Unitary Chiral Dynamics In Three-Body Systems

Alberto Martínez Torres

Departamento De Física Teórica

Universidad de Valencia

TESIS DOCTORAL

VALENCIA 2009

D. Eulogio Oset Báguena, Catedrático de Física Teórica de la Universidad de Valencia,

> CERTIFICA: Que la presente Memoria *Unitary Chiral Dynamics In Three-Body Systems* ha sido realizada bajo mi dirección en el Departamento de Física Teórica de la Universidad de Valencia por D. Alberto Martínez Torres como Tesis para obtener el grado de Doctor en Física.

Y para que así conste presenta la referida Memoria, firmando el presente certificado.

Fdo: Eulogio Oset Báguena

Contents

Agradecimientos

Parece que fue ayer pero ya han pasado cuatro años desde que me senté por primera vez en una de las sillas del despacho de Eulogio Oset, catedrático de física teórica de la Universidad de Valencia, para escuchar atentamente la idea que tenía para que realizase un doctorado con él en su grupo de investigación. Empezó a contarme que desde hacía tiempo tenía en mente que había bariones y mesones cuyas propiedades físicas podían entenderse si se consideraba que esos estados no eran sistemas ligados de tres quarks, en el caso de bariones, o de un par quark-antiquark, en el caso de mesones, sino estados ligados de tres hadrones y que, hasta la fecha, era un tema que no había sido estudiado con profundidad.

La verdad es que no necesitó mucho tiempo para contagiarme la misma ilusión que podía ver en su cara cuando hablaba conmigo sobre el tema y no tardó mucho en convencerme de que estudiar sistemas formados por tres hadrones podría servir para explicar las propiedades de alguno de los bariones y mesones observados en la naturaleza y que, en algunos casos, no estaban del todo claras. Sobre todo, de los diferentes argumentos que dijo hubo uno que fue muy convincente: una chica que acababa de realizar su doctorado en la India, Kanchan, iba a venir al grupo para colaborar en el mismo proyecto que Eulogio tenía

en mente. ¿Qué argumento puede haber que sea mejor que ese, no? En algún momento en la historia de cómo empecé con el estudio de sistemas de tres cuerpos resultó que Kanchan y yo acabamos casándonos, pero creo que esa parte me la guardo para mí y sigo hablando sobre sistemas de tres cuerpos que seguro que para esta Tesis resulta más interesante.

Eulogio junto con diversos grupos teóricos había desarrollado un modelo basado en Lagrangianos chirales y unitariedad en canales acoplados de gran éxito en el estudio de sistemas mesón-mesón y mesón-barión y ahora pretendía generalizar ese modelo para el estudio de sistemas formados, por ejemplo, por dos mesones y un barión, tres mesones, etc. Eulogio tenía (y sigue teniendo) una gran experiencia en el estudio de sistemas de dos cuerpos (pues ya son muchos los años que lleva trabajando en esto, aunque tal y como me dijo el día en el que le felicité por su 59 cumpleaños: "hoy hago 59, sí, pero todavía los disimulo"). Sin embargo, no había estudiado sistemas formados por tres cuerpos. Kanchan había estudiado sistemas de tres cuerpos, pero nunca había utilizado Lagrangianos chirales y yo ni había estudiado sistemas de tres cuerpos ni utilizado Lagrangianos chirales. Con lo cual, la probabilidad de que juntos fuésemos a hacer algo que diese como resultado algo positivo no sé si sería grande o no, pero los tres empezamos desde cero con la ilusión de encontrar estados ligados formados por tres hadrones, pasando días enteros desarrollando el formalismo que nos permitiría aplicar las técnicas quirales que tanto éxito habían dado en sistemas de dos cuerpos al caso de sistemas de tres cuerpos. Ninguno de nosotros pensó antes de empezar que iba a ser más complicado de lo que en un principio nos hubiéramos imaginado y pasaron dos años desde que comenzamos con el formalismo hasta ver por primera vez en la pantalla del ordenador el cuadrado de la matriz T para el canal $\pi\pi\Sigma$ en función de la energía que, por suerte nuestra, en lugar de obtener una línea recta mostraba un pico a una energía en la que había un estado físico, $\Sigma(1660)$, que ya había sido observado experimentalmente, concretamente en la reacción $K^-p \to \pi^0\pi^0\Sigma^0$. Ese fue el día en

el que creo que los tres pensamos que mereció la pena los dos años que nos costó desarrollar el formalismo, los dos años en los que sufrimos viendo que cada vez que resolvíamos un problema otro mayor aparecía, los dos años en los que más de una vez pensamos por separado "pero para qué me habré metido yo en esto", pero que ninguno se atrevía a decírselo al otro temiendo que le cogiese la palabra y hubiese que poner fin al proyecto comenzado, esos dos años en los que tuvimos que convencernos de que merecía la pena seguir a pesar de no obtener nada ni atisvar que algo fuese a salir de todo eso. Pero al final hubo suerte y poco a poco empezaron a aparecer resultados positivos que concordaban con las observaciones experimentales. Tal y como diría Eulogio: "al final resulta que ha habido baby".

Dicho esto, no me cabe más que agradecerles a Eulogio Oset y a Kanchan Pradeepkumar Khemchandani el gran esfuerzo que pusieron y la enorme cantidad de tiempo que dedicaron en desarrollar el modelo que he intentado explicar de la mejor manera posible en esta Tesis. Sin ellos, esta Tesis no hubiese sido posible. También quiero agradecerle a Eulogio el que me diese la oportunidad de realizar un doctorado con él y el haber sido tan paciente en momentos en los que uno tiraría a la basura todo lo que ha estado haciendo y le gustaría empezar con algo totalmente diferente.

El modelo que aparece en esta Tesis no sería lo que es sin la ayuda de muchas personas que pacientemente han escuchado todo lo que estábamos haciendo y nos han ayudado a obtener soluciones a problemas que teníamos. En concreto Manolo Vicente Vacas, Christoff Hanhart, Juan Nieves, José Ramón Peláez, José Antonio Oller, Carmen García-Recio, Enrique Ruiz Arriola, Angels Ramos y Felipe Llanes Estrada. Gracias por todas vuestras críticas y comentarios que han servido para mejorar este modelo.

Quiero agradecer a mis padres, Julián Martínez Rodríguez y Francisca Torres Moreno, el esfuerzo que a lo largo de estos años han realizado para que su hijo tuviese la educación que ellos no pudieron tener y a mi hermano Julián el apoyo que siempre me

ha brindado desde mi infancia.

मेरी बीबी के लिए

Introduction

Let me start this introduction with a question: what the hell is a hadron? This question was already formulated for the first time around 1964 when Murray Gell-Mann and George Zweig proposed, independently, that all hadrons are formed by elementary particles, which Gell-Mann named quarks. According to the quark model, every hadron could be either composed of three quarks, which is called baryon, or by a quark-antiquark pair, such hadron is called meson. Keeping this idea in mind, it was just a matter of time to build up the different baryons and mesons observed in Nature (for an elementary introduction see [1]). All one needed was to write all the possible combinations of three quarks or quark-antiquark pairs as a function of their charge and strangeness. Excitations of these quarks from the ground state to different high energy levels would generate more hadrons with a relatively short lifetime and which are called resonance. However, the quark model suffers one profound embarrassment: nobody has ever observed an individual quark! The quark model solved this problem by introducing the concept of quark confinement: the quarks in the baryons and mesons are absolutely confined, therefore, it does not matter what you do, you will never be able to get them out of the hadron. But even if all the quarks are confined inside the

hadrons, this does not imply that they are inaccessible for experimental purposes. One can study the inner structure of a proton in a way similar to the one in which Rutherford investigated the structure of an atom, i.e, by firing something into it. Another way of confirming the existence and the confinement of the quarks is through the study of the e^+e^- annihilation. When an e^+ collides with an e^- a quark-antiquark pair is produced. For a brief moment of time the quarks "fly" apart as free particles, but when they reach a separation distance of about 1fm (the diameter of a hadron) their interaction is so strong that it decelerates the quarks. The decelerated quarks emit new quark-antiquark pair(s) which form hadrons just as a decelerated charged particle emits photons via Bremsstrahlung. In all this process there is an unmistakable footprint left behind by the original quark-antiquark pair: the new quark-antiquark pair(s) emerge in opposite directions in order to conserve the momentum, therefore, the observed hadrons are produced in two "jets", one along the direction of the primordial quarks, and the other marking the direction of the antiquarks [1].

However, it seems that Nature is more complicated than this and the picture in which all the hadrons can be understood as three quarks or a quark-antiquark pair is too simple to describe the properties of all the known hadrons. For example, the lowest excited state found of the nucleon is the $N^*(1440)$. However, in a three-quark model for a baryon, the state $N^*(1535)$ should be expected to be the first excitation of the nucleon, with a radial excitation of a quark. From the kinematical point of view, this implies providing an energy of around 600 MeV to one of the three quarks in the nucleon in order to excite it to a higher energy level to get the $N^*(1535)$. This energy is sufficient to create, for example, a pion or two pions or an eta meson. Thus, if one tries to excite a quark to an energy level which is 600 MeV far from the ground state, before that happens, by analogy to the collision between an e^+ and an e^-, a pair quark-antiquark will be created in form of a meson, for example, a pion. Then it seems plausible to think that the in-

teraction between a pion/two pions/an eta and a nucleon can be more important for the description of the properties of the $N^*(1535)$ than its possible three-quark structure, of course, if the interaction amongst hadrons is attractive in Nature.

Obviously, this does not mean that if one has to construct a wave function for the $N^*(1535)$ only the pion-nucleon component will be present. The wave function, for instance, must contain a three quark seed, but each of the components, three quarks, meson-baryon, etc., will have a different weight. Various investigations show that the properties of the $N^*(1535)$ can be understood by taking into account only the part of its wave function which is related to the meson-baryon component, which means that the other possible constituents, like, for example, three quarks, are much less important for the description of its properties. Thus, the $N^*(1535)$ can be considered mainly as a kind of πN "molecular" state. Such "molecular" states, in which the weight of the meson-baryon component in the wave function overcomes the rest, are called dynamically generated resonances, since they appear as poles in the scattering matrix due to the interaction of the mesons and baryons.

Therefore, a theory which uses the hadrons as degrees of freedom instead of quarks can be more reliable to understand the properties of some of the mesons and baryons found in Nature. This situation is in fact far more expected when ones studies interactions of hadrons in a low and an intermediate energy region. Here, due to the inherent confinement of the quarks, the quarks can not be considered as the asymptotic states of the theory. In the recent past, Chiral Perturbation Theory (χPT) has emerged as an appropriate formalism to deal with hadrons at low and intermediate energies. χPT describes the interaction between hadrons by taking them as the building blocks of the theory and by incorporating them into a series of effective Lagrangians in an expansion in powers of momenta. The expansion scale is of the order of 1 GeV, which implies that the series is valid for momenta smaller than 1 GeV. This theory, however has two basic limitations: the first one is that its

range of convergence is just a few hundreds of MeV, which corresponds to the energy region where the first meson resonances appear. This implies the presence of the corresponding poles in the scattering amplitude and an expansion in a power series can not reproduce a pole; the second one is that the number of free parameters increases tremendously with the increase in the order of the expansion in momenta. Thus, the theory loses its predictive power.

In the last years, non-perturbative unitarity techniques based on chiral Lagrangians have been developed to extend the validation range of the chiral theories up to energies of the order of 2 GeV. These unitarity extensions of the χPT have been applied to the study of different two-body meson-baryon and meson-meson systems, for example, $\bar{K}N$, $\pi\Sigma$, $\pi\Lambda$, πN, $\pi\pi$, $K\bar{K}$, $\pi\eta$, etc., and dynamical generation of many baryon and meson resonances in these systems has been found, for instance, the $\Lambda(1405)$, $\Lambda(1520)$, $N^*(1535)$, etc., in the baryon sector and the $f_0(980)$, $a_0(980)$, $\sigma(600)$, etc., in the meson sector [2–20]. It has also been found that all these states contain important meson-baryon and meson-meson components, respectively, in their wave functions, which play an important role in the description of their physical properties [21].

Since the interaction in such two-body systems is strongly attractive, it seems plausible to anticipate that the addition of one more meson or baryon could lead to the generation of new states in which case the interaction of the three particles could be determinant in understanding some of the experimental findings. This mean that there could exist some hadrons having, dominantly, a three-body structure. The properties of such hadrons would not be easily understood if their three-body structure is ignored. In fact, in the $S = -1$ baryonic sector, there exist Λ and Σ resonances with poor or controversial status, e.g., $\Sigma(1560)$, $\Sigma(1580)$, $\Sigma(1620)$, etc., [22]. Also some of these seem to remain unexplained in terms of two-body dynamics, e.g., a study of the $K^-p \to \pi^0\pi^0\Lambda$ reaction in a coupled channel approach [16] involving $\pi\Sigma(1385)$, $K\Xi(1530)$, $\bar{K}N$ and

$\pi\Sigma$ channels, and where the $\Lambda(1520)$ gets dynamically generated, provides an explanation for the bulk of the data [23], but fails to explain a bump in the $\Lambda(1600)$ region. Further, in [24] the excitation of the $\Sigma(1660)$ has been indicated in the data on the $K^-p \to \pi^0\pi^0\Sigma^0$ reaction. These findings naturally demand a study of three-body system(s) such as $\pi\pi\Sigma$, $\pi\pi\Lambda$, etc. There are many more hadron resonances which strongly suggest that their three-body structure should be explored for a clear understanding of their characteristics and that it is this missing information which has created a confusion about the properties of these resonances. We shall discuss some examples of such states in detail below.

In the $S = 0$ baryonic sector, the excited states of the nucleon have been studied extensively theoretically as well as experimentally. This is evident from the fact that many of these states, especially those in the energy region below 1750 MeV, have been assigned either three or four stars by the particle data group (PDG) [22]. Even then, there are some resonances in this low energy region which still need unanimous agreement on their characteristics or existence, e.g., the $J^\pi = 1/2^+$ resonances in the isospin $1/2$ domain. The $N^*(1440)$ or Roper resonance is a subject of continuous debate and the existence of the $N^*(1710)$ is even questioned. The quark models face difficulties in reproducing both these states [25–27]. In case of the $N^*(1710)$, some partial wave analyses [28, 29] do not find any pole corresponding to it, while others claim a clear manifestation of this resonance [30–33]. On the other hand, the authors of [34] claim an undisputable existence of the $N^*(1710)$ from their study of the $\pi N \to \eta N$ reaction in the coupled channel formalism and suggest that the status of this resonance should be upgraded from three-star to four-star.

Another controversy about the $N^*(1710)$ started after the finding of a narrow peak in the $\gamma A \to (K^+n)X$ reaction at LEPS [35], suggesting the existence of a pentaquark state which some groups associated to a SU(3) antidecuplet to which the $N^*(1710)$ would also belong (see, for example, [36, 37]). In or-

der to be compatible with the Θ^+, the $N^*(1710)$ is required to be narrow. However, the width of this resonance is not known precisely, but the widths listed in [22] for it rang from $\sim$ 90 - 480 MeV. The authors of [38] reanalyzed the $\pi N \to K\Lambda$ reaction and found that a narrow width of the $N^*(1710)$ [22] was incompatible with the data and proposed the existence of another narrow resonance in this energy region. The partial wave analyses group who do not find a pole for the $N^*(1710)$ suggested to look for another resonance in this energy region as a possible narrow, non-strange partner of the θ^+ [39, 40]. The debate on this issue has continued with new analyses which do not find a signal for the θ^+, as a consequence of which, the case for this state has weakened (see [41] for a review).

In the case of the Roper resonance, which is the lowest excited state of the nucleon and, hence, in the simplest quark model should be expected to be a 3-quark state with a radial excitation of a quark, alternative descriptions, like a 3-quark-gluon structure [42], a quark core dressed by meson clouds [43], a dynamically generated resonance from interaction of mesons and a baryon [44], etc., are posed in order to reproduce its properties.

Looking at the characteristics of both these $1/2^+$ resonances in [22], i.e., a large branching ratio for the $\pi\pi N$ decay channel, ($\sim$ 30-40 % for the $N^*(1440)$ and 40-90 % for the $N^*(1710)$), it seems that they couple strongly to two meson-one baryon systems. There are many findings which support this idea, e.g., a strong σN coupling to the Roper resonance reported in [44,45], an important contribution from the two meson cloud to the masses of the SU(3) antidecuplet members found in [21], and a good reproduction of the data on the $\Sigma\pi$ distribution in the $\pi^- p \to K^0 \Sigma\pi$ reaction by taking the $\pi\pi N$ decay channel of the $N^*(1710)$ into account [46]. Hence, it looks like a study of the three-body structure of these resonances could shed more light on their properties.

In the meson sector there are also several states which could be possible candidates for three-body resonances. For example,

the $X(2175)$. The discovery of the X(2175) 1^{--} resonance in $e^+e^- \to \phi f_0(980)$ with initial state radiation at BABAR [47,48], also confirmed at BES in $J/\Psi \to \eta\phi f_0(980)$ [49], has stimulated research around its nontrivial nature in terms of quark components. The possibility of it being a tetraquark $s\bar{s}s\bar{s}$ is investigated within QCD sum rules in [50], and as a gluon hybrid $s\bar{s}g$ state has been discussed in [51,52]. A recent review on this issue can be seen in [53], where the basic problem of the expected large decay widths into two mesons of the states of these models, contrary to what is experimentally observed, is discussed. The basic data available on this resonance from [47,48] are $M_X = 2175 \pm 10$ MeV and $\Gamma = 58 \pm 16 \pm 20$ MeV, which are consistent with the numbers quoted by BES $M_X = 2186 \pm 10 \pm 6$ MeV and $\Gamma = 65 \pm 25 \pm 17$ MeV. In Ref. [48] an indication of this resonance is seen as an increase of the $K^+K^-K^+K^-$ cross section around 2150 MeV. A detailed theoretical study of the $e^+e^- \to \phi f_0(980)$ reaction was done in Ref. [54] by means of loop diagrams involving kaons and K^*, using chiral amplitudes for the $K\bar{K} \to \pi\pi$ channel which contains the $f_0(980)$ pole generated dynamically by the theory. The study revealed that the loop mechanisms reproduced the background but failed to produce the peak around 2175 MeV, thus reinforcing the claims for a new resonance around this mass. In the chiral models the $f_0(980)$ gets dynamically generated in the $\pi\pi$ and $K\bar{K}$ interaction. Therefore there is a possibility to generate dynamically the $X(2175)$ in the $\phi\pi\pi$ and $\phi K\bar{K}$ system. There are many similar examples like the $Y(4260)$, $X(1750)$, $Y(4460)$, etc.

With the motivation to search for all such states and to understand their properties, we have extended the well studied two-body chiral formalism to three-body systems.

The study of three-body systems requires solving of Faddeev equations [55] which in its exact form is a cumbersome task, due to which one often resorts to approximations. While most conventional studies of three-body systems use potentials in coordinate space, usually separable potentials to make the solution of the Faddeev equations feasible, we used two parti-

cle amplitudes generated within the unitary chiral approach in momentum space. The most novel finding in this work is the realization that, for s-waves and in the SU(3) limit, there is an exact cancellation between the off-shell part of the two-body amplitudes and the three-body forces generated by the same chiral Lagrangians [56–58]. To be more precise, the on-shell amplitude means that the s-wave amplitude is calculated as a function of the Mandelstam variable s imposing $q^2 = m^2$ for the external momenta of the two body amplitudes. When these lines are inside the Faddeev diagrams where some line can be off-shell, the full amplitude is separated into this "on-shell" part plus and "off-shell" part which goes as $q^2 - m^2$ for mesons and $q^0 - E(q)$ for baryons and vanishes when the external lines are on-shell. This off-shell part contains an inverse particle propagator and cancels one particle propagator while iterating the Faddeev equations, rendering a three-body diagram with two two-body t-matrices into a three-body contact term, which has the same topology as genuine three-body forces that stem from the chiral Lagrangians. We find that the sum of all these three-body forces is null in the SU(3) limit. As a consequence, one needs only the on-shell two-body t-matrices and can ignore these three-body forces. This finding is novel for such studies and simplifies the work technically, although not much, since loops involve a changing s-variable, and consequently the s-dependent t-matrices must be inserted into the loop functions. This makes this approach different and technically more involved than the study of the two body interaction, where using arguments of the N/D method one can factorize on shell amplitudes outside the loop functions which involve only two hadron propagators [4]. The greatest benefit of this finding in the three-body problem is that the results do not depend upon the off-shell extrapolations of the amplitudes which is a source of uncertainty in the three-body calculations that rely upon a potential. Indeed, it is well known that given a certain physical amplitude, on-shell in nature, one has an infinite number of potentials that give this amplitude upon solving the Schrödinger equation. The dif-

ferences between the different potentials will only show in the off-shell extrapolation of the amplitudes. However, this information enters the solution of the Faddeev equations and, hence, different potentials leading to the same on shell amplitude will provide different results upon solution of the Faddeev equations.

The problem stated above is most probably the main reason why recent works dealing with the $\bar{K}NN$ system lead to quite different results in the binding and the width. In this sense, we find a series of works based on Faddeev equations which lead to relatively large binding, of the order of $50 - 70$ MeV [59–62], while other works based on variational methods lead to smaller bindings of the order of 20-30 MeV [63–65]. The widths also vary from $50 - 100$ MeV.

The arbitrariness of the off-shell amplitude is also well known in field theory, where the implementation of unitary transformations of the fields in the Lagrangian maintains the same on-shell amplitudes but changes their off-shell extrapolation. In this sense it is interesting to note that, although the cancellation of the off-shell part of the three-body amplitude versus the three-body forces discussed here is not explicitly shown in other three-body works using also chiral dynamics [66, 67], these approaches are invariant under unitary transformations, indicating that the mentioned cancellations apparently occur in the full calculation [68]. A similar independence of results from the off-shell extrapolation has been shown in different reactions like the $\pi N \to \pi\pi N$ reaction [69] and the study of the interacting two pion exchange in the NN interaction [70]. However, the explicit realization of the off-shell versus three-body forces indicates that one can neglect the three-body forces from the beginning, certainly simplifying the approach, and use only the two-body on-shell amplitudes.

As shall be explained in the subsequent chapters of this Thesis, we start with the lowest order chiral Lagrangian for the two-body interaction and use the on-shell factorization of the potentials and t-matrices in the Bethe-Salpeter equation [5–7, 10, 18], which replaces the solving of the integral equations to that of

algebraic equations. This simplification makes the solution of the few body equations conceivable, even if the unitary chiral approach demands inclusion of large number of coupled channels in order to implement the SU(3) symmetry. Following the method of the on-shell factorization in the Bethe-Salpeter equation, we have developed a similar approach to solve the Faddeev equations and the procedure shall be explained in the following chapters.

This theory has been applied to the $\pi \bar{K} N$ and its coupled channels, where all the Λ and Σ $1/2^+$ resonances listed in the Particle Data book [22], in the $1480 - 1800$ MeV region, have been found to get dynamically generated. Further, calculations using the same formalism have been done for $S = 0$ baryon resonances. Concretely, we have studied the $\pi\pi N$, $\pi\eta N$, $\pi K \Lambda$, $\pi K \Sigma$ and $K\bar{K}N$ systems considering them as coupled channels. As a result, two N^*'s, the $N^*(1710)$ and the $N^*(2100)$, and one Δ resonance, the $\Delta(1910)$, have been found in the three-body amplitudes. Also a new N^* state, which was predicted in [71], appears around 1920 MeV in the $NK\bar{K}$ system when the $K\bar{K}$ is resonating as the $f_0(980)$ or the $a_0(980)$.

Also, a two meson-one baryon system with total strangeness $+1$ have been studied with the aim of describing the Θ^+ pentaquark state as a $N\pi K$ bound state. We do not find any trace of the Θ^+ but we find a broad structure with 200 MeV of width at an energy of 1700 MeV [72].

In the case of three-meson systems, a calculation for the $\phi K\bar{K}$ and $\phi\pi\pi$ systems has been done which has revealed the dynamical generation of the $X(2175)$ state when the $\pi\pi$ and $K\bar{K}$ subsystem is projected in isospin zero and its invariant mass is close to 980 MeV. This confirms the experimental findings of BABAR and BES [47–49] that the $X(2175)$ has a very strong coupling to the $\phi f_0(980)$ channel. We have also investigated the $J/\psi\pi\pi$ and $J/\psi K\bar{K}$ systems where we find the charm partner of the $X(2175)$, i.e, $Y(4260)$, which gets dynamically generated when the J/ψ with two pseudoscalars rearrange as $J/\psi f_0(980)$.

In the next chapter of this Thesis a formalism is developed

to solve the Faddeev equations using two-body amplitudes obtained from chiral Lagrangians. In subsequent chapters we focus on using this formalism for different three-hadron systems and give details of the calculation and the results obtained in each case. The Thesis ends with a summary of the whole study and with a list of future plans.

CHAPTER 1

Formalism I: Faddeev equations and $U\chi PT$

For the last eight years strong interaction physics has
been concerned mainly with two-particle systems. My
own opinion is that two-particle systems are now finished.
By this I do not mean that we have done everything we
hoped to do, but rather we have done everything we are
going to be able to do. I think the future of strong
interactions now lies with many-particle systems. Here the
surface has barely been scratched.

C. LOVELACE [73]

In this chapter, we shall discuss the formalism to study the
three-body systems made up of two mesons and one baryon or
three mesons. Obviously, this requires the study of the meson-
meson and the meson-baryon interactions , which has been de-
scribed using unitary chiral perturbation theory ($U\chi PT$). Fol-
lowing a brief discussion on the two-body interaction an intro-
duction to the Faddeev equations is given. These equations are
then rederived using field theory. Finally, a reformulation of

the Faddeev equations is obtained by using unitary chiral dynamics for the two-body interactions. The motivation for the reformulation and its benefits are also discussed. The novel and one of the most important finding of the cancellation between three-body forces and the off-shell contribution of the two-body t-matrices to the three-body diagrams is shown analytically in this chapter for the two meson-one baryon as well as the three-meson case. The chapter ends with the new set of equations obtained, which are solved for different three-hadron systems as explained in the subsequent chapters.

1.1   Two-body interactions in $U\chi PT$

Quantum Chromodynamics or QCD is the theory which describes the strong interaction in terms of the fundamental constituents of the hadrons: quarks and gluons. However, while in the high energy region, due to the asymptotic freedom of the quarks, the theory has been successfully tested by the experiment, this is not the situation for low and intermediate energies. The introduction of the effective chiral Lagrangians formalism to account for the basic symmetries of QCD and its application through chiral perturbation theory (χPT) to the study of meson-meson interaction [74] or meson-baryon interaction [75–77] has shed new light on these problems and allowed a systematic approach. The standard chiral perturbative model, i.e., an expansion in powers of the typical momenta involved in the process, is constrained to the low energy region, where it has had remarkable success, but makes unaffordable the study of the intermediate energy region where resonances appear, since the singularities associated to the resonance cannot be generated perturbatively. In recent years, the combination of the information of the chiral Lagrangians, together with the use of non-perturbative schemes, has allowed one to make predictions beyond those of the chiral perturbation expansion. The main idea to extend the range of applicability of χPT to higher energies is the inclusion of unitarity in coupled channels. Within

the framework of chiral dynamics, the combination of unitarity in coupled channels together with a reordering of the chiral expansion provides a faster convergence and a larger convergence radius of a new chiral expansion, such that the lowest energy resonances are generated within those models. This then advances the chiral perturbation theory (χPT) to the unitary chiral perturbation theory ($U\chi PT$).

One starts from the standard chiral Lagrangians in the lowest order of chiral perturbation theory (χPT) coupling the octet of pseudoscalar mesons to the octet of $1/2^+$ baryons for the pseudosclar meson-baryon interaction and with itself for the pseudoscalar-pseudoscalar meson interaction. These Lagrangians provide the potentials which we use to solve the coupled channel Lipmann-Schwinger equation with relativistic propagators in the intermediate states (or Bethe-Salpeter equation) to obtain the two-body t-matrices.

The interaction chiral Lagrangians are given by [2, 5]

$$\mathcal{L}_{MB} = \frac{1}{4f^2}\langle \bar{B}i\gamma^\mu[(\partial_\mu\Phi\Phi - \Phi\partial_\mu\Phi))B$$
$$- B(\partial_\mu\Phi\Phi - \Phi\partial_\mu\Phi))\rangle \tag{1.1}$$

for the interaction of a pseudoscalar meson with a baryon of the $1/2^+$ octet and

$$\mathcal{L}_{MM} = \frac{1}{12f^2}\langle(\partial_\mu\Phi\Phi - \Phi\partial_\mu\Phi)^2 + M\Phi^4\rangle \tag{1.2}$$

for the pseudoscalar-pseudoscalar meson interaction. In Eqs. (1.1, 1.2) f is the pion decay constant and the symbol $\langle\ \rangle$ denotes the trace in the flavor space of the $SU(3)$ matrices Φ, B and M

$$\Phi = \begin{pmatrix} \frac{1}{\sqrt{2}}\pi^0 + \frac{1}{\sqrt{6}}\eta & \pi^+ & K^+ \\ \pi^- & -\frac{1}{\sqrt{2}}\pi^0 + \frac{1}{\sqrt{6}}\eta & K^0 \\ K^- & \bar{K}^0 & -\frac{2}{\sqrt{6}}\eta \end{pmatrix} \tag{1.3}$$

$$B = \begin{pmatrix} \frac{1}{\sqrt{2}}\Sigma^0 + \frac{1}{\sqrt{6}}\Lambda & \Sigma^+ & p \\ \Sigma^- & -\frac{1}{\sqrt{2}}\Sigma^0 + \frac{1}{\sqrt{6}}\Lambda & n \\ \Xi^- & \Xi^0 & -\frac{2}{\sqrt{6}}\Lambda \end{pmatrix} \qquad (1.4)$$

$$M = \begin{pmatrix} m_\pi^2 & 0 & 0 \\ 0 & m_\pi^2 & 0 \\ 0 & 0 & 2m_K^2 - m_\pi^2 \end{pmatrix}.$$

In the M matrix we have taken the isospin limit ($m_u = m_d$). Using the equations (1.1), (1.2) and (1.4) we can get the potentials for the different coupled channels of the system under consideration. For the pseudoscalar meson-baryon case, the potential has a common structure for the different channels (m, n) [17], i.e.,

$$\mathcal{V}_{mn} = -C_{mn}\frac{1}{4f^2}\bar{u}_s(\vec{p}')\gamma^\mu u_s(\vec{p})(k_\mu + k'_\mu) \qquad (1.5)$$

with $u_s(\vec{p})$ $[u_s(\vec{p}')]$ being the initial (final) baryon spinor and k (k') the momentum of the incoming (outgoing) meson. The matrix C_{ij}, which is symmetric, contains the coefficients which show the $SU(3)$ symmetry of the problem and can be found, for example, in [5,17]. If the interest is in S-wave interactions, the potentials (1.5) are projected in S-wave, getting

$$\mathcal{V}_{ij}(E) = -C_{ij}\frac{1}{4f_i f_j}(2E - M_i - M_j)\sqrt{\frac{M_i + E_i(E)}{2M_i}}$$
$$\times \sqrt{\frac{M_j + E_j(E)}{2M_j}} \qquad (1.6)$$

where E is the total energy in the CM system of the two particles, E_i and M_i (E_f and M_f) are the energy and the mass,

respectively, of the initial (final) baryon. Note that a different decay constant is introduced for each meson ($f_\pi = 93$ MeV, $f_K = 1.22 f_\pi$, $f_\eta = 1.3 f_\pi$ [74]).

In the case of the pseudoscalar-pseudoscalar meson interaction the potentials do not have a general form (see [2] as an example for the case of two pseudoscalars). These potentials are inserted in the coupled channel Bethe-Salpeter equation

$$t_{ij} = \mathcal{V}_{ij} + \mathcal{V}_{il} G_l t_{lj} \tag{1.7}$$

with

$$\mathcal{V}_{il} G_l t_{lj} = i \int \frac{d^4 q}{(2\pi)^4} \frac{M_l}{E_l(\vec{q})} \frac{\mathcal{V}_{il}(k,q) t_{lj}(q,k')}{k^0 + p^0 - q^0 - E_l(\vec{q}) + i\epsilon}$$
$$\times \frac{1}{q^2 - m_l^2 + i\epsilon} \tag{1.8}$$

in the pseudoscalar meson-baryon case, while

$$\mathcal{V}_{il} G_l t_{lj} = i \int \frac{d^4 q}{(2\pi)^4} \frac{\mathcal{V}_{il}(k,q) t_{lj}(q,k')}{q^2 + m_{1l}^2 + i\epsilon}$$
$$\times \frac{1}{(P-q)^2 - m_{2l}^2 + i\epsilon} \tag{1.9}$$

for the pseudoscalar-pseudoscalar meson interaction. In (1.8) only the positive energy component of the fermion propagator has been kept. The quantities M_l and E_l correspond to the mass and the energy of the intermediate baryon and m_l to the mass of the intermediate meson. Equation (1.7) can be represented as an infinite sum of the series of diagrams shown in Fig.1.1.
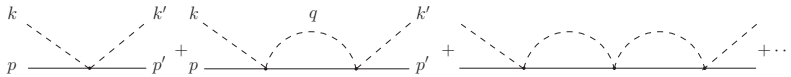

Figure 1.1: *Diagrammatic representation of the Bethe-Salpeter equation.*

The Bethe-Salpeter equation (1.7) is an integral equation and hence requires off-shell $\mathcal{V}$ and t for its solution. However, the use of the off-shell part of $\mathcal{V}$ and t can be circumvented, as we show below, and only the on-shell information will be needed. To see this, let us take, for example, the one loop diagram of the Fig.1.1 for the pseudoscalar meson-baryon interaction, which can be mathematically expressed as $\mathcal{V}G\mathcal{V}$. For simplicity, we assume equal masses in the external and intermediate states. In the low energy region, where one can neglect the spatial components in Eq.(1.5) and only the γ^0 component becomes relevant, we have

$$
\begin{aligned}
(\mathcal{V}_{on} + \mathcal{V}_{off})^2 &= C^2(k^0 + q^0)^2 = C^2(2k^0 + q^0 - k^0)^2 \\
&= C^2(2k^0)^2 + 2C^2(2k^0)(q^0 - k^0) \\
&\quad + C^2(q^0 - k^0)^2
\end{aligned}
\tag{1.10}
$$

with C a constant and hence

$$
\begin{aligned}
\mathcal{V}G\mathcal{V} = i \int \frac{d^4q}{(2\pi)^4} &\frac{M}{E(\vec{q})} \\
\times &\frac{C^2(2k^0)^2 + 2C^2(2k^0)(q^0 - k^0) + C^2(q^0 - k^0)^2}{k^0 + p^0 - q^0 - E(\vec{q}) + i\epsilon} \\
\times &\frac{1}{q^2 - m^2 + i\epsilon}.
\end{aligned}
\tag{1.11}
$$

It is obvious that the first term of the equation (1.10) is the on-shell contribution $\mathcal{V}_{on}^2$, $\mathcal{V}_{on}$ being $C(2k^0)$. A typical approximation for the heavy baryon propagation is to neglect the difference $p^0 - E(\vec{q})$ in Eq.(1.11) [78]. In this form, the one loop integral for the second term on the right hand side of Eq.(1.11) becomes

$$
\begin{aligned}
2iC\mathcal{V}_{on} &\int \frac{d^3q}{(2\pi)^3} \int \frac{dq^0}{2\pi} \frac{M}{E(\vec{q})} \frac{q^0 - k^0}{k^0 - q^0} \frac{1}{(q^0)^2 - \omega(\vec{q})^2 + i\epsilon} \\
&= -2C\mathcal{V}_{on} \int \frac{d^3q}{(2\pi)^3} \frac{M}{E(\vec{q})} \frac{1}{2\omega(\vec{q})} \sim \mathcal{V}_{on}q_{max}^2
\end{aligned}
\tag{1.12}
$$

where $w(\vec{q}) = \sqrt{\vec{q}^2 + m^2}$. This term is proportional to $\mathcal{V}_{on}$, therefore, it has the same structure as the tree level term in the

Bethe-Salpeter equation (1.7). Hence, it can be reabsorbed in the lowest order Lagrangian by making a suitable renormalization of the coupling constant f, giving then an effective chiral Lagrangian with the physical couplings. However, since we are already taking the physical values for the coupling constant f ($f = f_\pi = 93$ MeV) and the masses in the Lagrangians, this term should be omitted. Similarly, the last term of (1.11), proportional to $(q^0 - k^0)^2$, gets canceled with the $(k^0 - q^0)$ term in the denominator, i.e., the baryon propagator, and the integral of the remaining factor gives a term proportional to k^0 (and therefore to $\mathcal{V}_{on}$) and another proportional to q^0, which vanishes for parity reasons. These arguments can be easily extended to higher order loops and also for the meson-meson interaction (either pseudoscalar or vector mesons) [2, 5, 79]. An alternative derivation has been done using the N/D method starting from the unitarity condition $Im\{t^{-1}\} = -Im\{G\}$ and using a dispersion relation to get t^{-1}. In such a case, just from the beginning, only the on-shell part of $\mathcal{V}$ is needed [4, 6].

To conclude, only the on-shell part of the potential is needed in order to solve the Bethe-Salpeter equation (1.7) and, therefore, the potential can be extracted outside the loop integral leaving the loop function

$$
\begin{aligned}
G_l(E) &= i \int \frac{d^4q}{(2\pi)^4} \frac{M_l}{E_l(\vec{q})} \frac{1}{k^0 + p^0 - q^0 - E_l(\vec{q}) + i\epsilon} \\
&\quad \times \frac{1}{q^2 - m_l^2 + i\epsilon} \\
&= \int \frac{d^3q}{(2\pi)^3} \frac{1}{2w_l(\vec{q})} \frac{M_l}{E_l(\vec{q})} \\
&\quad \times \frac{1}{p^0 + k^0 - w_l(\vec{q}) - E_l(\vec{q}) + i\epsilon}
\end{aligned}
\tag{1.13}
$$

in the pseudoscalar meson-baryon case, while

$$G_l(E) = i \int \frac{d^4q}{(2\pi)^4} \frac{1}{q^2 + m_{1l}^2 + i\epsilon} \frac{1}{(P-q)^2 - m_{2l}^2 + i\epsilon}$$

$$= \int \frac{d^3q}{(2\pi)^3} \frac{w_1 + w_2}{w_1 w_2 [E^2 - (w_1 + w_2)^2 + i\epsilon]} \qquad (1.14)$$

with $w_1 = \sqrt{\vec{q}^{\,2} + m_{1l}^2}$ and $w_1 = \sqrt{\vec{q}^{\,2} + m_{2l}^2}$ for the pseudoscalar-pseudoscalar meson interaction.

The integral in equations (1.13) and (1.14) is logarithmically divergent. In χPT these divergences are canceled by counterterms of chiral Lagrangians at higher order and some finite contribution remains from the loops and the counterterms. Also one can regularize the loops by using a cut off q_{max} for the maximum value of the modulus of the momentum $|\vec{q}\,|$, typically of the order of 1 GeV, or through the dimensional regularization method, in which case

$$G_l(E) = \frac{N_l}{(4\pi)^2} \left\{ a_l(\mu) + ln\frac{\tilde{m}_{1l}^2}{\mu^2} + \frac{\tilde{m}_{2l}^2 - \tilde{m}_{1l}^2 + E}{2E} ln\frac{\tilde{m}_{2l}^2}{\tilde{m}_{1l}^2} \right.$$

$$+ \frac{Q_l(E)}{E} \times \left[ln\{E - (\tilde{m}_{2l}^2 - \tilde{m}_{1l}^2) + 2EQ_l(E)\} \right.$$

$$+ ln\{E + (\tilde{m}_{2l}^2 - \tilde{m}_{1l}^2) + 2EQ_l(E)\}$$

$$- ln\{-E + (\tilde{m}_{2l}^2 - \tilde{m}_{1l}^2) + 2EQ_l(E)\}-$$

$$\left. \left. - ln\{-E - (\tilde{m}_{2l}^2 - \tilde{m}_{1l}^2) + 2EQ_l(E)\} \right] \right\} \qquad (1.15)$$

where μ is the regularization scale ($\mu \simeq 1.2\, q_{max}$) and $N_l = 2M_l$, $\tilde{m}_{1l} = m_l$ and $\tilde{m}_{2l} = M_l$ in the pseudoscalar meson-baryon interaction, while in the pseudoscalar-pseudoscalar meson interaction $N_l = 1$ and $\tilde{m}_{1l}$, $\tilde{m}_{2l}$ are both the meson masses of the intermediate state. $Q_l(E)$ is the on-shell center of mass momentum of the system under consideration. The first term in Eq. (1.15) is a real constant and stands for the finite contribution of the counterterms. We treat these $a_l(\mu)$ constants as unknown

parameters and determine them from fits to the data [7, 17], requiring, however, that they are of natural size [6], which in terms of the cut off regularization means a cut off of the order of 1 GeV (the scale of these effective theories). In the same way, if one regularizes the loops with the cut off, one can vary it to fix some characteristics of the data (for example the position of the maximum of an experimental cross section). After this is done (by choosing a cut off, or by dimensional regularization), there is no free parameter left in the model.

Note that the imaginary part of the $G_l(E)$ (1.15) can be written as

$$Im\{G_l(E)\} = -\frac{N_l Q_l(E)}{8\pi E}. \tag{1.16}$$

From (1.7) it is easy to see that $Im\{t\} = t\,ImG\,t^*$, or

$$Im\{t^{-1}(E)]_{lj} = \delta_{lj}\frac{N_l Q_l(E)}{8\pi E} \tag{1.17}$$

which expresses the unitarity condition in the present normalization [80].

To summarize this discussion, it has been shown that only the on-shell part of the potentials together with the energy dependent loop function (1.14) is required to solve the coupled channel Bethe-Salpeter equation (1.7), reducing it to an algebraic equation. In matrix form

$$t(E) = \mathcal{V}(E) + \mathcal{V}(E)G(E)t(E) \tag{1.18}$$

which upon reordering give the two-body t-matrix as

$$t(E) = [1 - \mathcal{V}(E)G(E)]^{-1}\mathcal{V}(E). \tag{1.19}$$

1.2   The Faddeev equations

Let us consider three particles, labeled as 1, 2, 3, interacting by means of two-body potentials. We denote $\mathcal{V}^1$ as the potential acting between particles 2 and 3, $\mathcal{V}^2$ between the particles 1 and 3 and $\mathcal{V}^3$ between 1 and 2 [81]. By analogy with the two-body problem, one could consider solving the Bethe-Salpeter

equation for the three particle system with a kernel $K = G\mathcal{V}$, where $\mathcal{V} = \mathcal{V}^1 + \mathcal{V}^2 + \mathcal{V}^3$ and G the three-body Green function $1/(E - H)$. Unfortunately, there are two serious problems in using the Bethe-Salpeter equation (1.7) for the scattering of three or more particles. The first difficulty, as pointed out by Faddeev [55], is that the kernel of the Bethe-Salpeter equation is not square integrable[1] ($\mathcal{L}^2$) for the scattering of three or more particles. It should be stressed that the kernel of the Bethe-Salpeter equation for the two-body case written in an arbitrary reference frame is also non integrable. However, this problem is trivially solved by working in the two-body center of mass, as it is well known, which is not so for the case of three or more particles. To see this, let us evaluate the norm of the operator K, $\parallel K \parallel$, [81]

$$\parallel K \parallel = [Tr\{KK^\dagger\}]^{1/2} = \int d\alpha d\alpha' \, |< \alpha' \mid K \mid \alpha >|^2 \quad (1.20)$$

with α being a complete set of variables. In the momentum space, the matrix element in (1.20) is given by

$$< \vec{k}'_1, \vec{k}'_2, \vec{k}'_3 \mid K \mid \vec{k}_1, \vec{k}_2, \vec{k}_3 > = \delta^4(\vec{k}_1 + \vec{k}_2 + \vec{k}_3 - \vec{k}'_1 - \vec{k}'_2 - \vec{k}'_3)$$
$$\times \frac{1}{E - E_1(\vec{k}_1) - E_2(\vec{k}_2) - E_3(\vec{k}_3) + i\epsilon}[\delta^3(\vec{k}_1 - \vec{k}'_1)$$
$$\times < \vec{k}'_1 \mid \mathcal{V}^1 \mid \vec{k}_1 > +\delta^3(\vec{k}_2 - \vec{k}'_2) < \vec{k}'_2 \mid \mathcal{V}^2 \mid \vec{k}_2 >$$
$$+ \delta^3(\vec{k}_3 - \vec{k}'_3) < \vec{k}'_3 \mid \mathcal{V}^3 \mid \vec{k}_3 >]. \quad (1.21)$$

If we work in the global center of mass, i.e., in the center of mass system of the three particles, we can eliminate the total momentum conserving delta function. However, there will be still terms like $[\delta(\vec{k}_1 - \vec{k}'_1)]^2$ in the integrand of the equation (1.20), making the $Tr\{KK^\dagger\}$ infinite and the kernel K not $\mathcal{L}^2$. The second difficulty is that the Bethe-Salpeter equations do not have a unique solution when the limit $\epsilon \to 0^+$ is taken for

---

[1]If $K(x,y)$ is a finite and continuous function in the domain $a \leq x \leq b$, $a \leq y \leq b$, the condition $K(x,y) \in \mathcal{L}^2$ imply that: $\parallel K \parallel^2 = \int_a^b dx \int_a^b dy \mid K(x,y) \mid^2 < \infty$; $\int_a^b dy \mid K(x,y) \mid^2 < \infty \, \forall \, x$; $\int_a^b dx \mid K(x,y) \mid^2 < \infty \, \forall \, y$

the three-body case before solving the equation [81]. These two problems are totally new with respect to the two-body scattering and are intrinsic to the case of three (or more) particles.

In order to remove these difficulties, Faddeev [55] suggested to write the T-matrix operator as a sum of three partitions

$$T = T^1 + T^2 + T^3 \tag{1.22}$$

where T^i, $i = 1$, 2, 3 includes all the possible interactions contributing to the three-body T-matrix with the particle i being a spectator in the last interaction (Fig.1.2). Obviously, the sum of T^1, T^2 and T^3 contains all the possible diagrams obtained by permutations of the different interactions between the three particles. The Faddeev equations can be deduced by several methods[2], however, a derivation in terms of perturbation theory and the corresponding Feynman diagrams can give a more intuitive picture and a better understanding of the physical content of the equations. For this reason, we adopt this procedure to write the contribution of the different diagrams with different set of three-body interactions in order to derive the Faddeev equations.

We now list a set of conventions which we follow while representing the mathematical expressions diagrammatically:

- Particles are represented by horizontal lines, with those in the initial state on the left side being labeled by the four-momentum $k_i = (\omega_i, \vec{k}_i)$, and those in the final state by the four-momentum $k_i' = (\omega_i', \vec{k}_i')$ on the right side. With this convention the diagrams have to be read from right to left.

- A dashed line between two particles represent a two-body interaction (potential, $\mathcal{V}$).

- An empty blob between a pair of particle lines correspond to a two-body t-matrix.

---

[2]For example, by defining the operators T^1, T^2, T^3 as $T^i = \mathcal{V}^i + \mathcal{V}^i G T$, with $i = 1, 2, 3$, and using the Bethe-Salpeter equation to describe the interaction between the two particle subsystems.

- A filled grey blob indicates any three-body interaction.

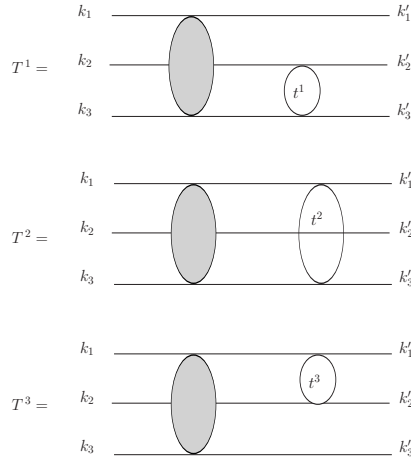Figure 1.2: *Diagrammatic representation of the Faddeev partitions.*

The diagrams contributing to the T^1 partition can thus be represented as those shown in Fig. 1.3.   Let us consider the
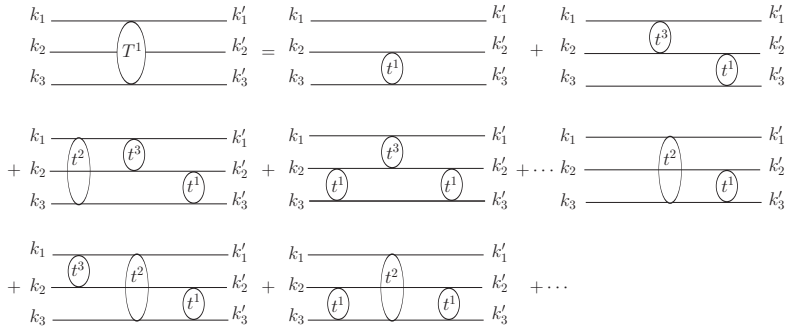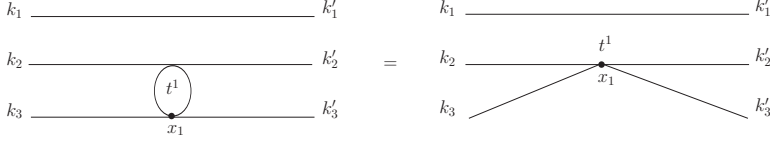

Figure 1.3: *Perturbation series of diagrams which contribute to the T^1 partition.*

particular case in which particles labeled by 1 and 2 are mesons and particle labeled by 3 is a baryon. Denoting the contribution

Figure 1.4: *Lowest order diagram that contribute to T^1.*

of each diagram of the Fig.1.3 to the $S - matrix$ corresponding to the T^1 partition, $S^{(1)}$, as $S_j^{(i)}$, where the upper index refers to the Faddeev partition under consideration and the lower index indicates the number of t-matrices (pair interactions) contained in the diagram, we have $S^{(1)} = S_1^{(1)} + S_2^{(1)} + S_3^{(1)} + \cdots$, with the first term (Fig.1.4) written as

$$< \vec{k}_1', \vec{k}_2', \vec{k}_3' \mid S_1^{(1)} \mid \vec{k}_1, \vec{k}_2, \vec{k}_3 > = \int d^4x_1 \prod_{l=2}^{3} \frac{1}{\sqrt{2\omega_l}}$$

$$\times \prod_{k=2}^{3} \frac{1}{\sqrt{2\omega_k'}} \sqrt{2m_3} \sqrt{2m_3'} \frac{1}{V^2} e^{i(k_2'+k_3')x_1}(-it_1)$$

$$\times e^{-i(k_2+k_3)x_1} \delta_{\vec{k}_1, \vec{k}_1'}$$

$$= -i \frac{(2\pi)^4}{V^2} \sqrt{2m_3} \sqrt{2m_3'} \prod_{l=1}^{3} \frac{1}{\sqrt{2\omega_l}} \prod_{k=1}^{3} \frac{1}{\sqrt{2\omega_k'}} (2\pi)^3$$

$$\times \delta^4(k_2 + k_3 - k_2' - k_3') \sqrt{2\omega(\vec{k}_1)} \sqrt{2\omega(\vec{k}_1')} \, t^1 \delta_{\vec{k}_1, \vec{k}_1'} \quad (1.23)$$

The m_1, m_2 (m_1', m_2') are the masses of the mesons in the initial (final) state and m_3 (m_3') is the mass of the baryon in the initial (final) state. The plane waves are normalized to unity in the volume V. There is a δ-Kronecker in (1.23) , $\delta_{\vec{k}_1, \vec{k}_1'}$, because the first particle is not interacting. According to our normalization

$$\delta_{\vec{k}_1, \vec{k}_1'} = \frac{1}{V} \int d^3x \, e^{i(\vec{k}_1 - \vec{k}_1')\vec{x}} = \frac{(2\pi)^3}{V} \delta^3(\vec{k}_1 - \vec{k}_1'). \quad (1.24)$$

Therefore, Eq. (1.23) can be written as

$$< \vec{k}'_1, \vec{k}'_2, \vec{k}'_3 \mid S_1^{(1)} \mid \vec{k}_1, \vec{k}_2, \vec{k}_3 >= -i\frac{(2\pi)^4}{V^3}\sqrt{2m_3}$$

$$\times \sqrt{2m'_3}\delta^4(k - k')\prod_{l=1}^{3}\frac{1}{\sqrt{2\omega_l}}\prod_{k=1}^{3}\frac{1}{\sqrt{2\omega'_k}}(2\pi)^3$$

$$\times \sqrt{2\omega(\vec{k}_1)}\sqrt{2\omega(\vec{k}'_1)}\delta^3(\vec{k}_1 - \vec{k}'_1)t_1 \qquad (1.25)$$

with $k = k_1 + k_2 + k_3$ the total four-momentum in the initial state and $k' = k'_1 + k'_2 + k'_3$ in the final state.

The contribution from the second diagram on the right hand side of the Fig.1.3 (redrawn in Fig. 1.5) can be written as
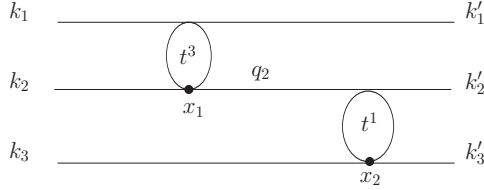
Figure 1.5: *Diagram at second order in t which contribute to T^1.*

$$< \vec{k}'_1, \vec{k}'_2, \vec{k}'_3 \mid S_2^{(1)} \mid \vec{k}_1, \vec{k}_2, \vec{k}_3 >= \int d^4x_2 \int d^4x_1 \prod_{l=1}^{3}\frac{1}{\sqrt{2\omega_l}}$$

$$\times \prod_{k=1}^{3}\frac{1}{\sqrt{2\omega'_k}}\sqrt{2m_3}\sqrt{2m'_3}\frac{1}{V^3}e^{i(k'_2+k'_3)x_2}(-it_1)e^{-ik_3x_2}$$

$$\times \int \frac{d^4q_2}{(2\pi)^4}\,i\frac{e^{iq_2(x_1-x_2)}}{q_2^2 - \tilde{m}_2^2 + i\epsilon}e^{ik'_1x_1}(-it_3)e^{-i(k_1+k_2)x_1} \qquad (1.26)$$

with $\tilde{m}_i$ the mass of the particle i in the intermediate state, such

that

$$< \vec{k}_1', \, \vec{k}_2', \, \vec{k}_3' \mid S_2^{(1)} \mid \vec{k}_1, \, \vec{k}_2, \, \vec{k}_3 >= -i \int \frac{dq_2^0}{(2\pi)} \int \frac{d^3q_2}{(2\pi)^3} \int dx_2^0$$

$$\times \, e^{-i(k_3^0 + q_2^0 - k_2^{0'} - k_3^{0'})x_2^0} \int dx_1^0 e^{-i(k_1^0 + k_2^0 - q_2^0 - k_1^{0'})x_1^0} \prod_{l=1}^{3} \frac{1}{\sqrt{2\omega_l}}$$

$$\times \prod_{k=1}^{3} \frac{1}{\sqrt{2\omega_k'}} \sqrt{2m_3} \sqrt{2m_3'} \frac{1}{V^3} \int d^3x_2 e^{-i(\vec{k}_3 + \vec{q}_2 - \vec{k}_2' - \vec{k}_3')\vec{x}_2}$$

$$\times \int d^3x_1 e^{-i(\vec{k}_1 + \vec{k}_2 - \vec{q}_2 - \vec{k}_1')\vec{x}_1} t_1 \frac{1}{(q_2^0)^2 - E_2^2(\vec{q}_2) + i\epsilon} t_3 \quad (1.27)$$

where $E_i(\vec{q}_i) = \sqrt{(\vec{q}_i)^2 + \tilde{m}_i^2}$. After integrating in d^4x_1 and d^4x_2 the expression (1.27) results in

$$< \vec{k}_1', \, \vec{k}_2', \, \vec{k}_3' \mid S_2^{(1)} \mid \vec{k}_1, \, \vec{k}_2, \, \vec{k}_3 >= -i \int \frac{dq_2^0}{(2\pi)} \int \frac{d^3q_2}{(2\pi)^3}$$

$$\times \frac{1}{V^3} (2\pi)^2 \delta(k_3^0 + q_2^0 - k_2^{0'} - k_3^{0'}) \delta(k_1^0 + k_2^0 - q_2^0 - k_1^{0'})$$

$$\times \prod_{l=1}^{3} \frac{1}{\sqrt{2\omega_l}} \prod_{k=1}^{3} \frac{1}{\sqrt{2\omega_k'}} \sqrt{2m_3} \sqrt{2m_3'} (2\pi)^3 \delta^3(\vec{k}_3 + \vec{q}_2 - \vec{k}_2' - \vec{k}_3')$$

$$\times (2\pi)^3 \delta^3(\vec{k}_1 + \vec{k}_2 - \vec{q}_2 - \vec{k}_1') \, t_1 \frac{1}{(q_2^0)^2 - E_2^2(\vec{q}_2) + i\epsilon} t_3.$$

Integrating the $\delta's$ we get

$$< \vec{k}_1', \, \vec{k}_2', \, \vec{k}_3' \mid S_2^{(1)} \mid \vec{k}_1, \, \vec{k}_2, \, \vec{k}_3 >= -i \frac{(2\pi)^4}{V^3} \delta^4(k - k')$$

$$\times \prod_{l=1}^{3} \frac{1}{\sqrt{2\omega_l}} \prod_{k=1}^{3} \frac{1}{\sqrt{2\omega_k'}} \sqrt{2m_3} \sqrt{2m_3'} \, t_1$$

$$\times \frac{1}{(k_1^0 + k_2^0 - k_1^{0'})^2 - E_2^2(\vec{k}_1 + \vec{k}_2 - \vec{k}_1') + i\epsilon} t_3.$$

Further, decomposing the propagators in the positive and neg-

ative energy parts

$$\frac{1}{(q^0)^2 - E^2(\vec{q}) + i\epsilon} = \frac{1}{2E(\vec{q})} \left[\frac{1}{q^0 - E(\vec{q}) + i\epsilon} \right.$$

$$\left. - \frac{1}{q^0 + E(\vec{q}) - i\epsilon} \right]$$

$$\frac{\slashed{q} + M}{(q^0)^2 - E^2(\vec{q}) + i\epsilon} = \frac{M}{E(\vec{q})} \left[\frac{\sum_s u_s(\vec{q})\bar{u}_s(\vec{q})}{q^0 - E(\vec{q}) + i\epsilon} \right.$$

$$\left. + \frac{\sum_s v_s(-\vec{q})\bar{v}_s(-\vec{q})}{q^0 + E(\vec{q}) - i\epsilon} \right] \qquad (1.28)$$

and neglecting the negative energy part of the propagators[3], since the calculations will be made in the low energy region we get,

$$\frac{1}{(q^0)^2 - E^2(\vec{q}) + i\epsilon} \Rightarrow \frac{1}{2E(\vec{q})} \frac{1}{q^0 - E(\vec{q}) + i\epsilon}$$

$$\frac{\slashed{q} + M}{(q^0)^2 - E^2(\vec{q}) + i\epsilon} \Rightarrow \frac{M}{E(\vec{q})} \frac{1}{q^0 - E(\vec{q}) + i\epsilon} \qquad .$$

Note that the operator $\sum_s u_s(\vec{q})\bar{u}_s(\vec{q})$ is used to construct the vertices, i.e., $\bar{u}_s(\vec{p}')\gamma^\mu u_s(\vec{q})$, $\bar{u}_s(\vec{q})\gamma^\nu u_s(\vec{p}')$ (see Eq.(1.5)), where $\bar{u}_s(\vec{p}')$, $u_s(\vec{p}')$ would be the external spinors.

Thus, for the diagram shown in Fig. 1.5 we have

$$< \vec{k}_1', \vec{k}_2', \vec{k}_3' \mid S_2^{(1)} \mid \vec{k}_1, \vec{k}_2, \vec{k}_3 > = -i\frac{(2\pi)^4}{V^3}\delta^4(k - k')$$

$$\times \prod_{l=1}^3 \frac{1}{\sqrt{2\omega_l}} \prod_{k=1}^3 \frac{1}{\sqrt{2\omega_k'}} \sqrt{2m_3}\sqrt{2m_3'} \, t_1 \frac{1}{2E_2}$$

$$\times \frac{1}{k_1^0 + k_2^0 - k_1^{0'} - E_2(\vec{k}_1 + \vec{k}_2 - \vec{k}_1') + i\epsilon} t_3 \qquad .$$

The next diagram of Fig.1.3 contains a loop (as shown in Fig.1.6) In this case,

---

[3]In the vicinity of the pole ($q^0 = M$, $\mid \vec{q} \mid$ small), $q^0 - E \sim \vec{q}^2/(2M)$, while $p^0 + E$ gives a much larger value of about $2M$.
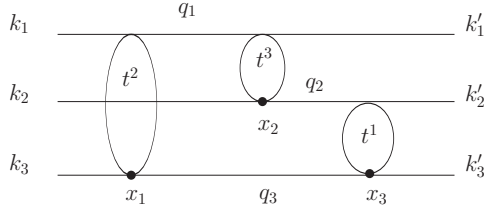
Figure 1.6: *Diagram with three successive interactions for the T^1 partition.*

$$< \vec{k}'_1, \vec{k}'_2, \vec{k}'_3 \mid S_3^{(1)} \mid \vec{k}_1, \vec{k}_2, \vec{k}_3 > = \int d^4 x_3 \int d^4 x_2$$

$$\times \int d^4 x_1 \prod_{l=1}^{3} \frac{1}{\sqrt{2\omega_l}} \prod_{k=1}^{3} \frac{1}{\sqrt{2\omega'_k}} \sqrt{2m_3} \sqrt{2m'_3} \frac{1}{V^3}$$

$$\times e^{i(k'_2 + k'_3)x_3}(-it_1) \int \frac{d^4 q_2}{(2\pi)^4} i \frac{e^{iq_2(x_2 - x_3)}}{(q_2)^2 - \tilde{m}_2^2 + i\epsilon}$$

$$\times e^{ik'_1 x_2}(-it_3)e^{-ik_2 x_2} \int \frac{d^4 q_3}{(2\pi)^4} i \frac{(\slashed{q}_3 + \tilde{m}_3)}{(q_3)^2 - \tilde{m}_3^2 + i\epsilon}$$

$$\times e^{iq_3(x_1 - x_3)} \int \frac{d^4 q_1}{(2\pi)^4} i \frac{e^{iq_1(x_1 - x_2)}}{(q_1)^2 - \tilde{m}_1^2 + i\epsilon}$$

$$\times (-it_2)e^{-i(k_1 + k_3)x_1} \tag{1.29}$$

where $\tilde{m}_i$ are the masses of the particles in the intermediate

states. Integrating in d^4x_i

$$
< \vec{k}_1', \vec{k}_2', \vec{k}_3' \mid S_3^{(1)} \mid \vec{k}_1, \vec{k}_2, \vec{k}_3 >= \frac{1}{V^3} \prod_{l=1}^{3} \frac{1}{\sqrt{2\omega_l}} \prod_{k=1}^{3} \frac{1}{\sqrt{2\omega_k'}}
$$

$$
\times \sqrt{2m_3}\sqrt{2m_3'} \int d^4q_1 \int d^4q_2 \int d^4q_3 \delta(q_2^0 + q_3^0 - k_2^{0'} - k_3^{0'})
$$

$$
\times \delta(k_2^0 + q_1^0 - q_2^0 - k_1^{0'})\delta(k_1^0 + k_3^0 - q_3^0 - q_1^0)
$$

$$
\times \delta(\vec{q}_2 + \vec{q}_3 - \vec{k}_2' - \vec{k}_3')\delta(\vec{k}_2 + \vec{q}_1 - \vec{q}_2 - \vec{k}_1')
$$

$$
\times \delta(\vec{k}_1 + \vec{k}_3 - \vec{q}_3 - \vec{q}_1)t_1 \frac{1}{(q_2)^2 - \tilde{m}_2^2 + i\epsilon}
$$

$$
\times t_3 \frac{\slashed{q}_3 + \tilde{m}_3}{(q_3)^2 - \tilde{m}_3^2 + i\epsilon} \frac{1}{(q_1)^2 - \tilde{m}_1^2 + i\epsilon} t_2. \tag{1.30}
$$

Solving the $\delta's$ functions and neglecting the negative energy part of the propagators we get

$$
< \vec{k}_1', \vec{k}_2', \vec{k}_3' \mid S_3^{(1)} \mid \vec{k}_1, \vec{k}_2, \vec{k}_3 >= \frac{1}{V^3} \prod_{l=1}^{3} \frac{1}{\sqrt{2\omega_l}}
$$

$$
\times \prod_{k=1}^{3} \frac{1}{\sqrt{2\omega_k'}} \sqrt{2m_3}\sqrt{2m_3'} \delta^4(k-k') \int d^3q_3 \int dq_3^0
$$

$$
\times t_1 \frac{1}{2\tilde{E}_2} \frac{1}{k_2^{0'} + k_3^{0'} - q_3^0 - \tilde{E}_2(\vec{k}_2' + \vec{k}_3' - \vec{q}_3) + i\epsilon}
$$

$$
\times t_3 \frac{2\tilde{m}_3}{2\tilde{E}_3} \frac{1}{q_3^0 - \tilde{E}_3(\vec{q}_3) + i\epsilon} \frac{1}{2\tilde{E}_1}
$$

$$
\times \frac{1}{k_1^0 + k_3^0 - q_3^0 - \tilde{E}_1(\vec{k}_1 + \vec{k}_3 - \vec{q}_3) + i\epsilon} t_2.
$$

$$
\tag{1.31}
$$

The two-body t-matrices depend on the total energy of the interacting pair, i.e., on its invariant mass. Therefore, $t_1 = t_1(s_{23})$, $t_2 = t_2(s_{31})$ and $t_3 = t_3(s_{12})$, hence, for the diagram in Fig.1.6, $s_{23} = (k_2' + k_3')^2$, $s_{31} = (k_1 + k_3)^2$ and $s_{12} = (k - q_3)^2$, with k being the total four-momentum. This implies that t_1 and t_2 can be taken out of the integral (1.31), but not t^3, which

depends on the loop variable q_3. Using energy conservation $E = k_1^0 + k_2^0 + k_3^0 = k_1^{0'} + k_2^{0'} + k_3^{0'}$ the previous equation can be written as

$$
< \vec{k}_1', \vec{k}_2', \vec{k}_3' \mid S_3^{(1)} \mid \vec{k}_1, \vec{k}_2, \vec{k}_3 > = \frac{1}{V^3} \prod_{l=1}^{3} \frac{1}{\sqrt{2\omega_l}} \prod_{k=1}^{3} \frac{1}{\sqrt{2\omega_k'}}
$$

$$
\times \sqrt{2m_3} \sqrt{2m_3'} \delta^4(k - k') t_1 \left[\int d^3 q_3 \int dq_3^0 \frac{1}{2\tilde{E}_2} \right.
$$

$$
\times \frac{1}{E - E_1'(\vec{k}_1') - \tilde{E}_2(\vec{k}_2' + \vec{k}_3' - \vec{q}_3) - q_3^0 + i\epsilon}
$$

$$
\times t_3 \frac{2\tilde{m}_3}{2\tilde{E}_3} \frac{1}{q_3^0 - \tilde{E}_3(\vec{q}_3) + i\epsilon} \frac{1}{2\tilde{E}_1}
$$

$$
\left. \times \frac{1}{E - \tilde{E}_1(\vec{k}_1 + \vec{k}_3 - \vec{q}_3) - E_2(\vec{k}_2) - q_3^0 + i\epsilon} \right] t_2
$$

$$(1.32)$$

where we have used that $k_1^{0'} = E_1(\vec{k}_1')$ and $k_2^0 = E_2(\vec{k}_2)$. To make the integration in dq_3^0 it is necessary to know the pole position of the t-matrix which is in the integrand. Consider the following diagram
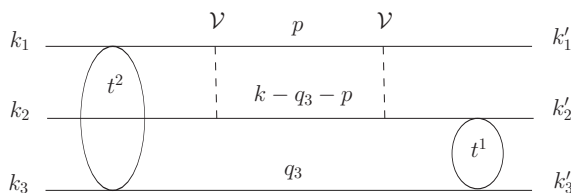

Figure 1.7: *Pole contribution from the two-body t-matrix.*

where we have split the t^3-matrix in terms of potential $\mathcal{V}$.

Using Feynman rules, the contribution to the t^3-matrix is

$$\int \frac{d^4p}{(2\pi)^4} \mathcal{V}[(k-q_3)^2] \frac{1}{2E(\vec{p})} \frac{1}{p^0 - E(\vec{p}) + i\epsilon} \frac{1}{2E(\vec{q}_3 + \vec{p})}$$

$$\times \frac{1}{k^0 - q_3^0 - p^0 - E(\vec{q}_3 + \vec{p}) + i\epsilon} \mathcal{V}[(k-q_3)^2] \qquad (1.33)$$

where there are two poles $(p^0)_1 = E(\vec{p}) - i\epsilon$ and $(p^0)_2 = k^0 - q_3^0 - E(\vec{q}_3 + \vec{p}) + i\epsilon$. Using Cauchy's theorem to evaluate the dp^0 integration in Eq.(1.33) we have

$$\int \frac{d^3p}{(2\pi)^3} \mathcal{V}[(k-q_3)^2] \frac{1}{2E(\vec{p})} \frac{1}{2E(\vec{q}_3 + \vec{p})}$$

$$\times \frac{1}{k^0 - q_3^0 - E(\vec{p}) - E(\vec{q}_3 + \vec{p}) + i\epsilon} \mathcal{V}[(k-q_3)^2]. \qquad (1.34)$$

And the pole in Eq.(1.34) for the variable of the loop in Eq.(1.32), q_3^0, is in the upper plane. Closing the contour of integration clockwise in the lower half plane (Fig.1.8) while applying the Cauchy's theorem to calculate the integral in Eq.(1.32) is a suitable choice, because in this way we avoid complications due to the presence of multiple poles in the upper half plane.

In this way,

$$< \vec{k}_1', \vec{k}_2', \vec{k}_3' \mid S_3^{(1)} \mid \vec{k}_1, \vec{k}_2, \vec{k}_3 >= -i\frac{(2\pi)^4}{V^3} \delta^4(k - k')$$

$$\times \prod_{l=1}^{3} \frac{1}{\sqrt{2\omega_l}} \prod_{k=1}^{3} \frac{1}{\sqrt{2\omega_k'}} \sqrt{2m_3} \sqrt{2m_3'} \int \frac{d^3q_3}{(2\pi)^3} \frac{1}{2\tilde{E}_1} \frac{1}{2\tilde{E}_2}$$

$$\times \frac{\tilde{m}_3}{\tilde{E}_3} t_1 \frac{1}{E - E_1'(\vec{k}_1') - \tilde{E}_2(\vec{k}_2' + \vec{k}_3' - \vec{q}_3) - \tilde{E}_3(\vec{q}_3) + i\epsilon}$$

$$\times t_3 \frac{1}{E - \tilde{E}_1(\vec{k}_1 + \vec{k}_3 - \vec{q}_3) - E_2(\vec{k}_2) - \tilde{E}_3(\vec{q}_3) + i\epsilon} t_2 \qquad (1.35)$$

with

$$t_3 = t_3[(k - q_3)^2 \mid_{q_3^0 = \tilde{E}_3(\vec{q}_3)}]. \qquad (1.36)$$
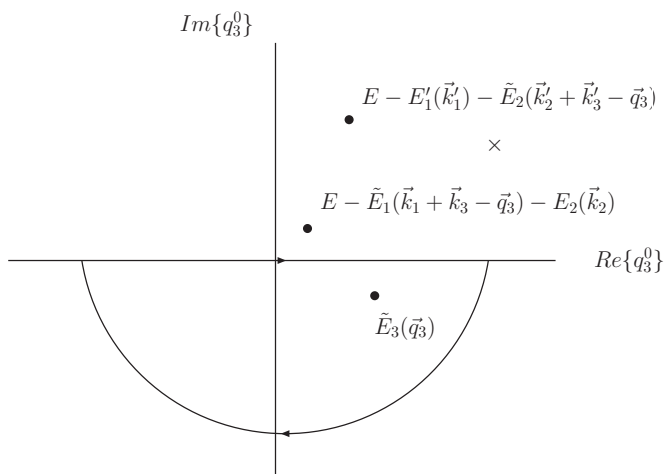
Figure 1.8: *Argand diagram.* ($\times$) *indicates the position of the pole of the t^3-matrix.*

Similarly, for diagrams with four, five or more interactions the $S_4^{(1)}$, $S_5^{(1)}$, etc., contribution to the $S^{(1)}$-matrix can be calculated to get

$$S^{(1)} = S_1^{(1)} + S_2^{(1)} + S_3^{(1)} + \cdots \tag{1.37}$$

Using the relation between the S and the T matrices

$$< \vec{k}_1', \vec{k}_2', \vec{k}_3' \mid S^{(1)} \mid \vec{k}_1, \vec{k}_2, \vec{k}_3 > = \delta_{\vec{k}_1,\vec{k}_1'} \delta_{\vec{k}_2,\vec{k}_2'} \delta_{\vec{k}_3,\vec{k}_3'}$$
$$- N < \vec{k}_1', \vec{k}_2', \vec{k}_3' \mid T^1 \mid \vec{k}_1, \vec{k}_2, \vec{k}_3 >$$

with

$$N = i \frac{(2\pi)^4}{V^3} \delta^4(k - k') \prod_{l=1}^{3} \frac{1}{\sqrt{2\omega_l}} \prod_{k=1}^{3} \frac{1}{\sqrt{2\omega_k'}} \sqrt{2m_3} \sqrt{2m_3'} \tag{1.38}$$

we obtain the three-body T^1 matrix which sums all those diagrams contributing to the three-body system where the last interaction is between particles 2 and 3.

$$T^1 = t^1 + t^1 G[t^3 + t^3 G t^1 + t^3 G t^2 \cdots]$$
$$+ t^1 G[t^2 + t^2 G t^1 + t^2 G t^3 + \cdots] \tag{1.39}$$

where G is the Green-function

$$
G = \begin{cases} \dfrac{1}{2E}\dfrac{1}{E-H} & \text{meson-meson interaction} \\[3mm] \dfrac{M}{E}\dfrac{1}{E-H} & \text{meson-baryon interaction} \end{cases} \tag{1.40}
$$

The factors $1/2E$ and M/E have their origin in the relativistic kinematics. In the same way, we can get the equations for the sum of the contribution of all those diagrams where the last interaction is between particles 1 and 3, and between particles 1 and 2

$$
\begin{aligned}
T^2 &= t^2 + t^2 G[t^1 + t^1 G t^2 + t^1 G t^3 + \cdots] \\
&\quad + t^2 G[t^3 + t^3 G t^1 + t^3 G t^2 + \cdots] \\
T^3 &= t^3 + t^3 G[t^1 + t^1 G t^2 + t^1 G t^3 + \cdots] \\
&\quad + t^3 G[t^2 + t^2 G t^1 + t^2 G t^3 + \cdots].
\end{aligned}
$$

The series T^1, T^2 and T^3 can be rewritten to get the Faddeev equations

$$
\begin{aligned}
T^1 &= t^1 + t^1 G\Big[T^2 + T^3\Big] \\
T^2 &= t^2 + t^2 G\Big[T^1 + T^3\Big] \\
T^3 &= t^3 + t^3 G\Big[T^1 + T^2\Big].
\end{aligned} \tag{1.41}
$$

1.3　Faddeev equations within Unitary Chiral Dynamics

The Faddeev equations, like the Bethe-Salpeter equation, are integral equations. However, we have seen in section (1.1) that in the Bethe-Salpeter equation the off-shell part of the potentials in the unitary chiral approach is such that its contribution can be reabsorbed by making a suitable renormalization of the coupling constants in the Lagrangians. This allows to extract the two-body potentials out of the integral and, therefore, one

only needs the on-shell two-body t-matrices to solve the Bethe-Salpeter equation, which gets simplified to an algebraic one. The question now is if there is a possibility to develop a similar technique for the Faddeev equations by using unitary chiral dynamics.

In this section, we discuss the origins of three-body forces: (a) Due to the off-shell contribution of the two-body t-matrices; (b) From the Chiral Lagrangians. We show that these three-body forces cancel in the $SU(3)$ limit leading to a reformulation of the Faddeev equations with a formalism that makes solving them technically faster.

1.3.1 Three-body forces

As suggested by Faddeev himself and discussed by others, e.g., in [82], in order to study the genuine three-body dynamics (for instance, poles of the three-body T-matrix) the terms with disconnected diagrams, i.e., the ones which contain only one t-matrix (obviously, with an associated delta function) can be neglected. Let us then consider the lowest order connected diagrams of the Faddeev equations Eq. (1.41) which are second order in t, i.e., the terms which contain two t-matrices. There are six terms of this kind as shown in the diagrams of Fig. 1.9
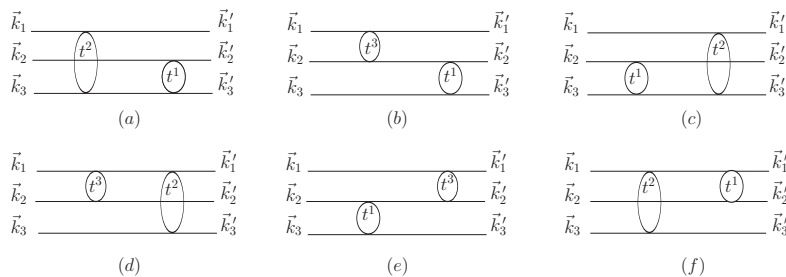

Figure 1.9: *All the diagrams at second order in t which give rise to a three-body force.*

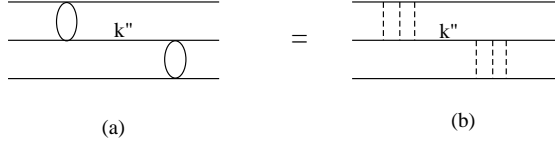Mathematically, the contribution of these diagrams can be ex-

(a)   =   (b)

Figure 1.10: *A diagrammatic representation of the $t^1 g^{13} t^3$ term. The blob in (a) represents a t-matrix which can be expressed mathematically as $\mathcal{V} + \mathcal{V}\tilde{g}\mathcal{V} + \mathcal{V}\tilde{g}\mathcal{V}\tilde{g}\mathcal{V} + \mathcal{V}\tilde{g}\mathcal{V}\tilde{g}\mathcal{V}\tilde{g}\mathcal{V} + ...$ And (b) shows the term $(\mathcal{V}^1\tilde{g}^1\mathcal{V}^1\tilde{g}^1\mathcal{V}^1)g^{13}(\mathcal{V}^3\tilde{g}^3\mathcal{V}^3\tilde{g}^3\mathcal{V}^3)$ of Eq. (1.42).*

pressed as $t^i g^{ij} t^j$, and which can be expanded in terms of the potentials as

$$
\begin{aligned}
t^i g^{ij} t^j &= \left[\mathcal{V}^i + \mathcal{V}^i\tilde{g}^i\mathcal{V}^i + \mathcal{V}^i\tilde{g}^i\mathcal{V}^i\tilde{g}^i\mathcal{V}^i + \cdots\right] g^{ij} \\
&\quad \times \left[\mathcal{V}^j + \mathcal{V}^j\tilde{g}^j\mathcal{V}^j + \mathcal{V}^j\tilde{g}^j\mathcal{V}^j\tilde{g}^j\mathcal{V}^j + \cdots\right] \\
&= \mathcal{V}^i g^{ij}\mathcal{V}^j + \mathcal{V}^i\tilde{g}^i\mathcal{V}^i g^{ij}\mathcal{V}^j + \mathcal{V}^i g^{ij}\mathcal{V}^j\tilde{g}^j\mathcal{V}^j + \cdots \quad (1.42)
\end{aligned}
$$

For example, a term of $t^1 g^{13} t^3$ expanded as in Eq. (1.42) is shown in Fig. 1.10.

All the terms of the kind $t^i g^{ij} t^j$ in our formalism give rise to a three-body force. This can be easily understood if we pay attention to the form of the potentials obtained from the chiral Lagrangians. The potentials in chiral dynamics can be split into an on-shell part which depends on the center of mass energy of the interacting particles and an off-shell part proportional to $k''^2 - m^2$ for each of the meson legs, in case of meson-meson interaction (where k'' is the four vector of the off-shell particle and m is its mass). In case of the meson-baryon interaction, the off-shell part of the potential behaves as $p^0 - k^0$, where $p^0(k^0)$ is the energy corresponding to the off-shell (on-shell) momentum. Due to this behavior, the off-shell part of the potential cancels a propagator in the loops, giving rise effectively to a three body force, for example, the one shown in Fig. 1.11 corresponding to the $t^1 g^{13} t^3$ term shown in Fig. 1.10. In both cases we show that these three-body forces together with the three-body contact term coming from the chiral Lagrangian is null.

Figure 1.11: *An induced effective three-body force generated by the cancellation of the off-shell part of the potential and a propagator as explained in the text.*

Similar effective three-body forces arise from other terms too. We shall now write the contributions for the first terms of all six $t^i g^{ij} t^j$ terms (Eq. (1.42)) including the off-shell parts of the t-matrices, first for a system of two pseudoscalar mesons and a baryon from the octet and later for a system of two pseudoscalar mesons and one vector meson.

1.3.1.1 Three-body forces for two pseudoscalars and one baryon system

Let us take the $\pi^+\pi^- n$ channel as an example for this case and evaluate the total effect of the three-body forces.

We label the initial (final) four-momentum of the π^+ as p (p'), that of the π^- as k (k') and that of the neutron as q (q') as shown in Fig. 4. We assign a four vector k'' to the intermediate states (see Fig. 1.10).
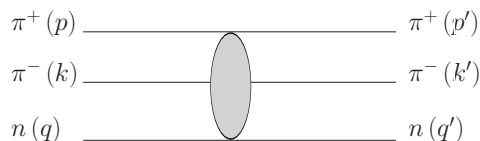
Figure 1.12: *Assigning four momenta to the $\pi^+\pi^- n$ system.*

The potentials calculated from the chiral Lagrangians Eqs. (1.1, 1.2) for the three possible two-body interactions are

$$\mathcal{V}_{\pi^+\pi^- \to \pi^+\pi^-} = -\frac{1}{6f^2}\left[3s_{\pi\pi} - \sum_i (p_i^2 - m_i^2)\right], \qquad (1.43)$$

$$\mathcal{V}_{\pi^- n \to \pi^- n} = -\frac{1}{4f^2}(k_\pi^0 + k_\pi'^{\,0}), \qquad (1.44)$$

$$\mathcal{V}_{\pi^+ n \to \pi^+ n} = -\mathcal{V}_{\pi^- n \to \pi^- n}, \qquad (1.45)$$

where $s_{\pi\pi}$ is the invariant mass of the $\pi - \pi$ subsystem, f is the pion decay constant and k_π^0 ($k_\pi'^{\,0}$) is the energy of the pion before (after) the πN interaction.

In this way, the contribution of the first term of Eq. (1.42) for $i = 1$ and $j = 2$, which corresponds to the first diagram in Fig. 1.9, is given by

$$T_a = -\frac{1}{16f^4}(k^0 + k'^{\,0})\frac{m_n}{E_n}$$
$$\times \frac{1}{k'^{\,0} + q'^{\,0} - k^0 - E_n(\vec{p}\,' + \vec{k}) + i\epsilon}$$
$$\times (p^0 + p'^{\,0}) \equiv T_a^{on}. \qquad (1.46)$$

m_n in Eq.(1.46) is the neutron mass and the superscript "on" on T_a denotes that there is no off-shell dependence in this equation.

For the diagram (b) of Fig. 1.9

$$T_b = \frac{1}{24f^4}\left[2k'^{\,0} + (k''^{\,0} - k'^{\,0})\right]\frac{1}{k''^2 - m_\pi^2}$$
$$\times \left[3(p+k)^2 - (k''^2 - m_\pi^2)\right]$$
$$\equiv T_b^{on} + T_b^{off} \qquad (1.47)$$

with

$$T_b^{on} = \frac{1}{4f^4}k'^{\,0}\frac{1}{(p+k-p')^2 - m_\pi^2}(p+k)^2 \qquad (1.48)$$

$$T_b^{off} = \frac{1}{24f^4}\left[-k'^{\,0} - p^0 - k^0 + p'^{\,0}\right.$$
$$\left. + 3(p+k)^2\frac{k''^0 - k'^{\,0}}{k''^2 - m_\pi^2}\right] \qquad (1.49)$$

representing the on-shell and off-shell contributions to T_b. In Eq. (1.48) and in the first term of Eq. (1.49), k'' has been

replaced by $p + k - p'$ using the energy-momentum conservation law from the initial state. For the second term of Eq. (1.49) we apply energy-momentum conservation from the final state

$$k''^2 = (k' + q' - q)^2 \quad . \tag{1.50}$$

Defining $\Delta q = q' - q$, Eq. (1.50) becomes

$$k''^2 = m_\pi^2 + (\Delta q)^2 + 2k' \cdot \Delta q$$

and, hence

$$\frac{k''^0 - k'^0}{k''^2 - m_\pi^2} = \frac{(\Delta q)^0}{(\Delta q)^2 + 2k' \cdot \Delta q} \quad . \tag{1.51}$$

Therefore,

$$T_b^{off} = \frac{1}{24 f^4} \left[-k'^0 - p^0 - k^0 + p'^0 \right.$$
$$\left. + 3(p + k)^2 \frac{(\Delta q)^0}{(\Delta q)^2 + 2k' \cdot \Delta q} \right]. \tag{1.52}$$

The contribution of the diagram (c) of Fig. 1.9 is

$$T_c = -\frac{1}{16 f^4} (p^0 + p'^0) \frac{m_n}{E_n} \frac{1}{k^0 + q^0 - k'^0 - E_n(\vec{p} + \vec{k}')}$$
$$\times (k^0 + k'^0)$$
$$\equiv T_c^{on}. \tag{1.53}$$

Similarly,

$$T_d = -\frac{1}{24 f^4} (2p'^0 + p''^0 - p'^0) \frac{1}{p''^2 - m_\pi^2}$$
$$\times [3(p + k)^2 - (p''^2 - m_\pi^2)]$$
$$\equiv T_d^{on} + T_d^{off} \tag{1.54}$$

with

$$T_d^{on} = -\frac{1}{4f^4}p'^0\frac{1}{(p+k-k')^2 - m_\pi^2}(p+k)^2 \qquad (1.55)$$

$$T_d^{off} = -\frac{1}{24f^4}\Bigg[-p'^0 - p^0 - k^0 + k'^0$$

$$+ 3(p+k)^2\frac{p''^0 - p'^0}{p''^2 - m_\pi^2}\Bigg] \qquad (1.56)$$

Analogous to Eq. (1.51), we write

$$\frac{p''^0 - p'^0}{p''^2 - m_\pi^2} = \frac{(\Delta q)^0}{(\Delta q)^2 + 2p'\cdot\Delta q} \qquad (1.57)$$

which gives

$$T_d^{off} = -\frac{1}{24f^4}\Bigg[-p'^0 - p^0 - k^0 + k'^0$$

$$+ 3(p+k)^2\frac{(\Delta q)^0}{(\Delta q)^2 + 2p'\cdot\Delta q}\Bigg]. \qquad (1.58)$$

For the next diagram, we have

$$T_e = \frac{1}{24f^4}[3(p'+k')^2 - (k''^2 - m_\pi^2)]$$

$$\times \frac{1}{k''^2 - m_\pi^2}(2k^0 + k''^0 - k^0)$$

$$\equiv T_e^{on} + T_e^{off} \qquad (1.59)$$

where

$$T_e^{on} = \frac{1}{4f^4}(p'+k')^2\frac{1}{(p'+k'-p)^2 - m_\pi^2}k^0 \qquad (1.60)$$

$$T_e^{off} = \frac{1}{24f^4}\Bigg[-k^0 - p'^0 - k'^0 + p^0$$

$$+ 3(p'+k')^2\frac{k''^0 - k^0}{k''^2 - m_\pi^2}\Bigg] \qquad (1.61)$$

In this case $k'' = k - \Delta q$ and therefore

$$\frac{k''^0 - k^0}{k''^2 - m_\pi^2} = -\frac{(\Delta q)^0}{(\Delta q)^2 - 2k \cdot \Delta q} \tag{1.62}$$

leading to

$$T_e^{off} = \frac{1}{24f^4}\left[-k^0 - p'^0 - k'^0 + p^0 \right.$$

$$\left. - 3(p' + k')^2 \frac{(\Delta q)^0}{(\Delta q)^2 - 2k \cdot \Delta q} \right]. \tag{1.63}$$

For the last diagram of Fig. 1.9 we have

$$T_f = -\frac{1}{24f^4}[3(p' + k')^2 - (p''^2 - m_\pi^2)]$$

$$\times \frac{1}{p''^2 - m_\pi^2}(2p^0 + p''^0 - p^0) \tag{1.64}$$

$$\equiv T_f^{on} + T_f^{off}$$

where

$$T_f^{on} = -\frac{1}{4f^4}(p' + k')^2\frac{1}{(p' + k' - k)^2 - m_\pi^2}p^0 \tag{1.65}$$

$$T_f^{off} = -\frac{1}{24f^4}\left[-p^0 - p'^0 - k'^0 + k^0 \right.$$

$$\left. + 3(p' + k')^2\frac{p''^0 - p^0}{p''^2 - m_\pi^2} \right] \tag{1.66}$$

Following the same method as in the previous equations

$$\frac{p''^0 - p^0}{p''^2 - m_\pi^2} = -\frac{(\Delta q)^0}{(\Delta q)^2 - 2p \cdot \Delta q}. \tag{1.67}$$

then

$$T_f^{off} = -\frac{1}{24f^4}\left[-p^0 - p'^0 - k'^0 + k^0 \right.$$

$$\left. - 3(p' + k')^2\frac{(\Delta q)^0}{(\Delta q)^2 - 2p \cdot \Delta q} \right]. \tag{1.68}$$
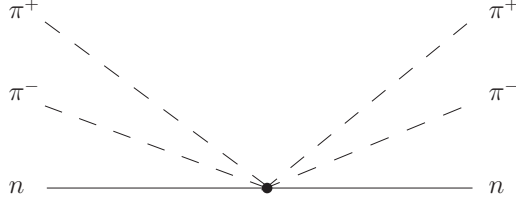
Figure 1.13: *Source of three-body force from the chiral Lagrangians.*

On the other hand, genuine three-body forces also originate directly from the chiral Lagrangian , where we can find a contact term as the one shown in Fig. (1.13) (such diagrams were considered for example in [83]).

In order to find the contribution of the diagram shown in Fig. 1.13 we consider the interaction Lagrangian between mesons and baryon at lowest order in momentum, which is

$$\mathcal{L} = i\langle \bar{B}\gamma^\mu [\Gamma_\mu, B]\rangle \tag{1.69}$$

where

$$\Gamma_\mu = \frac{1}{2}(u^\dagger \partial_\mu u + u \partial_\mu u^\dagger), \quad u^2 = e^{i\sqrt{2}\Phi/f} \tag{1.70}$$

and ϕ, B are same as those defined in Eqs. (1.3, 1.4). If we expand Γ_μ up to the terms which contain four meson fields, we get

$$\Gamma_\mu = \frac{1}{32f^4}\left[\frac{1}{3}\partial_\mu \Phi\Phi^3 - \Phi\partial_\mu\Phi\Phi^2 + \Phi^2\partial_\mu\Phi\Phi - \frac{1}{3}\Phi^3\partial_\mu\Phi\right] \tag{1.71}$$

For the case under consideration, i.e., $\pi^+\pi^-n$, using Γ_μ from Eq. (1.71), the Eq. (1.69) becomes

$$\mathcal{L} = \frac{i}{32f^4}\bar{n}\left[\frac{1}{3}\partial\!\!\!/\pi^-\pi^+\pi^-\pi^+ - \pi^-\partial\!\!\!/\pi^+\pi^-\pi^+\right.$$

$$\left. + \pi^-\pi^+\partial\!\!\!/\pi^-\pi^+ - \frac{1}{3}\pi^-\pi^+\pi^-\partial\!\!\!/\pi^+\right]n. \tag{1.72}$$

In this way, the contribution of the diagram in Fig. 1.13 is

$$T_{3b} = \frac{1}{24f^4}\bar{u}_r(\vec{q}\,')(2\not{p} - 2\not{k}' - 2\not{k} + 2\not{p}')u_r(\vec{q}). \qquad (1.73)$$

Since we are interested in the low energy region, only the γ^0 component of Eq. (1.73) is relevant, then

$$T_{3b} = \frac{1}{24f^4}(2p^0 - 2k'^0 - 2k^0 + 2p'^0). \qquad (1.74)$$

Adding this to the off-shell contributions from the Faddeev equations at second order in t-matrices, we get

$$\sum_{i=a}^{e} T_i^{off} + T_{3b} = \frac{1}{24f^4}\left[-4k^0 + 4p'^0 - 4k'^0 + 4p^0 \right.$$

$$+ 3(p+k)^2(\Delta q)^0 \left\{ \frac{1}{(\Delta q)^2 + 2k'\cdot\Delta q} \right.$$

$$\left. - \frac{1}{(\Delta q)^2 + 2p'\cdot\Delta q} \right\} + 3(p'+k')^2(\Delta q)^0$$

$$\left. \times \left\{ \frac{1}{(\Delta q)^2 - 2p\cdot\Delta q} - \frac{1}{(\Delta q)^2 - 2k\cdot\Delta q} \right\} \right] \qquad (1.75)$$

If we consider small momentum transfer for the baryon, i.e., $|\Delta\vec{q}| << 1$, Eq. (1.75) can be expressed as

$$\sum_{i=1}^{6} T_i^{off} + T_{3b} = \frac{1}{24f^4}\left[-4k^0 + 4p'^0 - 4k'^0 + 4p^0 \right.$$

$$+ 3(p+k)^2 \left\{ \frac{1}{(\Delta q)^0 + 2k'^0} - \frac{1}{(\Delta q)^0 + 2p'^0} \right\}$$

$$\left. + 3(p'+k')^2 \left\{ \frac{1}{(\Delta q)^0 - 2p^0} - \frac{1}{(\Delta q)^0 - 2k^0} \right\} \right] \qquad (1.76)$$

And there is a cancellation of the terms in the $SU(2)$ limit, assuming equal average energies for the pion. Furthermore, if

the propagators in the Eq. (1.75) are projected over s-wave, as we do in our study, the curly brackets become

$$\left\{ \frac{1}{2 \mid \vec{k}' \mid \mid \vec{\Delta q} \mid} ln\left(\frac{(\Delta q)^2 + 2k'^0(\Delta q)^0 + 2 \mid \vec{k}' \mid \mid \vec{\Delta q} \mid}{(\Delta q)^2 + 2k'^0(\Delta q)^0 - 2 \mid \vec{k}' \mid \mid \vec{\Delta q} \mid} \right) \right.$$
$$\left. - \frac{1}{2 \mid \vec{p}' \mid \mid \vec{\Delta q} \mid} ln\left(\frac{(\Delta q)^2 + 2p'^0(\Delta q)^0 + 2 \mid \vec{p}' \mid \mid \vec{\Delta q} \mid}{(\Delta q)^2 + 2p'^0(\Delta q)^0 - 2 \mid \vec{p}' \mid \mid \vec{\Delta q} \mid} \right) \right\}$$

and

$$\left\{ \frac{1}{2 \mid \vec{p} \mid \mid \vec{\Delta q} \mid} ln\left(\frac{(\Delta q)^2 - 2p^0(\Delta q)^0 + 2 \mid \vec{p} \mid \mid \vec{\Delta q} \mid}{(\Delta q)^2 - 2p^0(\Delta q)^0 - 2 \mid \vec{p} \mid \mid \vec{\Delta q} \mid} \right) \right.$$
$$\left. - \frac{1}{2 \mid \vec{k} \mid \mid \vec{\Delta q} \mid} ln\left(\frac{(\Delta q)^2 - 2k^0(\Delta q)^0 + 2 \mid \vec{k} \mid \mid \vec{\Delta q} \mid}{(\Delta q)^2 - 2k^0(\Delta q)^0 - 2 \mid \vec{k} \mid \mid \vec{\Delta q} \mid} \right) \right\}$$

respectively, and the cancellation is exact.

1.3.1.2 Three-body forces for two pseudoscalars and one vector meson system

Analogously to the cancellation shown in the previous section, here we are going to show that a similar cancellation also occurs in the case of one vector and two pseudoscalar mesons. We consider, as an example, the channel $\rho^+\pi^+\pi^-$ and, in order to simplify the formulation, we take no other coupled channels of the system into account.

The interaction of a vector and any number of pseudoscalar mesons is described by the chiral Lagrangian [79]

$$\mathcal{L} = -Tr\{[V^\mu, \partial^\nu V_\mu]\Gamma_\nu\} \qquad (1.77)$$

where

$$
V_\mu = \begin{pmatrix} \frac{1}{\sqrt{2}}\rho^0 + \frac{1}{\sqrt{2}}w & \rho^+ & K^{*+} \\ \rho^- & -\frac{1}{\sqrt{2}}\rho^0 + \frac{1}{\sqrt{2}}w & K^{*0} \\ K^{*-} & \bar{K}^{*0} & \phi \end{pmatrix}_\mu
$$

$$
\Gamma_\nu = \frac{1}{2}(u^\dagger \partial_\nu u + u \partial_\nu u^\dagger)
$$

$$
u^2 = e^{i\frac{\sqrt{2}}{f}P}
$$

$$
P = \begin{pmatrix} \frac{1}{\sqrt{2}}\pi^0 + \frac{1}{\sqrt{2}}\eta_8 & \pi^+ & K^+ \\ \pi^- & -\frac{1}{\sqrt{2}}\pi^0 + \frac{1}{\sqrt{6}}\eta_8 & K^0 \\ K^- & \bar{K}^0 & -\frac{2}{\sqrt{6}}\eta_8 \end{pmatrix}
$$

If we expand u in series up to terms containing two pseudoscalar fields P, we obtain

$$
\Gamma_\nu = \frac{1}{4f^2}[P, \partial_\nu P] \tag{1.78}
$$

and Eq. (1.77) becomes

$$
\mathcal{L}_{VP} = -\frac{1}{4f^2} Tr\{[V^\mu, \partial^\nu V_\mu][P, \partial_\nu P]\}. \tag{1.79}
$$

For the case under consideration, we need to calculate the $\rho^+\pi^+ \to \rho^+\pi^+$ and $\rho^+\pi^- \to \rho^+\pi^-$ amplitudes. In this case, Eq. (1.79) has the form

$$
\mathcal{L} = -\frac{1}{2f^2}\left(\partial^\mu \rho_\nu^- \rho^{+\nu} - \rho_\nu^- \partial^\mu \rho^{+\nu}\right)
$$
$$
\times \left(\partial_\mu \pi^- \pi^+ - \pi^- \partial_\mu \pi^+\right) \tag{1.80}
$$

leading to (see Fig. (1.14))

$$
\mathcal{V}_{\rho^+\pi^+ \to \rho^+\pi^+} = -\frac{1}{2f^2}(k_1 + k_1')(k_2 + k_2')(\epsilon \cdot \epsilon')
$$
$$
\mathcal{V}_{\rho^+\pi^- \to \rho^+\pi^-} = -\mathcal{V}_{\rho^+\pi^+ \to \rho^+\pi^+}. \tag{1.81}
$$
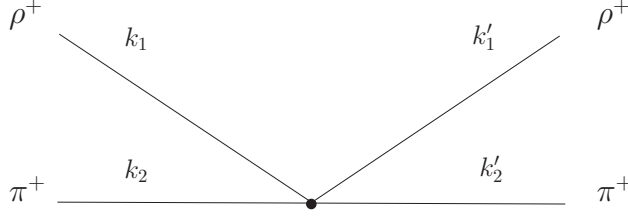
Figure 1.14: Lowest order diagram contributing to the $\rho^+\pi^+$ interaction.

The $\pi^+\pi^-$ amplitude, from Eq. (7.4), is

$$\mathcal{V}_{\pi^+\pi^- \to \pi^+\pi^-} = -\frac{1}{6f^2}\Big[3s_{\pi\pi} - \sum_i (k_i^2 - m_i^2)\Big], \qquad (1.82)$$

where k_i and m_i represent the momentum and mass, respectively, of the external particles for the $\pi^+\pi^-$ interaction.
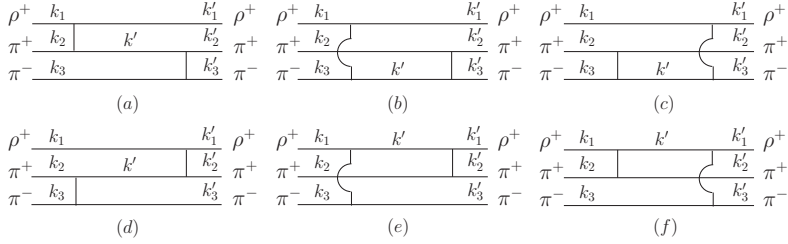
Figure 1.15: Diagrams in which the off-shell part of the t matrices lead to a three-body force.

In this way, the contribution of the first diagram in Fig. (1.15) is given by

$$
\begin{aligned}
T_a &= -\frac{1}{6f^2}\Big[3(k_2' + k_3')^2 - (k'^2 - m_\pi^2)\Big]\frac{1}{k'^2 - m_\pi{}^2} \\
&\quad \times \Big[-\frac{1}{2f^2}(k_1 + k_1')(2k_2 + k' - k_2)\Big](\epsilon \cdot \epsilon') \\
&= T_a^{on} + T_a^{off}, \qquad\qquad\qquad\qquad\qquad (1.83)
\end{aligned}
$$

with T_a^{on} (T_a^{off}) being the contribution which comes from the on-shell (off-shell) part of the t matrices:

$$
\begin{aligned}
T_a^{on} &= \frac{1}{2f^4}(k_2' + k_3')^2 \frac{1}{(k_1 + k_2 - k_1')^2 - m_\pi^2} \\
&\quad \times (k_1 + k_1')k_2(\epsilon \cdot \epsilon') \\
T_a^{off} &= \left[\frac{1}{4f^4}(k_2' + k_3')^2(k_1 + k_1') \left[\frac{k' - k_2}{k'^2 - m_\pi^2} \right]_{k'=k_1+k_2-k_1'} \right. \\
&\quad - \frac{1}{12f^4} \frac{k'^2 - m_\pi^2}{k'^2 - m_\pi^2}(k_1 + k_1') \\
&\quad \left. \times (k_2 + k')_{k'=k_1+k_2-k_1'} \right] (\epsilon \cdot \epsilon')
\end{aligned}
\tag{1.84}
$$

From the results obtained in the previous section for two meson-one baryon system, we expect that the contribution of the off-shell part for the different diagrams of Fig. (1.15), together with one of the vector-pseudoscalar-pseudoscalar contact terms of the chiral Lagrangian, vanishes in the limit of equal masses for the pseudoscalars and equal masses for the vectors. Following the algebra of the previous section for Eq. (1.84)

$$
\begin{aligned}
T_a^{off} &= \left[\frac{1}{4f^4}(k_2' + k_3')^2(k_1 + k_1') \frac{\Delta k_1}{(\Delta k_1)^2 + 2k_2\Delta k_1} \right. \\
&\quad \left. - \frac{1}{12f^4}(k_1 + k_1')(2k_2 + \Delta k_1) \right] (\epsilon \cdot \epsilon')
\end{aligned}
\tag{1.85}
$$

with $\Delta k_1 = k_1 - k_1'$. Using that

$$
(k_1 + k_1')\Delta k_1 = k_1^2 - {k_1'}^2 = m_1^2 - {m_1'}^2
\tag{1.86}
$$

is zero in the limit of equal masses, we have

$$
T_a^{off} = -\frac{1}{6f^4}(k_1 + k_1')k_2(\epsilon \cdot \epsilon')
\tag{1.87}
$$
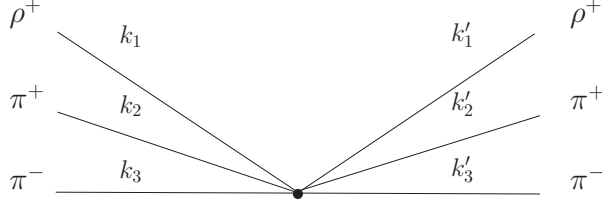
Figure 1.16: Contact term whose origin is in the chiral Lagrangian.

Analogously, for the rest of the diagrams in Fig. (1.15) we have

$$T_b^{off} = \frac{1}{6f^4}(k_1 + k_1')k_3(\epsilon \cdot \epsilon')$$

$$T_c^{off} = \frac{1}{6f^4}(k_1 + k_1')k_3'(\epsilon \cdot \epsilon')$$

$$T_d^{off} = -\frac{1}{6f^4}(k_1 + k_1')k_2'(\epsilon \cdot \epsilon')$$

$$T_e^{off} = 0$$

$$T_f^{off} = 0$$

Adding all these T^{off} we get

$$\sum_{i=a}^{i=f} T_i^{off} = \frac{1}{6f^4}(k_1 + k_1')(k_3' - k_2 + k_3 - k_2')(\epsilon \cdot \epsilon') \qquad (1.88)$$

In order to evaluate the vector-pseudoscalar-pseudoscalar (VPP) contact term, we have to expand Γ_ν up to terms with four pseudoscalar fields

$$\Gamma_\nu = \frac{1}{32f^4}\left[\frac{1}{3}\partial_\nu PP^3 - P\partial_\nu PP^2 + P^2\partial_\nu PP - \frac{1}{3}P^3\partial_\nu P\right] \quad (1.89)$$

and, therefore, using Eq. (1.77), the chiral Lagrangian for the VPP contact term for the $\rho^+\pi^+\pi^-$ interaction is (Fig. (1.16))

$$\mathcal{L}_{VPP} = -\frac{1}{12f^4}(\partial^\mu \rho_\nu^- \rho^{+\nu} - \rho_\nu^- \partial^\mu \rho^{+\nu})$$
$$\times (\pi^- \pi^- \pi^+ \partial_\mu \pi^+ - \pi^- \partial_\mu \pi^- \pi^+ \pi^+) \qquad (1.90)$$

which implies

$$T^{3b}_{\rho^+ \pi^+ \pi^-} = -\frac{1}{6f^4}(k_1 + k_1')(k_3' - k_2 + k_3 - k_2')(\epsilon \cdot \epsilon') \quad (1.91)$$

The sum of Eq. (1.88) and Eq. (1.91) results in

$$\sum_{i=a}^{f} T_i^{off} + T^{3b}_{\rho^+ \pi^+ \pi^-} = 0 \qquad (1.92)$$

The proof of the cancellation stated above has proceeded taking the potentials (tree level amplitudes) derived from the lowest order chiral Lagrangians. The extension of the proof made to the corresponding one using t-matrices is straight forward, since the t-matrices would be generated by further iterations of the tree level amplitudes in the Faddeev diagrams, as done in [2,17], where the off-shell part of the potential in these iterations is reabsorbed in constants of the on-shell potential. Hence the cancellations are guaranteed when iterations are done to obtain Faddeev diagrams in terms of t-matrices rather than potentials.

Thus, we have proved that the off-shell dependence of the t-matrices in the three-body diagrams is found to cancel exactly with the three-body forces generated from the chiral Lagrangian for 2 pseudoscalar meson + baryon (or vector meson) $\rightarrow$ 2 pseudoscalar meson + baryon (or vector meson) contact term in the SU(3) limit. If this limit is not considered, the total contribution of the off-shell part of the t-matrices is found to be less than 5% of the total on-shell contribution . Therefore, for a hadronic model as ours, it is enough to retain the on-shell parts of the t-matrices, which depend on the invariant mass of the interacting pair, and neglect the contribution from the off-shell part of the
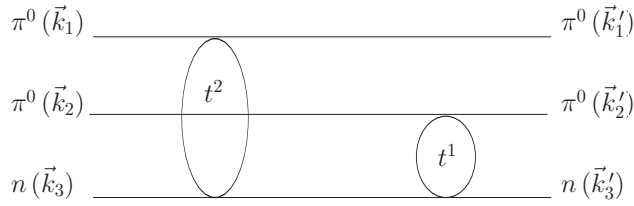
Figure 1.17: *An example of a simplest possible interaction amongst the three particles, $\pi^0\pi^0 n$. The labels $\vec{k}_i$ $(\vec{k}_i')$ on the particle lines denote the momenta corresponding to the initial (final) state. The meaning of the blob is shown in Fig. 1.18.*
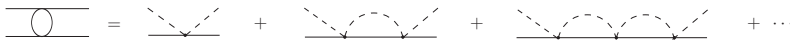
Figure 1.18: *The blob in the Fig. 1.17, which is a t-matrix.*

t-matrices together with the three-body forces present in the system.

In the next sections, having this idea in mind, we are going to start evaluating the contribution of the different diagrams involved in the three-body interaction.

1.3.2 Lowest order diagrams

Our aim is to calculate the three-body scattering matrix which includes all the possible "connected" diagrams between three particles. In order to develop the formalism, let us take the $\pi^0\pi^0 n$ system as an example. The simplest possible three-body connected diagram we can have is the one which contains two t-matrices, for example the one shown in Fig. 1.17 for the considered channel. This diagram can be expressed mathematically as (reading Fig. 1.17 from right to left as a convention)

$$t^1 g^{12} t^2 \tag{1.93}$$

where the superscript on t denotes the particle which is not interacting in the three-body system. Hence, t^1 is the t-matrix for the interaction of particles 2 and 3 and t^2 is that for particles 1 and 3. The discussion of the last section makes it clear that both t^1 and t^2 matrices in Eq. (1.93) are on-shell, meaning they depend on the invariant mass of the interacting pairs. These t-matrices are always obtained by solving the Bethe-Salpeter equation, Eq. (1.19), in the coupled channel approach with the potentials obtained from the Lagrangians given by Eqs. (1.1), (1.2).

For example, to obtain the $\pi^0 n \rightarrow \pi^0 n$ t-matrix for the diagram of Fig. 1.17, we would take πN, ηN, $K\Lambda$ and $K\Sigma$ as the coupled channels, which means Eq. (1.19) is solved with the potential,

$$
\mathcal{V} = \begin{pmatrix}
\mathcal{V}_{\pi^0 n \rightarrow \pi^0 n} & \mathcal{V}_{\pi^0 n \rightarrow \pi^- p} & \mathcal{V}_{\pi^0 n \rightarrow \eta n} & \cdots \\
\mathcal{V}_{\pi^- p \rightarrow \pi^0 n} & \mathcal{V}_{\pi^- p \rightarrow \pi^- p} & \mathcal{V}_{\pi^- p \rightarrow \eta n} & \cdots \\
\mathcal{V}_{\eta n \rightarrow \pi^0 n} & \mathcal{V}_{\eta n \rightarrow \pi^- p} & \mathcal{V}_{\eta n \rightarrow \eta n} & \cdots \\
\mathcal{V}_{K^+ \Sigma^- \rightarrow \pi^0 n} & \mathcal{V}_{K^+ \Sigma^- \rightarrow \pi^- p} & \mathcal{V}_{K^+ \Sigma^- \rightarrow \eta n} & \cdots \\
\mathcal{V}_{K^0 \Sigma^0 \rightarrow \pi^0 n} & \mathcal{V}_{K^0 \Sigma^0 \rightarrow \pi^- p} & \mathcal{V}_{K^0 \Sigma^0 \rightarrow \eta n} & \cdots \\
\mathcal{V}_{K^0 \Lambda \rightarrow \pi^0 n} & \mathcal{V}_{K^0 \Lambda \rightarrow \pi^- p} & \mathcal{V}_{K^0 \Lambda \rightarrow \eta n} & \cdots
\end{pmatrix}
$$

and the $t_{\pi^0 n \rightarrow \pi^0 n}$ element of the resulting matrix would be in Eq. (1.93) as t^2 and t^1. As shown in Fig. 1.9, there are six possible three-body diagrams involving two t-matrices. To calculate all these diagrams for the $\pi^0 \pi^0 n$ channel, we would require the $\pi\pi$ t-matrices also, which we would calculate by solving the Bethe-Salpeter equation with $\pi\pi$, $\pi\eta$ and $K\bar{K}$ as coupled channels (as done in [2,3]), with the potentials obtained from the chiral Lagrangian of Eq. (1.2).

The g^{12} in Eq. (1.93) is a three-body Green's function which can be written as

$$
g^{12} = \frac{M_3}{E_3(\vec{k}_1' + \vec{k}_2)}
$$
$$
\times \frac{1}{\sqrt{s} - E_1(\vec{k}_1') - E_2(\vec{k}_2) - E_3(\vec{k}_1' + \vec{k}_2) + i\epsilon} \quad (1.94)
$$
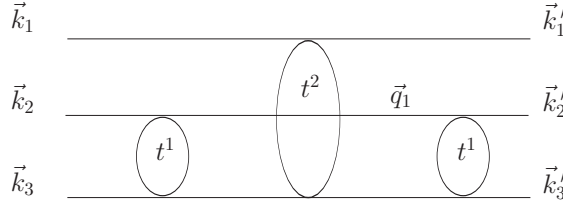
Figure 1.19: *A diagram involving three t-matrices.*

Therefore, all the diagrams in Fig. 1.9 can be expressed mathematically as $t^i g^{ij} t^j$ with $i \neq j = 1, 2, 3$. In this discussion we have taken one channel, $\pi^0 \pi^0 n$, as an example but normally our calculations require taking several coupled channels into account. Hence t^i, g^{ij} and t^j are normally matrices and the elements of the g^{ij} matrix have a general form

$$g_\xi^{ij}(\vec{k_i}', \vec{k_j}) = \left(\prod_{r=1}^{D} \frac{N_r}{2E_r} \right)$$
$$\times \frac{1}{\sqrt{s} - E_i(\vec{k_i}') - E_l(\vec{k_i}' + \vec{k_j}) - E_j(\vec{k_j}) + i\epsilon}, l \neq i, l \neq j, = 1, 2, 3$$
$$(1.95)$$

where the subscript ξ represents an element of the matrix[4], D is the number of particles propagating between two t-matrices. Following the normalization of [80], $N_r = 1$ for a meson and $N_r = 2M_r$ for a baryon with M_r being the mass of the baryon. $\vec{k_i}'$ ($\vec{k_j}$) in Eq. (1.95) denotes the momentum of the ith (jth) particle in the final (initial) state.

1.3.3 Higher order diagrams

The calculation of diagrams with more than two t-matrices involve a loop of three propagators and three two-body t-matrices,

---

[4]In this Thesis the subscript "ξ" shall always represent an element of a matrix

as shown in Fig. 1.19. The contribution of this diagram can be written mathematically as

$$\int \frac{d^3q_1}{(2\pi)^3} t^1(s_{23}) g^{12}(\vec{k}_1', \vec{q}_1) t^2(s_{31}^{q_1}) g^{21}(\vec{q}_1, k_1) t^1(s_{23}) \qquad (1.96)$$

Note that, while s_{23} in Eq. (1.96) can be defined from the external variables for the diagram shown in Fig. 1.19, the argument s_{31} of the t^2-matrix is a function of the loop variable and must be kept in the loop integral. The $s_{31}^{q_1}$ can be defined in terms of the loop variable, q_1, which is the four vector of the particle 2 with $\vec{q}_1$ defined in the global center of mass system (see Eq. 1.36)

$$s_{31}^{q_1} = (P - q_1|_{q_1^0 = E_2(\vec{q}_1)})^2. \qquad (1.97)$$

In the equation written above, P is the total four momentum of the three-body system

Therefore, the two t^1 matrices can be extracted out of the loop integral, but not t^2. However, we would like to factorize the $t^2 g^{21} t^2$ term outside the integral, because in this way the multifunction integral (1.96) simplifies to that of a single function, which could ultimately speed up the numerical calculation of the Faddeev equations. The expression in Eq. (1.96) can be rearranged as

$$t^1(s_{23}) \left[\int \frac{d^3q_1}{(2\pi)^3} g^{12}(\vec{k}_1', \vec{q}_1) t^2(s_{31}^{q_1}) g^{21}(\vec{q}_1, k_1) \right.$$

$$\left. \times [g^{21}]^{-1} [t^2(s_{31})]^{-1} \right] t^2(s_{31}) g^{21} t^1(s_{23}) \qquad (1.98)$$

where an identity expression depending on the on-shell variables has been introduced, i.e., $[g^{21}]^{-1}[t^2(s_{31})]^{-1}t^2(s_{31})g^{21}$.

We define the expression in the square bracket in Eq. (1.98) as

$$G^{121} = \int \frac{d\vec{q}_1}{(2\pi)^3} \hat{g}^{12} F^{121}(\vec{q}_1, \vec{k}_2', \vec{k}_1, s_{31}^{q_1}) \qquad (1.99)$$

with

$$F^{121}(\vec{q}_1, \vec{k}'_2, \vec{k}_1, s^{q_1}_{31}) = t^2(s^{q_1}_{31}) \times g^{21}(\vec{q}_1, \vec{k}_1)$$
$$\times [g^{21}(\vec{k}'_2, \vec{k}_1)]^{-1}[t^2(\sqrt{s_{31}})]^{-1}. \tag{1.100}$$

In this way, the contribution of the diagram in Fig. 1.19, thus, can be expressed as

$$t^1 G^{121} t^2 g^{21} t^1 = t^1(\sqrt{s_{23}}) G^{121} t^2(\sqrt{s_{31}})$$
$$\times g^{21}(\vec{k}'_2, \vec{k}_1) t^1(\sqrt{s_{23}}). \tag{1.101}$$

The F^{121} function contains the inverse of t^2 calculated as a function of s_{31}, which is evaluated in terms of on-shell variables. It also depends on the g^{21} propagator which is a function of the loop variable, and also involves the inverse of g^{21} on-shell. In this way, $[g^{21}(\vec{k}'_2, \vec{k}_1)]^{-1} \times [t^2(\sqrt{s_{31}})]^{-1}$ in F^{121} (and hence in G^{121}) when multiplied to $t^2(\sqrt{s_{31}})g^{21}(\vec{k}'_2, \vec{k}_1)$ in Eq. (1.101) give an identity leaving $t^2 g^{21}$ evaluated with the loop variable in the loop integral. Simplifying Eq. (1.101) we arrive to Eq. (1.96), which is the appropriate contribution of the diagram in Fig. 1.19. However, for convenience, we will replace in Eq. (1.99) the g^{12} propagator by the corresponding one written in the rest frame of particles 2 and 3, $\hat{g}^{12}$.

$$\hat{g}^{12}_\xi = \frac{1}{2E_2(\vec{q}_1)} \frac{M_3}{E_3(\vec{q}_1)} \frac{1}{\sqrt{s_{23}} - E_2(\vec{q}_1) - E_3(\vec{q}_1) + i\epsilon}$$

There are six possible diagrams for the three-body scattering with two successive (pair) interactions amongst them (Fig.1.9). There are two possibilities to add another interaction to these diagrams giving rise to a total of twelve possible diagrams for three successive interactions and, therefore, twelve corresponding G-functions, with a general definition

$$G^{ijk} = \int \frac{d^3 k''}{(2\pi)^3} \hat{g}^{ij}(s_{lm}, \vec{k}'') F^{ijk}(\vec{k}'', \vec{k}'_j, \vec{k}_k, s^{k''}_{l'k'}) \tag{1.102}$$
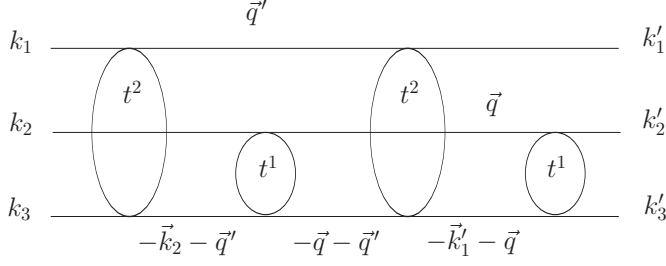
Figure 1.20: *A diagram with two concatenated loops.*

with $i \neq j$, $j \neq k = 1, 2, 3$, $l \neq m \neq i$, $l' \neq k' \neq j$, where the elements of the $\hat{g}^{ij}$ matrix are given by

$$
\begin{aligned}
\hat{g}_\xi^{ij} = {} & \frac{N_l}{2E_l(\vec{k}'')} \frac{N_m}{2E_m(\vec{k}'')} \\
& \times \frac{1}{\sqrt{s_{lm}} - E_l(\vec{k}'') - E_m(\vec{k}'') + i\epsilon}
\end{aligned}
\tag{1.103}
$$

and the matrix

$$
\begin{aligned}
F^{ijk}(\vec{k}'', \vec{k}'_j, \vec{k}_i, s_{l'k'}^{k''}) = {} & t^j(s_{l'k'}^{k''}) \times g^{jk}(\vec{k}'', \vec{k}_k) \\
& \times [g^{jk}(\vec{k}'_j, \vec{k}_k)]^{-1} [t^j(s_{l'k'})]^{-1}.
\end{aligned}
\tag{1.104}
$$

The integrals of G^{ijk} are regularized with a cut-off of 1 GeV in the modulus of the momentum, which if changed to 1.5 GeV introduces less than 1% of a change in G. A diagram with three t-matrices is, thus, written as $t^i G^{ijk} t^j g^{jk} t^k$ instead of $t^i g^{ij} t^j g^{jk} t^k$.

The formalism is further developed by repeating the above procedure for higher order diagrams too, i.e., by replacing the g^{ij} propagator by the G^{ijk} loop function every time a new interaction is added.

In case of the diagrams with more than three t-matrices, this scheme involves an approximation, since the introduction of a new interaction, to the diagrams of the kind shown in Fig.

1.19, replaces the external variables in the latter case by variables of a former loop. This procedure, which would render the integral Faddeev equations into a set of algebraic equations, is certainly very economical in terms of numerical solution and a justification for its use is given below.

Let us discuss in detail a diagram with four t-matrices as shown in Fig. 1.20, as an example. This diagram is written explicitly as (considering only one meson-meson-baryon channel for simplification)

$$
t^1 G^{121} t^2 G^{212} t^1 g^{12} t^2 = t^1(\sqrt{s_{23}}) \left(\int \frac{d\vec{q}_1}{(2\pi)^3} \frac{1}{2E_2(\vec{q}_1)} \right.
$$

$$
\times \frac{M_3}{E_3(\vec{q}_1)} \frac{1}{\sqrt{s_{23}} - E_2(\vec{q}_1) - E_3(\vec{q}_1) + i\epsilon} t^2(s_{31}^{q_1})
$$

$$
\left. \times g^{21}(\vec{q}_1, \vec{k}_1) \, [g^{21}(\vec{k}_2', \vec{k}_1)]^{-1} \, [t^2(\sqrt{s_{31}})]^{-1} \right) t^2(\sqrt{s_{31}})
$$

$$
\times \left(\int \frac{d\vec{q}_2}{(2\pi)^3} \frac{1}{2E_1(\vec{q}_2)} \frac{M_3}{E_3(\vec{q}_2)} \frac{1}{\sqrt{s_{31}} - E_1(\vec{q}_2) - E_3(\vec{q}_2) + i\epsilon} \right.
$$

$$
\left. \times t^1(s_{23}^{q_2}) \, g^{12}(\vec{q}_2, \vec{k}_2) \, [g^{12}(\vec{k}_1', \vec{k}_2)]^{-1} [t^1(\sqrt{s_{23}})]^{-1} \right)
$$

$$
\times t^1(\sqrt{s_{23}}) \, g^{12}(\vec{k}_1', \vec{k}_2) \, t^2(\sqrt{s_{31}}) \tag{1.105}
$$

which can be simplified to

$$
t^1(\sqrt{s_{23}}) \int \frac{d\vec{q}_1}{(2\pi)^3} \frac{1}{2E_2(\vec{q}_1)} \frac{M_3}{E_3(\vec{q}_1)}
$$

$$
\times \frac{1}{\sqrt{s_{23}} - E_2(\vec{q}_1) - E_3(\vec{q}_1) + i\epsilon} t^2(s_{31}^{q_1}) g^{21}(\vec{q}_1, \vec{k}_1)
$$

$$
\times [g^{21}(\vec{k}_2', \vec{k}_1)]^{-1} \int \frac{d\vec{q}_2}{(2\pi)^3} \frac{1}{2E_1(\vec{q}_2)} \frac{M_3}{E_3(\vec{q}_2)}
$$

$$
\times \frac{1}{\sqrt{s_{31}} - E_1(\vec{q}_2) - E_3(\vec{q}_2) + i\epsilon} t^1(s_{23}^{q_2})
$$

$$
\times g^{12}(\vec{q}_2, \vec{k}_2) t^2(\sqrt{s_{31}}), \tag{1.106}
$$

where $s_{23}^{q_2}$ is calculated analogously to Eq.(1.97). We compare our expression (1.106) with the corresponding one written in terms of the g propagators with the concatenated two loops

$$t^1(\sqrt{s_{23}}) \left[\int \frac{d\vec{q_1}}{(2\pi)^3} \int \frac{d\vec{q_2}}{(2\pi)^3} g^{12}(\vec{k_1'}, \vec{q_1}) t^2(s_{31}^{q_1}) \right.$$

$$\left. \times g^{21}(\vec{q_1}, \vec{q_2}) t^1(s_{23}^{q_2}) g^{12}(\vec{q_2}, \vec{k_2}) \right] t^2(\sqrt{s_{31}}). \qquad (1.107)$$

This exercise shows that the dependence of g^{21} on the two loop variables has been factorized in Eq. (1.106) as

$$g^{21}(\vec{q_1}, \vec{q_2}) = \mathscr{F}_1(\vec{q_1}) \mathscr{F}_2(\vec{q_2}), \qquad (1.108)$$

where

$$\mathscr{F}_1(\vec{q_1}) = g^{21}(\vec{q_1}, \vec{k_1})[g^{21}(\vec{k_2'}, \vec{k_1})]^{-1} \qquad (1.109)$$

and

$$\mathscr{F}_2(\vec{q_2}) = \tilde{g}^{21}(\vec{q_2}) = \frac{1}{2E_1(\vec{q_2})} \frac{M_3}{E_3(\vec{q_2})}$$

$$\times \frac{1}{\sqrt{s_{31}} - E_1(\vec{q_2}) - E_3(\vec{q_2})}. \qquad (1.110)$$

This factorization, which simplifies the calculations to a great extent, leads to very similar results to those obtained with the concatenated loop function as can be seen in Fig. 1.21 for the $\pi^0\pi^0 n$ system as an example. We show the mod-square of the Eq. (1.106) and Eq. (1.107) as a function of the invariant mass of the three particles in the energy region where, as we shall show in chapter 4, the $N^*(1710)$ gets dynamically generated.

The agreement of the results depicted in Fig. 1.21 shows that Eq. (1.106) is a good approximation of Eq. (1.107). Hence, this scheme is used to write the rest of the higher order diagrams which contribute to the three-body amplitude.
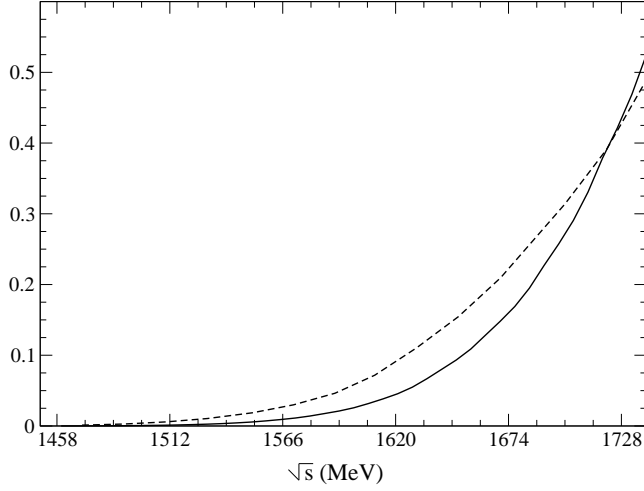
Figure 1.21: *The comparison of modulus square of Eq. (1.106) and Eq. (1.107) shown as dashed and solid lines, respectively, in units of $10^{-15}\ MeV^{-6}$.*

1.4   Reformulation of the Faddeev equations

If we sum Eqs. (1.17), (1.101), (1.105) and all the other possible diagrams with the last two t-matrices as t^2 and t^1, we get the series

$$t^1 g^{12} t^2 + t^1 G^{121} t^2 g^{21} t^1 + t^1 G^{121} t^2 G^{212} t^1 g^{12} t^2 + \cdots$$
$$+ t^1 G^{123} t^2 g^{23} t^3 + t^1 G^{123} t^2 G^{232} t^3 g^{32} t^2 + \cdots, \qquad (1.111)$$

which we define as T_R^{12}. Similarly, we consider all other possible diagrams obtained by permutating different interactions between the three hadrons and get the following equations upon

summing all the diagrams with the same last two t-matrices

$$T_R^{12} = t^1 g^{12} t^2 + t^1 \left[G^{121} T_R^{21} + G^{123} T_R^{23} \right]$$

$$T_R^{13} = t^1 g^{13} t^3 + t^1 \left[G^{131} T_R^{31} + G^{132} T_R^{32} \right]$$

$$T_R^{21} = t^2 g^{21} t^1 + t^2 \left[G^{212} T_R^{12} + G^{213} T_R^{13} \right] \tag{1.112}$$

$$T_R^{23} = t^2 g^{23} t^3 + t^2 \left[G^{231} T_R^{31} + G^{232} T_R^{32} \right]$$

$$T_R^{31} = t^3 g^{31} t^1 + t^3 \left[G^{312} T_R^{12} + G^{313} T_R^{13} \right]$$

$$T_R^{32} = t^3 g^{32} t^2 + t^3 \left[G^{321} T_R^{21} + G^{323} T_R^{23} \right]$$

In Eq. (1.112) all the loop dependence is assembled in the loop function G^{ijk}, therefore, they are algebraic equations. The T_R^{ij} partitions consider all the different contributions to the three-body T- matrix in which the last interactions are given in terms of the two-body t-matrices t^j and t^i, respectively. The T_R^{ij} matrices are related to the Faddeev partitions T^i through

$$T^i = \tilde{\delta}^3(\vec{k}_i - \vec{k}_i') t^i + \sum_{i=1}^{3} \sum_{j \neq i=1}^{3} T_R^{ij} \tag{1.113}$$

with $j \neq k \neq i = 1,\,2,\,3$ and $\tilde{\delta}^3(\vec{k}_i - \vec{k}_i') \equiv \left[(2\pi)^3 \tilde{N}_i \delta^3(\vec{k}_i - \vec{k}_i') \right]$ where

$$\tilde{N}_i = \begin{cases} \sqrt{2\omega(\vec{k}_i)} \sqrt{2\omega(\vec{k}_i')} & i = 1, 2 \\ \left(\sqrt{2\omega(\vec{k}_i)} \sqrt{2\omega(\vec{k}_i')} \right) / \left(\sqrt{2m_i} \sqrt{2m_i'} \right) & i = 3. \end{cases}$$

for a two meson-one baryon system and

$$\tilde{N}_i = \sqrt{2\omega(\vec{k}_i)} \sqrt{2\omega(\vec{k}_i')}, \quad i = 1, 2, 3$$

for a three meson system. The $\vec{k}_i$ ($\vec{k}_i'$) is the initial (final) momentum of the particle i. The subscription R on T^{ij} signifies that these equations do not contain the terms corresponding to

the disconnected diagrams but are composed of the rest of all the terms for the connected diagrams. Thus, the full three-body T-matrix is given by

$$T = \sum_{i=1}^{3} T^i = \sum_{i=1}^{3} t^i \tilde{\delta}^3(\vec{k}_i' - \vec{k}_i) + T_R$$

$$T_R \equiv \sum_{i=1}^{3} \sum_{j \neq i=1}^{3} T_R^{ij} \qquad (1.114)$$

As our objective is to search for peaks in the T-matrix which can be associated with physical states, we can restrict ourselves to the study of the properties of

$$T_R^* \equiv T_R - \sum_{i=1}^{3} \sum_{j \neq i=1}^{3} t^i g^{ij} t^j \qquad (1.115)$$

since neither $t^i \tilde{\delta}^3(\vec{k}_i' - \vec{k}_i)$ nor the $t^i g^{ij} t^j$ terms can give rise to any three-body resonance.

This chapter can be summarized as follows:

1. The Faddeev equations have been obtained by evaluating the contribution of the different Feynman diagrams with different interactions between the three particles which form the system under study.

2. The off-shell part of the two-body amplitudes calculated from the chiral Lagrangians gives rise to three-body forces, when plugged in the Faddeev equations. All such terms when added to the three-body contact term of the same Lagrangian cancel in the $SU(3)$ limit and give a negligible contribution for a realistic case. Then, in such a formalism, the Faddeev equations can be solved with the on-shell part of the two-body t matrices.

3. The contribution of diagrams with more than three t matrices is written by collecting all the loop dependence in the G^{ijk} functions.

4. Writing the higher order terms with the same procedure involves an approximation which has been illustrated to be excellent for our purpose.

5. Finally we obtain six coupled equations which appear as reformulation of the Faddeev equations. These equations have the advantage that they are algebraic equations instead of integral equations. The solution of these equations and its interpretation requires more technical information like kinematics, isospin algebra and the correspondence of the peaks found in the amplitude to poles. We will focus on all these topics in the next chapter.

Formalism II: Kinematics, Isospin and poles

In the last chapter we derived the equations which we will use to investigate three-hadron systems made of mesons and baryons. In this chapter we will define the kinematics for these equations and we will also discuss the algebra for the isospin projection of the three-body T matrix. This will be useful in interpreting the results in the subsequent chapters of this Thesis. Finally, we will show the correspondence of our results to the poles in the complex plane.

2.1 Kinematics

We now define the kinematics for the system. The first choice we make is that all the calculations will be carried out in S wave. There will be always two variables in the calculation: the total energy of the three-body system, denoted as $\sqrt{s}$, and the invariant mass of the particles 2 and 3, denoted as $\sqrt{s_{23}}$. The other invariant masses are obtained in terms of these variables as

$$s_{ij} = s + m_k^2 - \frac{\sqrt{s}(\sqrt{s} - E_1)(s_{23} + m_k^2 - m_j^2)}{s_{23}} \qquad (2.1)$$

with m_k being the mass of the non-interacting particle and

$$E_1 = \frac{s - s_{23} + m_1^2}{2\sqrt{s}}. \tag{2.2}$$

The definition in Eq. (2.1) implies an angular average between external momenta suited for the study of s-waves.

From all this we can calculate the momenta $|\vec{k}_1|, |\vec{k}_1'|$ of the particle 1 in the global center of mass system and that of the particles 2 and 3 in their rest frame (R_{23}), which we denote as $\vec{K}$ $(\vec{K}')$ in the initial (final) state;

$$\begin{aligned}
|\vec{k}_1| &= \frac{1}{2\sqrt{s}}\lambda^{1/2}(s, s_{23}, m_1^2) \\
|\vec{k}_1'| &= \frac{1}{2\sqrt{s}}\lambda^{1/2}(s, s_{23}, m_1'^{\,2}) \\
|\vec{K}| &= \frac{1}{2\sqrt{s_{23}}}\lambda^{1/2}(s_{23}, m_2^2, m_3^2) \\
|\vec{K}'| &= \frac{1}{2\sqrt{s_{23}}}\lambda^{1/2}(s_{23}, m_2'^{\,2}, m_3'^{\,2}).
\end{aligned} \tag{2.3}$$

The calculation of the g^{ij} propagators for different diagrams requires the momenta of the particles in the global center of mass. For this, we boost the momentum in R_{23} to the global center of mass using the relations [84]:

$$\begin{aligned}
\vec{k}_2 &= \left[\left(\frac{\sqrt{s} - E_1(\vec{k}_1)}{\sqrt{s_{23}}} - 1\right)\frac{\vec{K}\cdot\vec{k}_1}{\vec{k}_1^2} - \frac{E_2^{R_{23}}(\vec{K})}{\sqrt{s_{23}}}\right]\vec{k}_1 + \vec{K} \\
\vec{k}_3 &= \left[\left(\frac{\sqrt{s} - E_1(\vec{k}_1)}{\sqrt{s_{23}}} - 1\right)\frac{(-\vec{K})\cdot\vec{k}_1}{\vec{k}_1^2} - \frac{E_3^{R_{23}}(\vec{K})}{\sqrt{s_{23}}}\right]\vec{k}_1 - \vec{K} \\
\vec{k}_2' &= \left[\left(\frac{\sqrt{s} - E_1(\vec{k}_1')}{\sqrt{s_{23}}} - 1\right)\frac{\vec{K}'\cdot\vec{k}_1'}{\vec{k}_1'^2} - \frac{E_2^{R_{23}}(\vec{K}')}{\sqrt{s_{23}}}\right]\vec{k}_1' + \vec{K}' \\
\vec{k}_3' &= \left[\left(\frac{\sqrt{s} - E_1(\vec{k}_1')}{\sqrt{s_{23}}} - 1\right)\frac{(-\vec{K}')\cdot\vec{k}_1'}{\vec{k}_1'^2} - \frac{E_3^{R_{23}}(\vec{K}')}{\sqrt{s_{23}}}\right]\vec{k}_1' - \vec{K}'.
\end{aligned} \tag{2.4}$$

We are going to work with t-matrices calculated in S wave. Therefore, all the angular dependent expressions have to be projected in S wave. Having defined all the variables it should be noted that the projection in S-wave consists of integrating over the angles of these momenta

$$\frac{1}{(4\pi)^4} \int d\Omega(\hat{k}_1) \int d\Omega(\hat{K}) \int d\Omega(\hat{k}'_1) \int d\Omega(\hat{K}'). \qquad (2.5)$$

We define $\vec{k}_1$ to be along the z-axis, which implies a symmetry under a global rotation along the $\vec{k}_1$ axis, and $\vec{K}$ to form a plane with $\vec{k}_1$, i.e., its azimuthal angle $\phi = 0$:

$$\vec{k}_1 = \begin{pmatrix} 0 \\ 0 \\ |\vec{k}_1| \end{pmatrix} \qquad \vec{K} = \begin{pmatrix} |\vec{K}| \sin\theta \\ 0 \\ |\vec{K}| \cos\theta \end{pmatrix} \qquad (2.6)$$

$$\vec{k}'_1 = \begin{pmatrix} |\vec{k}'_1| \sin\theta'_1 \cos\phi'_1 \\ |\vec{k}'_1| \sin\theta'_1 \sin\phi'_1 \\ |\vec{k}'_1| \cos\theta'_1 \end{pmatrix} \qquad \vec{K}' = \begin{pmatrix} |\vec{K}'| \sin\theta' \cos\phi' \\ |\vec{K}'| \sin\theta' \sin\phi' \\ |\vec{K}'| \cos\theta' \end{pmatrix}.$$

with the definitions and expressions defined until now we can calculate the T_{ij}^R partitions up to second order in t using

1. The invariant mass $\sqrt{s_{23}}$ and others defined by Eq. (2.1) for calculation of the two-body t matrices.

2. The momenta $\vec{k}_i$, $\vec{k}'_i$ defined by Eqs. (2.3,2.4) along with the directions defined by Eq. (2.6) to obtain the g^{ij} function, which, as discussed earlier, are on-shell in nature since we know two of the three momenta in the global center of mass and the third one can be always obtained from the law of conservation of momentum in the global center of mass, i.e., $\vec{k}_1 + \vec{k}_2 + \vec{k}_3 = 0$.

Before we proceed with other definitions, we should discuss the kinematical dependence of the g^{ij} functions in more detail.

There are no problems in the calculations of the g^{ij} propagators if we are above the threshold(s) of a system but it gets non-trivial if we are below threshold(s). A three-body system composed of particles with different masses has multiple thresholds.

In our case, where all the kinematics is defined in terms of $\sqrt{s}$ and $\sqrt{s_{23}}$, we would have the three-body threshold $m_1+m_2+m_3$, other would be $\sqrt{s_{23}} = m_2+m_3$ and yet another threshold would be $\sqrt{s_{23}}+m_1$. When we calculate the three-body equations, depending on the energy range which we consider, one or more of the following conditions might be satisfied

I) $\sqrt{s} > m_1 + m_2 + m_3$.

II) $\sqrt{s_{23}} > m_2 + m_3$.

III) $\sqrt{s} > m_1 + \sqrt{s_{23}}$.

IV) $\sqrt{s} < m_1 + m_2 + m_3$.

V) $\sqrt{s_{23}} < m_2 + m_3$.

VI) $\sqrt{s} < m_1 + \sqrt{s_{23}}$.

If all the first three conditions are satisfied, the momenta and energies are real and trivial to calculate. However, if the condition V or VI or both are satisfied, we need a procedure to continue the T_{ij}^R equations below threshold. For example, if $\sqrt{s} < m_1 + \sqrt{s_{23}}$, then $|\vec{k}_1|$ gets purely imaginary, which makes the momenta $\vec{k}_2$ and $\vec{k}_3$ calculated from Eq. (2.4) complex, which in turn makes E_2 and E_3 complex. Another example is if $\sqrt{s_{23}} < m_2 + m_3$. In that case, we have $|\vec{K}|$ purely imaginary and its use in Eq. (2.4) again gives complex momenta and energy. In order to avoid such unphysical situations we do the following:

1. If $\sqrt{s} < m_1 + \sqrt{s_{23}}$, we fix $|\vec{k}_1|$ to a minimun value, $|\vec{k}_1| = p_{min} = 50$ MeV.

2. If $\sqrt{s_{23}} < m_2 + m_3$, we introduce a binding energy, B_{23}, such that

$$\sqrt{s_{23}} = -B_{23} + \frac{p_{min}^2}{2m_2} + \frac{p_{min}^2}{2m_3} + m_2 + m_3 \qquad (2.7)$$

and

$$E_2 = -\frac{B_{23}}{2} + \frac{p_{min}^2}{2m_2} + m_2$$

$$E_3 = -\frac{B_{23}}{2} + \frac{p_{min}^2}{2m_3} + m_3. \tag{2.8}$$

The B_{23} in Eq. (2.8) can be calculated by fixing the p_{min} (typically 50 MeV). The philosophy used is that the particles below threshold(s) are bound and have a physical momentum and energy. This is indeed the real case and our approach tries to stick closely to that situation.

With this philosophy, a binding energy can also be defined if the condition VI is satisfied. Let us assume that in the case of $\sqrt{s} < m_1 + \sqrt{s_{23}}$ the three-body problem is reduced to a bound state of particles with mass m_1 and $\sqrt{s_{23}}$ having a small center of mass momentum p_{min} and a binding energy B. Then,

$$\sqrt{s} = E_1 + \sqrt{s_{23} + p_{min}^2}$$
$$= \sqrt{(m_1 - B)^2 + p_{min}^2} + \sqrt{s_{23} + p_{min}^2}$$

Rearranging the equation written above, we get

$$\left(\sqrt{s} - \sqrt{s_{23} + p_{min}^2}\right)^2 = (m_1 - B)^2 + p_{min}^2$$

which means,

$$\left(\sqrt{s} - \sqrt{s_{23} + p_{min}^2}\right)^2 - p_{min}^2 = (m_1 - B)^2$$

and hence

$$m_1 - B = \pm\sqrt{\left(\sqrt{s} - \sqrt{s_{23} + p_{min}^2}\right)^2 - p_{min}^2}.$$

In the above equation, we choose the positive sign since otherwise we will have $m_1 < B$ which does not make sense. Thus,

$$B = m_1 - \sqrt{\left(\sqrt{s} - \sqrt{s_{23} + p_{min}^2}\right)^2 - p_{min}^2}. \qquad (2.9)$$

Although, as we will see in the following chapters, practically all the resonances found are far above any of the thresholds listed, in cases where we need to use the procedure described above, we have analyzed the dependence of the results on the p_{min}.

Finally it remains to obtain explicit expressions for the invariant masses in terms of the loop variable which will be necessary to calculate the two-body t matrices in the loop functions of Eq. (1.102). In general all these invariant masses can be defined as

$$s_{ij}^q = (P - q)^2 \big|_{q^0 = \tilde{E}(\vec{q})} \qquad (2.10)$$

where P is the four vector of the three-body system in the global center of mass frame, $P = (\sqrt{s}, \vec{0})$, and q is the four vector for the loop variable. This means

$$s_{ij}^q = s + \tilde{m}_k^2 - 2\sqrt{s} \cdot E_k(\vec{q}), \quad k \neq i \neq j \qquad (2.11)$$

with $E_k(\vec{q}) = \sqrt{\vec{q}^2 + m_k^2}$.

We shall always need the s_{ij}^q in the calculation of the G^{ijk} functions. As discussed in section 1.3.3 the loop variable, $\vec{q}$, in the G^{ijk} functions is defined in the center of mass of the two propagating particles of $\hat{g}^{ij}$ (see Eq. (1.103)). However, to calculate Eq. (2.11) we need to boost the $\vec{q}$ to the global center of mass frame.

We shall now describe the method to do this for one particular diagram as an example. In all other cases we can proceed in completely analogous manner. Let us consider the $t^1 G^{121} t^2 g^{21} t^1$ term, which has been discussed in section 1.3.3 and which is

shown diagrammatically in Fig. (1.19). In this case, we want to evaluate $s_{31}^{q_1}$ to calculate the t^2 matrix in the loop. From Eq. (2.11)

$$s_{31}^{q_1} = s + \tilde{m}_2^2 - 2\sqrt{s} \cdot E_2(\vec{q}_1) \qquad (2.12)$$

with $\tilde{m}_2$ the mass of the particle which has four momentum q_1 and $E_2(\vec{q}_1)$ the energy of that particle in the three-body center of mass frame. Since G^{121} contains a propagator $\hat{g}^{12}$ which is defined in the center of mass frame of particles 2 and 3, $\vec{q}_1$ and, hence, $E_2(\vec{q}_1)$ in the diagram Fig. 1.19 is defined in the rest frame of particles 2 and 3. Let us denote the rest frame of particles i and j by R^{ij}. Thus we need to boost $E_2(\vec{q}_1)$ from R^{23} to the global center of mass to calculate $s_{31}^{q_1}$. Using the Lorentz relations

$$E_2(\vec{q}_1) = \frac{E_2^{CM23}(\vec{q}_1) + \vec{v}\vec{q}_1}{\sqrt{1 - \vec{v}^2}} \qquad (2.13)$$

with $\vec{v}$ the speed. In this case

$$\vec{v} = -\frac{\vec{k}_1'}{\sqrt{s} - E_1(\vec{k}_1')}. \qquad (2.14)$$

Using the relation $E_2^{CM23}(\vec{q}_1) = \sqrt{\vec{q}_1^2 + \tilde{m}_2^2}$ in Eq. (2.13), we have

$$E_2(\vec{q}_1) = \frac{\sqrt{\vec{q}_1^2 + \tilde{m}_2^2}(\sqrt{s} - E_1(k_1')) - \vec{q}_1 \cdot \vec{k}_1'}{\sqrt{s_{23}}}, \qquad (2.15)$$

which when substituted in Eq. (2.12) after averaging over the angles gives

$$s_{31}^{q_1} = s + \tilde{m}_2^2 - 2\sqrt{s}\,\frac{\sqrt{\vec{q}_1^2 + \tilde{m}_2^2}(\sqrt{s} - E_1(\vec{k}_1'))}{\sqrt{s_{23}}}. \qquad (2.16)$$

We end the present section by stating that now we have all the information and expressions required to solve the T^R equations. Before going ahead and discussing the study of different

three hadron systems within our formalism, we need to define some isospin base in order to interpret our results. We give a short note on the method of projecting the T^R matrices on the isospin base.

2.2 Isospin base

We shall construct the three-body T_R-matrices using isospin symmetry, for which we must take an average mass for the isospin multiplets $\pi\,(\pi^+,\pi^0,\pi^-)$, $\rho\,(\rho^+,\rho^0,\rho^-)$, $\bar{K}\,(\bar{K}^0,K^-)$, $K\,(K^+,K^0)$, $\bar{K}^*\,(\bar{K}^{*0},K^{*-})$, $K^*\,(K^{*+},K^{*0})$, $\Sigma\,(\Sigma^+,\Sigma^0,\Sigma^-)$, $N\,(p,n)$, and $\Xi\,(\Xi^0,\Xi^-)$. However, the evaluation of the scattering matrix is done in the physical base of states. In order to identify the nature of the resulting states, we project the T_R-matrix on the isospin base. One appropriate base is the one where the states are classified by the total isospin of the three particles "I" and the total isospin of a subsystem "I_{sub}". We thus label the states in the isospin base as $|\,I, I_{sub}\rangle$. Obviously transitions between states with same total isospin but different isospin of a subsystem are possible. As we will show, the peaks in the amplitudes are nevertheless seen more clearly for some particular isospin of the subsystem, indicating that the dominant structure of the state found in the three-body system has a certain value of the total isospin and that of the isospin of a subsystem. We can thus write our T_R-matrix in the isospin base, in general, as $\langle I, I_{sub} \,|\, T_R(\sqrt{s}, \sqrt{s_{23}}) \,|\, I, I'_{sub}\rangle$.

Normally, if we consider three particles with isospin I_1, I_2 and I_3, respectively, we start by writing the three-body states as

$$|I_1, I_2, I_3\rangle = |I_1, I_1^z\rangle \otimes |I_2, I_2^z\rangle \otimes |I_3, I_3^z\rangle \qquad (2.17)$$

which could be written in one of the following ways

$$
\begin{aligned}
|I_1, I_2, I_3\rangle &= |I_{12}, I_{12}^z\rangle \otimes |I_3, I_3^z\rangle = |I, I_{12}\rangle \\
&= |I_1, I_1^z\rangle \otimes |I_{23}, I_{23}^z\rangle = |I, I_{23}\rangle \\
&= |I_2, I_2^z\rangle \otimes |I_{31}, I_{31}^z\rangle = |I, I_{31}\rangle
\end{aligned}
$$

where I_{lm} denotes the total isospin of the (lm) subsystem and the z superscript indicates the third isospin component.

Having classified the T_R matrices in the isospin configurations, we will plot the resulting modulus squared amplitudes for different channels as a function of the two variables of the formalism, $\sqrt{s}$ and $\sqrt{s_{23}}$. We would identify the peaks in these plots as resonances. The question now arises is if these peaks correspond to poles in the complex plane. We address this question in the next section.

2.3 Poles in the complex plane

The peaks obtained in our formalism are very neat and we associate them to physical resonance states. In the two body scattering it is customary to look for poles in the second Riemann sheet to associate them to resonances. In the three-body problem, the difficulty to work with two complex variables, $\sqrt{s}$ and $\sqrt{s}_{23}$ which induce complex three momenta needed in the evaluation of integrals are obvious. Yet, an approximate method can be devised for the case when a subsystem of two particles can be treated as a resonance. Therefore the three-body system can be interpreted as a system of a particle (P) and a resonance (R). As we will see in the next chapters, this is indeed the case for the different three-body systems studied, i.e., the resonances normally appear when two out of the three hadrons rearrange themselves as a know resonance. For example, the $NK\bar{K}$ system where a resonance around 1920 MeV is found can be considered as a $Na_0(980)$ or $Nf_0(980)$ system. In such cases, the three-body problem is reduced to a two-body scattering and usual poles can be identified in the complex energy ($\sqrt{s}$) plane. Thus, as long as the resonances found in our work follow an approximate Breit-Wigner shape, the poles in the second Riemann sheet are guaranteed. Yet, we have looked at it in more detail, though, in a simplified way. Let us consider, for example, a three meson system. We keep the variable $\sqrt{s_{23}}$ as real, and we fix its value to the one where the peak appears

and then study the PR (particle plus a two-body resonance) amplitude as a function of the complex $\sqrt{s}$ variable. We must move to the second Riemann sheet in the PR amplitude which is accomplished by changing the momentum in the PR center of mass system, $k_P \to -k_P$ in the PR loop function. We proceed as explained below.

The unitarity condition allows us to write [4]

$$T_{PR}^{-1} = V_{PR}^{-1} - \tilde{G}_{PR} \tag{2.18}$$

with V_{PR} the real potential and $\tilde{G}_{PR}$ the PR loop function used in Eq. (1.14)

Going to the second Riemann sheet implies substituting $\tilde{G}_{PR}$ by $\tilde{G}_{PR}^{II}$, where $\tilde{G}_{PR}^{II}$ is obtained by changing k_P with $-k_P$ in the analytical expression of $\tilde{G}_{PR}$ [79]

$$
\begin{aligned}
\tilde{G}_{PR}(\sqrt{s}) = \frac{1}{16\pi^2} \Bigg\{ & a(\mu) + ln\frac{m_P^2}{\mu^2} + \frac{m_R^2 - m_P^2 + s}{2s} ln\frac{m_R^2}{m_P^2} \\
& + \frac{k_P}{\sqrt{s}} \Big[ln\{ s - (m_P^2 - m_R^2) + 2k_P\sqrt{s} \} + ln\{ s + (m_P^2 - m_R^2) \\
& + 2k_P\sqrt{s} \} - ln\{ s - (m_P^2 - m_R^2) - 2k_P\sqrt{s} \} \\
& - ln\{ s + (m_P^2 - m_R^2) - 2k_P\sqrt{s} \} - 2\pi i \Big] \Bigg\}
\end{aligned} \tag{2.19}
$$

Thus we can write

$$
\begin{aligned}
(T_{PR}^{-1})^{II} &= (V_{PR}^{-1}) - (\tilde{G}_{PR})^{II} \\
&= (T_{PR}^{-1})^I + \tilde{G}_{PR} - (\tilde{G}_{PR})^{II} \\
&= (T_{PR}^{-1})^I - i\frac{k_P}{4\pi\sqrt{s}},
\end{aligned} \tag{2.20}
$$

where I and II superindices indicate the first and second Riemann sheet, respectively. We can approximate T_R of Eq. (1.114) by a Breit-Wigner form as

$$T_R \simeq \frac{g^2}{s - s_o + iM\Gamma(s)} \tag{2.21}$$

In the vicinity of a resonance, T_{PR} must be proportional to T_R, implying then $T_{PR} = \alpha T_R$. Assuming α to be real and using the unitarity condition $Im\{T_{PR}^{-1}\} = -Im\{G_{PR}\}$ we have

$$Im\{T_{PR}^{-1}\} = \alpha^{-1} Im\{T_R^{-1}\}$$
$$= -Im\{G_{PR}\} = \frac{k_P}{8\pi\sqrt{s}}, \qquad (2.22)$$

which determines α. Therefore

$$(T_{PR}^{-1})^I = (\alpha^{-1}T_R^{-1})^I$$
$$= \left(\frac{k_P}{8\pi\sqrt{s}\,Im\{T_R^{-1}\}}\right)_{\sqrt{s}=M} T_R^{-1} \qquad (2.23)$$

which leads to

$$(T_{PR}^{-1})^{II} = \left(\frac{k_P}{8\pi\sqrt{s}}\frac{1}{M\Gamma}\right)_{\sqrt{s}=M}$$
$$\times (s - s_o + iM\Gamma) - i\frac{k_P}{4\pi\sqrt{s}}, \qquad (2.24)$$

which upon taking into account that the decay width of a two meson system

$$\Gamma = \frac{1}{8\pi s}g^2 k_P, \qquad (2.25)$$

with k_P being real, results in

$$(T_{PR}^{-1})^{II} = \frac{1}{g^2}\left[s - s_0 - i\frac{k_P}{8\pi}\left(\frac{2\sqrt{s} - M}{s}\right)g^2\right]. \qquad (2.26)$$

Then $(T_{PR}^{-1})^{II}$ has a pole at

$$s - s_0 - i\frac{k_P}{8\pi}\left(\frac{2\sqrt{s} - M}{s}\right)g^2 = 0, \qquad (2.27)$$

which appears indeed very close to $Re\sqrt{s} \simeq \sqrt{s_0}$ and $Im\sqrt{s} \simeq \Gamma/2$ as we have checked numerically for different cases, taking s_0

and g^2 from the shape of T_R. We also get the complex conjugate pole taking another branch of the logarithm.

With the end of this discussion, we have completely prepared the base for the three-body calculations. In the next chapter we discuss the study of the $\pi \bar{K} N$ system and its coupled channels for strangeness -1 and total charge zero. As we will show, these meson-meson-baryon systems generate several resonances dynamically.

CHAPTER 3

The low lying $1/2^+$ Σ and Λ states

The formalism developed in chapters 1 and 2 shall now be applied to the $\pi\bar{K}N$ system. The calculations are carried out as a function of two variables: the total energy of the three-body system and that of the $\bar{K}N$ subsystem and its coupled channels. A short introduction is followed by a technical discussion. Finally, the results are projected on the isospin base and peaks in the total three-body T-matrix are shown.

3.1 Introduction

One of the successes of unitary chiral dynamics is the reproduction of the $\Lambda(1405)\,S_{01}$ $(J^P = 1/2^-)$ properties, which has been found to get dynamically generated (with a two pole structure [8]) from the $\bar{K}N$ interaction and its coupled channels. If another pseudoscalar meson is added to this system, in S-wave, it results into states with spin-parity $J^P = 1/2^+$. The lightest pseudoscalar meson which can be added is the pion. The resulting three-body system would posses a mass ~ 1570 MeV. This is exactly the region where the $1/2^+$ hyperon resonances have poor status. The poor status of these low-lying $S = -1$ states is evident from the following facts: a) The spin-parity assignment

for many of these states is unknown, e.g., for $\Sigma(1480)$, $\Sigma(1560)$, etc., b) the partial-wave analysis and production experiments have been often kept separately in the PDG listings, e.g., for $\Sigma(1620)$, $\Sigma(1670)$, c) other times, e.g., in case of $\Lambda(1600)$, it is stated that existence of two resonances, in this energy region, is quite possible [22]. Indeed, there are hints for some of them to decay to three-body final states, like $\Lambda(1600)$ [23], $\Sigma(1660)$ [24]. Therefore, some of the $1/2^+$ resonances in the $S = -1$ sector have an appreciable overlap with two-mesons and one baryon states. An additional encouragement comes from the finding that the two meson cloud gives a sizable contribution to the mass in the spectrum of the $1/2^+$ baryon antidecuplet [21]. The chiral dynamics has been used earlier in the context of the three nucleon problems, e.g., in [85]. Here we present the first study of two mesons-one baryon systems applying chiral dynamics to solve the Faddeev equations. As shall be described in this chapter, our calculations for the $\pi \bar{K} N$ system and its coupled channels reveal peaks which we identify with the resonances $\Sigma(1770)$, $\Sigma(1650)$, $\Sigma(1620)$, $\Sigma(1560)$, $\Sigma(1480)$, $\Lambda(1810)$ and $\Lambda(1600)$.

The strong coupling of the $\bar{K}N$ to the $\Lambda(1405)$ resonance implies that the correlation of the $\bar{K}N$ and its coupled channels should be largely kept during the three-body scattering. Thus to solve the equations (1.112) we assume a given invariant mass for the $\bar{K}N$ system and the three-body T-matrix is, therefore, evaluated as a function of this mass and the total energy, which we denote as s_{23} and s, respectively. The other variables on which the two-body t-matrices and the propagators depend are defined in chapter 2. As has been already mentioned in chapter 1, the two-body t-matrices depend on the total energy, s_{ij}, in the corresponding two-body center of mass. The expression for the s_{12} and s_{13} obtained from the energy conservation from the external (on-shell) variables is given by Eq. (2.1). Note, however, that in the loop functions the invariant mass of two particles, as we discussed in sections 1.3.3 and 2.1, is a running variable and it is taken as such in the integral Eq.(1.102).

3.2 Coupled channels

The three pair interactions in the $\pi \bar{K} N$ system are attractive in Nature and generate resonances in certain energy region. The $\pi \bar{K}$ system generates the scalar $\kappa(800)$ [3]. The $K\bar{K}$, $\pi\pi$ and $\pi\eta$ systems generates the $f_0(980)$ and $a_0(980)$ states. The πN and its coupled channels generate the $N^*(1535)$ and the $\bar{K}N$ interaction (and coupled channels) form the $\Lambda(1405)$. Certainly, we can choose to study the three-body interaction in an energy range where resonances get built in one or more pair interactions. This augments the possibility of formation of a three-hadron resonance. For example, if we vary the invariant mass of the $\bar{K}N$ system around that of the $\Lambda(1405)$ the total mass of the $\pi \bar{K} N$ system will be around 1540 MeV. By varying the total energy from 1500-1800 MeV, we can scan exactly that energy region where the $S = -1$ resonances are not well understood and which we expect to couple strongly to three-hadron channels. This, in a way, is equivalent to study the $\pi\Lambda(1405)$ interaction.

Hence, we start by taking all the combinations of a pseudoscalar meson of the 0^- $SU(3)$ octet and a baryon of the $1/2^+$ octet which couple to $S = -1$ with any charge. To this system we add a pion and obtain twenty-two coupled channels with net charge zero: $\pi^0 K^- p$, $\pi^0 \bar{K}^0 n$, $\pi^0 \pi^0 \Sigma^0$, $\pi^0 \pi^+ \Sigma^-$, $\pi^0 \pi^- \Sigma^+$, $\pi^0 \pi^0 \Lambda$, $\pi^0 \eta \Sigma^0$, $\pi^0 \eta \Lambda$, $\pi^0 K^+ \Xi^-$, $\pi^0 K^0 \Xi^0$, $\pi^+ K^- n$, $\pi^+ \pi^0 \Sigma^-$, $\pi^+ \pi^- \Sigma^0$, $\pi^+ \pi^- \Lambda$, $\pi^+ \eta \Sigma^-$, $\pi^+ K^0 \Xi^-$, $\pi^- \bar{K}^0 p$, $\pi^- \pi^0 \Sigma^+$, $\pi^- \pi^+ \Sigma^0$, $\pi^- \pi^+ \Lambda$, $\pi^- \eta \Sigma^+$, $\pi^- K^+ \Xi^0$.

Thus we solve the six coupled T_R^{ij} equations for the above mentioned twenty-two coupled channels. It is the cancellations found in section 1.3.1 along with the characteristics of the formalism, rid of uncertainties from the off-shell parts of the t-matrices, which makes the numerical calculation of the present order feasible.

3.3 Isospin formalism

In order to identify the nature of the resulting states, we project the T-matrix on the isospin base. We choose as base the one

where the states are classified by the total isospin of the three particles, I, and the total isospin of the two mesons, I_π in the case of two pions. Using the phase convention $\mid \pi^+ \rangle = - \mid 1,1 \rangle$, $\mid K^- \rangle = - \mid 1/2, -1/2 \rangle$, $\mid \Sigma^+ \rangle = - \mid 1,1 \rangle$ and $\mid \Xi^- \rangle = - \mid 1/2, -1/2 \rangle$ we have, for example, for the the $\pi\pi\Sigma$ channel

$$
\begin{aligned}
\mid \pi^0 \pi^0 \Sigma^0 \rangle =& \mid I_1 = 1, I_{1z} = 0 \rangle \otimes \mid I_2 = 1, I_{2z} = 0 \rangle \\
& \otimes \mid I_3 = 1, I_{3z} = 0 \rangle \\
=& \left\{ \sqrt{\frac{2}{3}} \mid I_\pi = 2, I_{\pi z} = 0 \rangle - \sqrt{\frac{1}{3}} \mid I_\pi = 0, I_{\pi z} = 0 \rangle \right\} \\
& \otimes \mid I_3 = 1, I_{3z} = 0 \rangle \\
=& \sqrt{\frac{2}{5}} \mid I = 3, I_\pi = 2 \rangle - \frac{2}{\sqrt{15}} \mid I = 1, I_\pi = 2 \rangle \\
& - \sqrt{\frac{1}{3}} \mid I = 1, I_\pi = 0 \rangle
\end{aligned}
$$

To simplify the notation, we omit the label I and I_π and write

$$
\mid \pi^0 \pi^0 \Sigma^0 \rangle = \sqrt{\frac{2}{5}} \mid 3, 2 \rangle - \frac{2}{\sqrt{15}} \mid 1, 2 \rangle - \sqrt{\frac{1}{3}} \mid 1, 0 \rangle. \qquad (3.1)
$$

Similarly,

$$| \pi^+ \pi^- \Sigma^0 \rangle = -\sqrt{\frac{1}{10}} \, | \, 3, 2 \rangle + \sqrt{\frac{1}{15}} \, | \, 1, 2 \rangle - \sqrt{\frac{1}{3}} \, | \, 2, 1 \rangle$$

$$+ \sqrt{\frac{1}{6}} \, | \, 0, 1 \rangle - \sqrt{\frac{1}{3}} \, | \, 1, 0 \rangle$$

$$| \pi^- \pi^+ \Sigma^0 \rangle = -\sqrt{\frac{1}{10}} \, | \, 3, 2 \rangle + \sqrt{\frac{1}{15}} \, | \, 1, 2 \rangle + \sqrt{\frac{1}{3}} \, | \, 2, 1 \rangle$$

$$- \sqrt{\frac{1}{6}} \, | \, 0, 1 \rangle - \sqrt{\frac{1}{3}} \, | \, 1, 0 \rangle$$

$$| \pi^+ \pi^0 \Sigma^- \rangle = -\sqrt{\frac{1}{10}} \, | \, 3, 2 \rangle - \frac{1}{2} \, | \, 2, 2 \rangle - \sqrt{\frac{3}{20}} \, | \, 1, 2 \rangle$$

$$- \sqrt{\frac{1}{12}} \, | \, 2, 1 \rangle - \frac{1}{2} \, | \, 1, 1 \rangle - \sqrt{\frac{1}{6}} \, | \, 0, 1 \rangle$$

$$| \pi^0 \pi^+ \Sigma^- \rangle = -\sqrt{\frac{1}{10}} \, | \, 3, 2 \rangle - \frac{1}{2} \, | \, 2, 2 \rangle - \sqrt{\frac{3}{20}} \, | \, 1, 2 \rangle$$

$$+ \sqrt{\frac{1}{12}} \, | \, 2, 1 \rangle + \frac{1}{2} \, | \, 1, 1 \rangle + \sqrt{\frac{1}{6}} \, | \, 0, 1 \rangle$$

$$| \pi^- \pi^0 \Sigma^+ \rangle = -\sqrt{\frac{1}{10}} \, | \, 3, 2 \rangle + \frac{1}{2} \, | \, 2, 2 \rangle - \sqrt{\frac{3}{20}} \, | \, 1, 2 \rangle$$

$$+ \sqrt{\frac{1}{12}} \, | \, 2, 1 \rangle - \frac{1}{2} \, | \, 1, 1 \rangle + \sqrt{\frac{1}{6}} \, | \, 0, 1 \rangle$$

$$| \pi^0 \pi^- \Sigma^+ \rangle = -\sqrt{\frac{1}{10}} \, | \, 3, 2 \rangle + \frac{1}{2} \, | \, 2, 2 \rangle - \sqrt{\frac{3}{20}} \, | \, 1, 2 \rangle$$

$$- \sqrt{\frac{1}{12}} \, | \, 2, 1 \rangle + \frac{1}{2} \, | \, 1, 1 \rangle - \sqrt{\frac{1}{6}} \, | \, 0, 1 \rangle.$$

These equations are written in a matrix form as

$$
\begin{pmatrix}
\sqrt{\dfrac{2}{5}} & 0 & -\dfrac{2}{\sqrt{15}} & 0 & 0 & 0 & -\sqrt{\dfrac{1}{3}} \\[2ex]
-\sqrt{\dfrac{1}{10}} & 0 & \sqrt{\dfrac{1}{15}} & -\sqrt{\dfrac{1}{3}} & 0 & \sqrt{\dfrac{1}{6}} & -\sqrt{\dfrac{1}{3}} \\[2ex]
-\sqrt{\dfrac{1}{10}} & 0 & \sqrt{\dfrac{1}{15}} & \sqrt{\dfrac{1}{3}} & 0 & -\sqrt{\dfrac{1}{6}} & -\sqrt{\dfrac{1}{3}} \\[2ex]
-\sqrt{\dfrac{1}{10}} & -\dfrac{1}{2} & -\sqrt{\dfrac{3}{20}} & -\sqrt{\dfrac{1}{12}} & -\dfrac{1}{2} & -\sqrt{\dfrac{1}{6}} & 0 \\[2ex]
-\sqrt{\dfrac{1}{10}} & -\dfrac{1}{2} & -\sqrt{\dfrac{3}{20}} & \sqrt{\dfrac{1}{12}} & \dfrac{1}{2} & \sqrt{\dfrac{1}{6}} & 0 \\[2ex]
-\sqrt{\dfrac{1}{10}} & \dfrac{1}{2} & -\sqrt{\dfrac{3}{20}} & \sqrt{\dfrac{1}{12}} & -\dfrac{1}{2} & \sqrt{\dfrac{1}{6}} & 0 \\[2ex]
-\sqrt{\dfrac{1}{10}} & \dfrac{1}{2} & -\sqrt{\dfrac{3}{20}} & -\sqrt{\dfrac{1}{12}} & \dfrac{1}{2} & -\sqrt{\dfrac{1}{6}} & 0
\end{pmatrix}
\cdot
\begin{pmatrix}
\mid 3,2\rangle \\[2ex]
\mid 2,2\rangle \\[2ex]
\mid 1,2\rangle \\[2ex]
\mid 2,1\rangle \\[2ex]
\mid 1,1\rangle \\[2ex]
\mid 0,1\rangle \\[2ex]
\mid 1,0\rangle
\end{pmatrix}
=
\begin{pmatrix}
\mid \pi^0\,\pi^0\,\Sigma^0\rangle \\[2ex]
\mid \pi^+\,\pi^-\,\Sigma^0\rangle \\[2ex]
\mid \pi^-\,\pi^+\,\Sigma^0\rangle \\[2ex]
\mid \pi^+\,\pi^0\,\Sigma^-\rangle \\[2ex]
\mid \pi^0\,\pi^+\,\Sigma^-\rangle \\[2ex]
\mid \pi^-\,\pi^0\,\Sigma^+\rangle \\[2ex]
\mid \pi^0\,\pi^-\,\Sigma^+\rangle
\end{pmatrix}
$$

Inverting this matrix we have

$$| 3, 2 \rangle = \frac{1}{\sqrt{10}} \Big[2 \mid \pi^0 \, \pi^0 \, \Sigma^0 \rangle - \mid \pi^+ \, \pi^- \, \Sigma^0 \rangle - \mid \pi^- \, \pi^+ \, \Sigma^0 \rangle$$
$$- \mid \pi^+ \, \pi^0 \, \Sigma^- \rangle - \mid \pi^0 \, \pi^+ \, \Sigma^- \rangle$$
$$- \mid \pi^- \, \pi^0 \, \Sigma^+ \rangle - \mid \pi^0 \, \pi^- \, \Sigma^+ \rangle \Big]$$

$$| 2, 2 \rangle = -\frac{1}{2} \Big[\mid \pi^+ \, \pi^0 \, \Sigma^- \rangle + \mid \pi^0 \, \pi^+ \, \Sigma^- \rangle - \mid \pi^- \, \pi^0 \, \Sigma^+ \rangle$$
$$- \mid \pi^0 \, \pi^- \, \Sigma^+ \rangle \Big]$$

$$| 1, 2 \rangle = \frac{1}{\sqrt{15}} \Big[-2 \mid \pi^0 \, \pi^0 \, \Sigma^0 \rangle + \mid \pi^+ \, \pi^- \, \Sigma^0 \rangle + \mid \pi^- \, \pi^+ \, \Sigma^0 \rangle \Big]$$
$$- \sqrt{\frac{3}{20}} \Big[\mid \pi^+ \, \pi^0 \, \Sigma^- \rangle + \mid \pi^0 \, \pi^+ \, \Sigma^- \rangle + \mid \pi^- \, \pi^0 \, \Sigma^+ \rangle$$
$$+ \mid \pi^0 \, \pi^- \, \Sigma^+ \rangle \Big]$$

$$| 2, 1 \rangle = \frac{1}{2\sqrt{3}} \Big[-2 \mid \pi^+ \, \pi^- \, \Sigma^0 \rangle + 2 \mid \pi^- \, \pi^+ \, \Sigma^0 \rangle - \mid \pi^+ \, \pi^0 \, \Sigma^- \rangle$$
$$+ \mid \pi^0 \, \pi^+ \, \Sigma^- \rangle + \mid \pi^- \, \pi^0 \, \Sigma^+ \rangle - \mid \pi^0 \, \pi^- \, \Sigma^+ \rangle \Big]$$

$$| 1, 1 \rangle = \frac{1}{2} \Big[-\mid \pi^+ \, \pi^0 \, \Sigma^- \rangle + \mid \pi^0 \, \pi^+ \, \Sigma^- \rangle - \mid \pi^- \, \pi^0 \, \Sigma^+ \rangle$$
$$+ \mid \pi^0 \, \pi^- \, \Sigma^+ \rangle \Big]$$

$$| 0, 1 \rangle = \frac{1}{\sqrt{6}} \Big[\mid \pi^+ \, \pi^- \, \Sigma^0 \rangle - \mid \pi^- \, \pi^+ \, \Sigma^0 \rangle - \mid \pi^+ \, \pi^0 \, \Sigma^- \rangle$$
$$+ \mid \pi^0 \, \pi^+ \, \Sigma^- \rangle + \mid \pi^- \, \pi^0 \, \Sigma^+ \rangle - \mid \pi^0 \, \pi^- \, \Sigma^+ \rangle \Big]$$

$$| 1, 0 \rangle = -\frac{1}{\sqrt{3}} \Big[\mid \pi^0 \, \pi^0 \, \Sigma^0 \rangle + \mid \pi^+ \, \pi^- \, \Sigma^0 \rangle + \mid \pi^- \, \pi^+ \, \Sigma^0 \rangle \Big].$$

Similarly, other channels can be projected on the isospin

base defined by the total isospin of the system and that of the two meson system.

3.4   Results

We plot the squared $\langle I, I_{sub} | T_R^* | I, I_{sub} \rangle$ amplitudes as a function of $\sqrt{s}$ and $\sqrt{s_{23}}$ (see Eq. (1.115) for the definition of T_R^*).
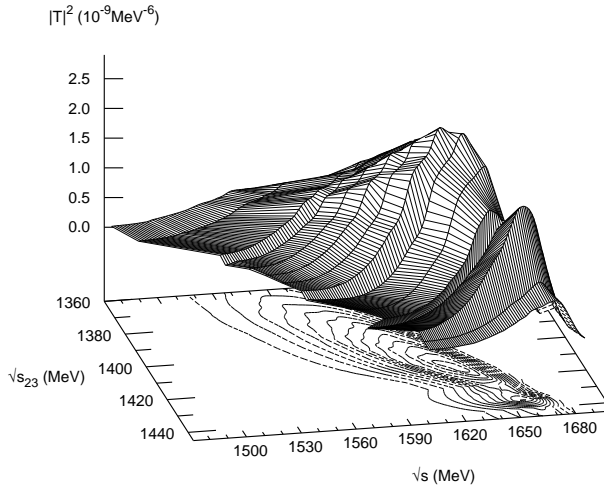
Figure 3.1: Two Σ resonances in the $\pi\pi\Sigma$ amplitude in $I = 1$, $I_\pi = 2$ configuration.

In Fig.3.1, we show a plot of the squared T_R^*-matrix and its projection, for the $\pi\pi\Sigma$ channel in the total isospin $I = 1$ configuration obtained for the two pions in isospin $I_\pi = 2$. We see two peaks; one at $\sqrt{s} = 1656$ MeV with the full width at half maximum ~ 30 MeV and another at $\sqrt{s} = 1630$ MeV with $\Gamma = 39$ MeV. We identify the peak at $\sqrt{s} = 1656$ MeV with the well established $\Sigma(1660 - i100/2)$ [22] as a resonance in the $\pi\pi\Sigma$ system. It is interesting to recall that the excitation of this resonance is claimed in the study of the $K^- p \to \pi^0 \pi^0 \Sigma^0$

reaction [23]. Note that since we are plotting the squared amplitude, which would be proportional to a cross section of a certain process, we can associate our results to the ordinary masses of the PDG and not to the "pole positions" also quoted there.

The peak in squared T_R^*-matrix observed at 1630 MeV with a width of 39 MeV needs a special attention. The two-star resonance $\Sigma(1620)$ [22], though listed as a $1/2^-$ state, seems to be a very unclear case. The partial wave analysis and the production experiments have been kept separately in [22] since it is difficult to know the quantum numbers from the production experiments and if more than one resonance contributes to a single bump. Interestingly, there is a $1/2^+$ state found by the partial wave analysis work of martin et. al. [86] in this region. The authors of [86] use a multichannel partial wave analysis of the $\bar{K}N$ data and find a resonance at 1597 MeV. This result has however been listed under the $\Sigma(1660)$ in [22]. Another partial wave analysis of the $\bar{K}N \to \Lambda\pi$ reaction made by Armenteros et. al. [87] find a $1/2^+$ P_{11} resonance at 1610 MeV with a width of 60 MeV. These findings would provide some phenomenological support to our claim of a $1/2^+$ Σ resonance around ~ 1620 MeV.

We find two more peaks in the $I = 1$ sector; one at $\sqrt{s} = 1590$ MeV with a width ~ 70 MeV in $I = 1$, $I_\pi = 0$ state and another at $\sqrt{s} = 1790$ MeV with $\Gamma = 24$ MeV in $I = 1$, $I_\pi = 2$ case. The former one supports the existence of the $\Sigma(1560)$ "bump", whose spin-parity is unknown [22]. Our results would associate a $1/2^+$ to the spin-parity of this resonance. The latter finding supports the one-star $\Sigma(1770)$.

Next, we discuss the three isospin zero states obtained in these calculations. First we look at states observed in $\pi\bar{K}N$ with $I_{\pi\bar{K}} = 1/2$. Two peaks in the $\Lambda(1600)$ MeV region have been found at $\sqrt{s} = 1568$ with a width of 60 MeV and at 1700 MeV with $\Gamma=136$ MeV. One should note that the PDG quotes a mass for the $\Lambda(1600)$ between 1560 MeV and 1700 MeV. We should also note the quoting of the PDG concerning this resonance, "There are quite possibly two P_{01} states in this region". Our results reinforce this hypothesis.

Finally, in the $\pi\pi\Lambda$ amplitude for the $I = 0$, $I_\pi = 0$ configuration we find a similar structure at 1740 MeV with the full width at half maximum being 20 MeV (which is shown in Fig.3.2). We identify this peak as the $\Lambda(1810 - i150/2)$ resonance, which is listed as a three-star $1/2^+$ resonance by the particle data group [22]. We note that there is a large variation in the peak positions as well as the widths reported by different partial wave analyses [22] for the $\Lambda(1810)$ resonance (the peak position changes from 1750 MeV to 1850 MeV and the width from 50-250 MeV). The value 1810 MeV is just an average of the results of different partial wave analyses.
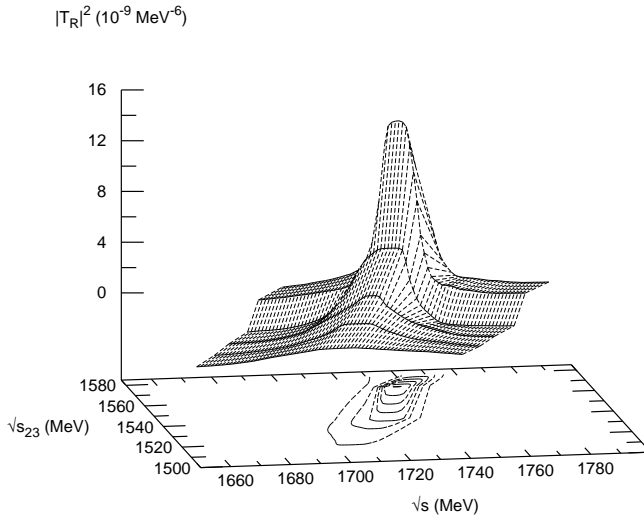

Figure 3.2: The $\Lambda(1810)$ resonance in the $\pi\pi\Lambda$ amplitude in $I = 0$, $I_\pi = 0$.

We do not find any states with exotic isospin.

We have investigated the theoretical uncertainties of the model. We have already mentioned in chapters 2 and 1 that p_{min} and the cut off in the three particle loops do not produce

practically changes in the results. In addition, we have checked the sensitivity of our results to the change in the two body input parameters. We have varied the pion decay constant and the two body cut offs, by about 5%, which still guarantees a fair agreement of our two body cross sections with the experimental ones. We find changes in the peak positions by less than 5 MeV from each source, or 7 MeV when summed in quadrature. This gives us an idea of the accuracy of our results.

The states obtained are not exotic and their quantum numbers can be reached with just three quarks. But our findings imply that in Nature these three quarks states unavoidably couple to two mesons and one baryon, and, that these components overcome the weight of the original three quarks seed. This particular nature could be tested experimentally by means of different reactions, among which, the strong three body decay channels and the radiative decays should play an important role and deserve further theoretical and experimental studies.

We conclude the discussion by emphasizing that all the low lying $1/2^+$ Σ and Λ resonances in the PDG [22], up to the 1800 MeV energy region, get dynamically generated as two meson-one baryon states in these calculations. In addition, we predict the quantum numbers of the $\Sigma(1560)$ and also find evidence for a $1/2^+$ Σ resonance at ~ 1620 MeV. It is rewarding to see that the widths obtained in this work, which correspond to decay into three body systems, are smaller than the total ones to which the two body decay widths also contribute. There would be no contradiction with these two body channels having a smaller weight in the resonance wave functions, as implicitly assumed in our study, and having a fair contribution to the total width, since some of the three body channels to which the resonances couple are kinematically closed for decay, and others which are open have a far smaller phase space than that available for two body decay channels.

We summarize our findings in Table 3.1.

	Γ (PDG) (MeV)	Peak position (this work) (MeV)	Γ (this work) (MeV)
Isospin = 1			
$\Sigma(1560)$	10 - 100	1590	70
$\Sigma(1620)$	10 - 100	1630	39
$\Sigma(1660)$	40 - 200	1656	30
$\Sigma(1770)$	60 - 100	1790	2
Isospin = 0			
$\Lambda(1600)$	50 - 250	1568, 1700	60, 136
$\Lambda(1810)$	50 - 250	1740	20

Table 3.1: A comparison of the resonances found in our work with the states listed by the PDG.

CHAPTER 4

Searching for $1/2^+$, $S = 0$ resonances

In this chapter we take the meson-meson-baryon systems with strangeness zero. We study the $\pi\pi N$ system and coupled channels using as input for the πN interaction, first, the amplitude obtained with the chiral model of [17] and, later, the corresponding one calculated with experimental phase shifts and inelasticities. The results within the two approaches are compatible, indicating, thus, that in our formalism it is possible to use experimental amplitudes as input for the Faddeev equations, since the model does not depend on off-shell parts of the t-matrices. As we will show, the interaction of the three hadrons considered in this case generates dynamically three N^* resonances, two of them listed in the PDG [22], the $N^*(1710)$ and the $N^*(2100)$, and a new one, not listed in the PDG, at 1920 MeV, and one Δ state, the $\Delta(1910)$.

4.1 Introduction

In the previous chapter, the study of systems with strangeness $S = -1$ like $\pi\pi\Sigma$, $\pi\pi\Lambda$, etc., produced resonant states which could be identified with the existing low lying baryonic $J^P = 1/2^+$ two Λ and four Σ resonances. In this chapter we will

see if, in similarity with the $S = -1$ system of the previous chapter, a study of three-hadron channels with $S = 0$ also reproduces all the $1/2^+$ resonances. According to the PDG, in the $S = 0$ sector, there are three N^* resonances, concretely, the $N^*(1440)$, $N^*(1710)$ and the $N^*(2100)$, and two Δ states, the $\Delta(1750)$ and $\Delta(1910)$, with $J^P = 1/2^+$. For the first two N^* resonances, the large branching ratio found experimentally to the $\pi\pi N$ [22] channel already indicates a possibility of interpreting these states as three-body resonances. A study of the $\pi\pi N$ system and coupled channels is thus important in order for clarify the nature of these states.

With this perspective and motivation let us tackle here the investigation of three-body systems with two mesons and a baryon with strangeness $S = 0$.

Before we start, we recall that the work of [17] shows that for the πN interaction the chiral unitary approach using the lowest order chiral Lagrangian provides a fair amplitude up to $\sqrt{s} = 1600$ MeV but fails beyond this energy. For instance, in [17] the $N^*(1535)$ gets dynamically generated but the $N^*(1650)$ does not appear in the approach. As a consequence, any three-body states which could cluster a πN subsystem into this resonance would not be obtained by solving the Faddeev equations with the chiral amplitude of [17]. We will first discuss the study of the $\pi\pi N$ system and its coupled channels made by taking the πN interaction from the correspondent chiral Lagrangian. It will be shown that such a study generates the $N^*(1710)$ which couples almost only to the $\pi\pi N$ channel. But no other $1/2^+$ resonances are found. Next we will investigate the same system but using experimental πN amplitudes and will show that in this case not only we reproduce the $N^*(1710)$ resonance without practically any modification with respect to the case in which chiral amplitudes are used as input in Eq. (1.112), but the use of a more realistic πN interaction at higher energies leads also to the generation of the $N^*(2100)$ and the $\Delta(1910)$ resonances too.

4.2   Studying the $\pi\pi N$ system with chiral amplitudes

Since the Roper and the $N^*(1710)$ resonances are expected to couple strongly to two meson-one baryon channels, we calculate the T_R matrix in Eq. (1.114) in s-wave for fourteen coupled channels: $\pi^0\pi^0 n$, $\pi^0\pi^- p$, $\pi^0 K^+\Sigma^-$, $\pi^0 K^0\Sigma^0$, $\pi^0 K^0\Lambda$, $\pi^0\eta n$, $\pi^+\pi^- n$, $\pi^+ K^0\Sigma^-$, $\pi^-\pi^+ n$, $\pi^-\pi^0 p$, $\pi^- K^+\Sigma^0$, $\pi^- K^0\Sigma^+$, $\pi^- K^+\Lambda$ and $\pi^-\eta p$ as a function of $\sqrt{s}$ and $\sqrt{s_{23}}$ in the energy region 1300-2000 MeV. However, we have checked that the effect of the $\pi K\Lambda$, $\pi K\Sigma$, $\pi\eta\Sigma$ and $\pi\eta\Lambda$ channels in the energy region studied is negligible and the results remain mostly unchanged by using only the five $\pi\pi N$ channels listed above. Since we work with interactions in S wave, all the angle dependent expressions are projected in s-wave. The T_R-matrix (Eq. (1.114)) is then projected on the isospin base defined in terms of the total isospin of the three body system, I, and the total isospin of two pions, $I_{\pi\pi}$, defining the states as $|I, I_{\pi\pi}\rangle$. These states are obtained assuming the phase convention for $|\pi^+\rangle$ as $-|1,1\rangle$. We write the state $|\pi^0\pi^0 n\rangle$, for example, as

$$
\begin{aligned}
|\pi^0\pi^0 n\rangle = & |1,0\rangle \otimes |1,0\rangle \otimes |1/2,-1/2\rangle \\
= & \left\{ \sqrt{\frac{2}{3}} \, |I_{\pi\pi}=2, I_{\pi\pi}^z=0\rangle - \sqrt{\frac{1}{3}} \, |I_{\pi\pi}=0, I_{\pi\pi}^z=0\rangle \right\} \\
& \otimes |1/2,-1/2\rangle \\
= & \sqrt{\frac{2}{5}} \, |I=5/2, I_{\pi\pi}=2\rangle + \frac{2}{\sqrt{15}} \, |I=3/2, I_{\pi\pi}=2\rangle \\
& - \sqrt{\frac{1}{3}} \, |I=1/2, I_{\pi\pi}=0\rangle
\end{aligned}
$$

To simplify the notation, we omit the label I and $I_{\pi\pi}$ and write

$$
|\pi^0\pi^0 n\rangle = \sqrt{\frac{2}{5}} \, |5/2,2\rangle + \frac{2}{\sqrt{15}} \, |3/2,2\rangle - \sqrt{\frac{1}{3}} \, |1/2,0\rangle .
$$

Similarly,

$$| \pi^+ \pi^- n \rangle = -\sqrt{\frac{1}{10}} | 5/2, 2 \rangle - \sqrt{\frac{1}{15}} | 3/2, 2 \rangle - \sqrt{\frac{1}{3}} | 3/2, 1 \rangle$$
$$- \sqrt{\frac{1}{6}} | 1/2, 1 \rangle - \sqrt{\frac{1}{3}} | 1/2, 0 \rangle$$

$$| \pi^- \pi^+ n \rangle = -\sqrt{\frac{1}{10}} | 5/2, 2 \rangle - \sqrt{\frac{1}{15}} | 3/2, 2 \rangle + \sqrt{\frac{1}{3}} | 3/2, 1 \rangle$$
$$+ \sqrt{\frac{1}{6}} | 1/2, 1 \rangle - \sqrt{\frac{1}{3}} | 1/2, 0 \rangle$$

$$| \pi^- \pi^0 p \rangle = \sqrt{\frac{1}{5}} | 5/2, 2 \rangle - \sqrt{\frac{3}{10}} | 3/2, 2 \rangle$$
$$- \sqrt{\frac{1}{6}} | 3/2, 1 \rangle + \sqrt{\frac{1}{3}} | 1/2, 1 \rangle$$

$$| \pi^0 \pi^- p \rangle = \sqrt{\frac{1}{5}} | 5/2, 2 \rangle - \sqrt{\frac{3}{10}} | 3/2, 2 \rangle + \sqrt{\frac{1}{6}} | 3/2, 1 \rangle$$
$$- \sqrt{\frac{1}{3}} | 1/2, 1 \rangle. \tag{4.1}$$

From Eqs. (4.1), one can obtain

$$| 5/2, 2 \rangle = \sqrt{\frac{1}{5}} \left(\sqrt{2} | \pi^0 \pi^0 n \rangle + | \pi^0 \pi^- p \rangle + | \pi^- \pi^0 p \rangle \right.$$
$$\left. - \sqrt{\frac{1}{2}} | \pi^+ \pi^- n \rangle - \sqrt{\frac{1}{2}} | \pi^- \pi^+ n \rangle \right)$$

$$| 3/2, 2 \rangle = \sqrt{\frac{1}{15}} \left(2 | \pi^0 \pi^0 n \rangle - \frac{3}{\sqrt{2}} | \pi^0 \pi^- p \rangle - \frac{3}{\sqrt{2}} | \pi^- \pi^0 p \rangle \right.$$
$$\left. - | \pi^+ \pi^- n \rangle - | \pi^- \pi^+ n \rangle \right) \tag{4.2}$$

$$| 1/2, 0 \rangle = -\sqrt{\frac{1}{3}} \left(| \pi^0 \pi^0 n \rangle + | \pi^+ \pi^- n \rangle + | \pi^- \pi^+ n \rangle \right).$$

One could equivalently define the states in terms of the total isospin and the isospin of a pion-nucleon subsystem ($I_{\pi N}$) by repeating the former procedure or using the Racah coefficients
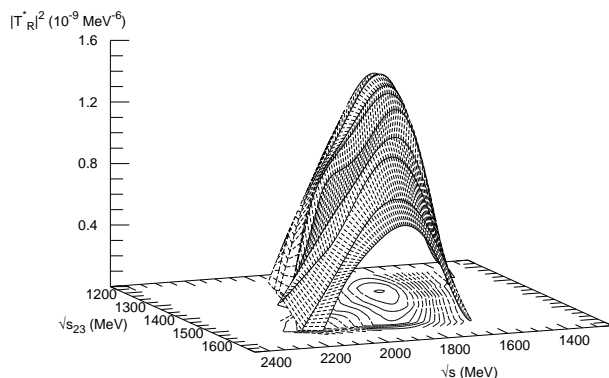
Figure 4.1: *The squared amplitude for the $\pi\pi N$ system in isospin 1/2 configuration as a function of $\sqrt{s}$ and $\sqrt{s_{23}}$.*

for the transformation of the $\mid I, I_{\pi\pi} \rangle$ states to $\mid I, I_{\pi N} \rangle$ states as explained in section 4.1. But we discuss only those amplitudes where we find a resonance.

In Fig. 4.1 we show the squared amplitude $\mid T_R^* \mid^2 = \mid T_R - \sum_{i \neq j=1}^{3} t^i g^{ij} t^j \mid^2$ for the $\pi\pi N$ system, calculated in s-wave and projected on the isospin base $\mid I, I_{\pi\pi} \rangle = \mid 1/2, 0 \rangle$. A peak at $\sqrt{s} = 1704$ MeV, with a full width at half maximum of 375 MeV (see also Fig. 4.2) is found. These results are in good agreement with the characteristics of the $N^*(1710)$ [22] and, hence, we relate the resonance shown in Fig. 4.1 with the $N^*(1710)$. To get further physical meaning of this peak, we show the same amplitude depicted in Fig. 4.1, but as a function of $\sqrt{s_{23}}$ and $\sqrt{s_{12}}$ in Fig. 4.3. The peak in $\sqrt{s_{12}}$ is very wide (width ~ 270 MeV) and is in the energy region of the σ resonance (see also Fig. 4.4). This means that the $N^*(1710)$ has a large $\pi\pi N$ component where the $\pi\pi$ subsystem rearranges itself as the σ reso-
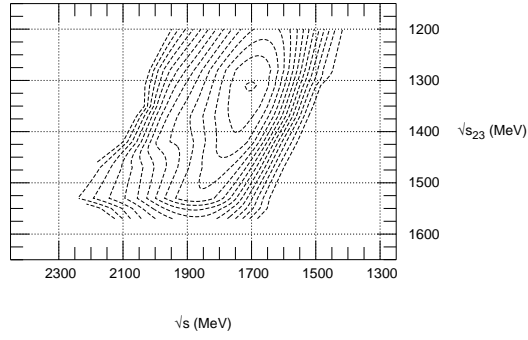
Figure 4.2: *The projection of the amplitude shown in Fig. 4.1.*
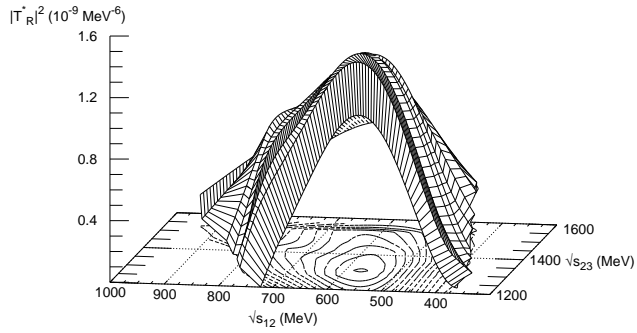

Figure 4.3: *The same as shown in Fig. 4.1 but as a function of the $\pi\pi$ invariant mass and that of the πN system.*
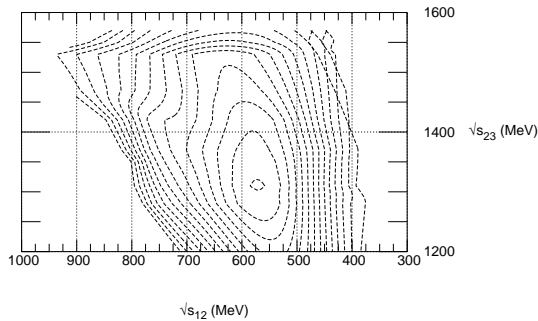
Figure 4.4: *The projection of the amplitude shown in Fig. 4.3*

nance. This gives a natural explanation for the large width of the $N^*(1710)$. The peak position and the width obtained from the $\pi\pi N$ amplitude in s-wave, where the $\pi\pi$ subsystem forms the σ resonance, show that our results are in good agreement with the information available from experimental analyses [22].

Although we find evidence for the $N^*(1710)$, this work fails to find any clear trace of the Roper resonance, which means that considering the $\pi\pi N$ system in s-wave interaction does not suffice to generate the Roper resonance, which is not surprising. Other works such as the Juelich model [44], which successfully describes the dynamical generation of the Roper resonance, contains additional information on the πN, $\pi\Delta, \rho N$ coupled channels and σN forces beyond the three body contact term of the chiral Lagrangians which we include here and which cancels the off-shell dependence of the amplitudes. An important contribution of the $\pi\Delta$ channel and $\pi\pi$ final state interaction (with one of the pions coming from the decay of the Δ resonance) to the Roper resonance has also been claimed in [88]. Such informa-

tion is not present in our formalism. Things are different in the case of the $N^*(1710)$ with its large empirical coupling to $\pi\pi N$ and weaker to πN and other coupled channels.

We also do not find any resonance corresponding to the $N^*(2100)$, $\Delta(1750)$ and $\Delta(1910)$. In any case, we did not expect to find any resonance in the energy region beyond 1800 MeV, since for that the πN t matrix is to be calculated for an invariant mass greater than 1600 MeV, where we know that our input is not good. Also, other three-body coupled channels may play an important role at these energies which we removed since they did not contribute much in the generation of the $N^*(1710)$.

Another important result of this work is that we do not find any resonant structure in the total isospin $I = 3/2$ and $I = 5/2$ configuration. Should we have found the latter, it would be exotic in the sense that it would not be possible to construct it with just three quarks.

4.3 Beyond the chiral description of the πN interaction

The total energy range studied in the previous section corresponded to a variation of the invariant masses of the πN pairs up to ~ 1550 MeV. The calculations developed there are limited to this energy range because, as it was mentioned in the Introduction, the input πN t-matrix used in that work was taken from [17] which reproduces the πN scattering data well up to about 1600 MeV.

The motivation in this section is to extend the previous calculations to higher energies by including the $N^*(1535)$ and $N^*(1650)$ in the input πN t-matrix and look for the other three-body isospin 1/2 and 3/2 states with $J^P = 1/2^+$ in the $\pi\pi N$ system and coupled channels. In order to do this, we use the experimental $L = 0$ phase shifts (δ) and inelasticities (η) [89] for the πN system in isospin 1/2 and 3/2 configurations (Fig. 4.5, 4.6) and calculate from them the πN amplitudes in the
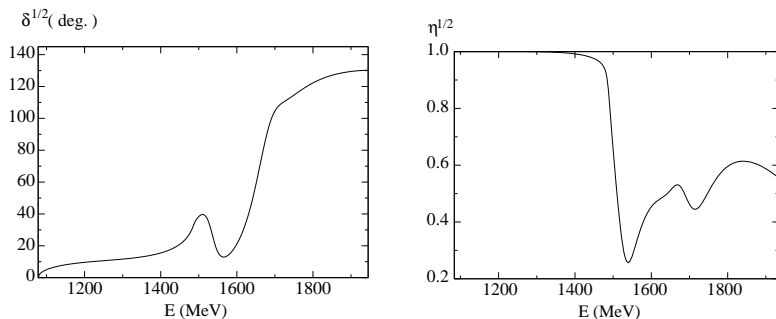
Figure 4.5: Experimental phase shifts and inelasticity for the πN interaction in isospin 1/2.
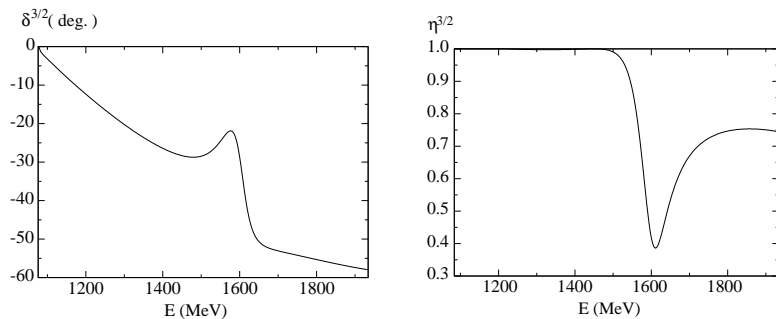
Figure 4.6: Experimental phase shifts and inelasticity for the πN interaction in isospin 3/2.

isospin base (Fig. 4.7) using the relation

$$t^I = -\frac{4\pi E}{M}f^I, \quad \text{I=1/2, 3/2} \tag{4.3}$$

with

$$f^I = \frac{\eta^I e^{2i\delta^I} - 1}{2iq} \tag{4.4}$$

where η^I is the inelasticity, δ^I the phase shift, M is the nucleon mass, E is the πN center of mass energy and q is the corresponding momentum.

We require the input two-body t-matrices in the charge base to solve the Faddeev equations in our model. For this we use

$|t^{1/2}|^2 (10^{-4}\,\text{MeV}^{-1})$

$|t^{3/2}|^2 (10^{-4}\,\text{MeV}^{-1})$

Figure 4.7: Experimental t-matrices for the πN interaction in isospin $1/2$ and $3/2$.

the relations

$$t_{\pi^0 n \to \pi^0 n} = \frac{2}{3}t^{3/2} + \frac{1}{3}t^{1/2}, \quad t_{\pi^0 n \to \pi^- p} = \frac{\sqrt{2}}{3}t^{3/2} - \frac{\sqrt{2}}{3}t^{1/2},$$

$$t_{\pi^- p \to \pi^- p} = \frac{1}{3}t^{3/2} + \frac{2}{3}t^{1/2}, \quad t_{\pi^- n \to \pi^- n} = t^{3/2},$$

$$t_{\pi^+ n \to \pi^+ n} = t_{\pi^- p \to \pi^- p}, \quad t_{\pi^0 p \to \pi^0 p} = t_{\pi^0 n \to \pi^0 n}, \tag{4.5}$$
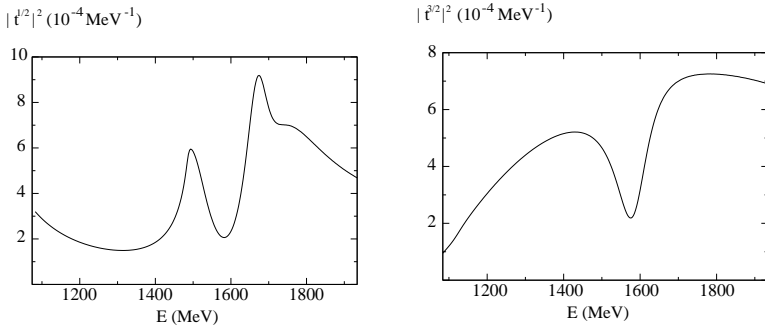
$$t_{\pi^0 p \to \pi^+ n} = -t_{\pi^0 n \to \pi^- p}.$$

Using these πN t-matrices as input for Eqs. (1.41), we can extend the model for the $\pi\pi N$ interaction of [57] to higher energies where the invariant masses of the πN subsystems can be varied around 1650 MeV.

At this point we would like to make some comments about the cancellation of the off-shell part of the t-matrices with the three-body forces discussed in section 1.3.1. There, in order to prove the cancellation we have made used of chiral amplitudes. This is fine for the $S = -1$ system studied in chapter 3. However, the situation is different for $S = 0$, since, as mentioned in the introduction, the results of the calculations done with the lowest order chiral Lagrangian already fail beyond the total energy of 1600 MeV of the πN system. Thus we could formally make no claims in this region about cancellations between the off-shell part of the T_R-matrices and the three-body forces.

However, we also insist on the fact that the results cannot depend on the off-shell part of the amplitudes, because these are unphysical.

The finding of the exact cancellation of the off-shell part with the three-body forces is very useful because it implies that the Faddeev equations can be solved using only the physical information, that is the on-shell amplitudes. This feature certainly must sustain even when one goes beyond that realm where the lowest order chiral Lagrangian reproduces the experimental data. Further, one could also wonder if such a cancellation would also occur in those cases where the higher order terms of the Lagrangian would be necessary. Technically our assertion, that one can use only the on-shell amplitudes, is rigorous as long as the amplitudes obtained with the lowest order chiral Lagrangian, upon unitarization, can reproduce the experimental data. This seems to be the case, for example, in S=-1 systems, for the energy range considered here. Indeed, calculations done in [10] using higher order terms of the Lagrangians show that the results obtained by using the lowest order Lagrangian fall well within the accepted uncertainties in the model. It would be interesting to study cancellations similar to those found in section 1.3.1 for the present case by using higher order Lagrangians but this is beyond the scope of this Thesis.

It should be also said, when using higher order terms in the Lagrangians, that although the elimination of the off-shell (unphysical) part is guaranteed, because the results cannot depend on unphysical amplitudes, it is not clear that the cancellation mentioned above would not leave some finite remanent part. It is also not guaranteed that, apart from three-body forces originating from the chiral Lagrangians, there are no other genuine three-body forces which would remain after necessary cancellations of off-shell terms.

However, let us make the following observation. We used a theory suited to the study of the $\pi\pi N$ system up to $\sqrt{s} \simeq 1750 - 1850$ MeV and concluded that one can study the system using only on-shell amplitudes, which one can get from experi-

ment. Although proved within a certain theory, the conclusion "one can use Faddeev equations with experimental amplitudes" is not linked to any model. With this in mind we make an ansatz that this conclusion should not be linked to the theory used to prove it and should be a characteristic of the dynamics of these systems for a wider range of energies than the one where we could establish a proof based on a particular theoretical framework.

After all we will only extend our calculation to energies up to $\sqrt{s} \simeq 2200$ MeV which is not too far from the energies at which the calculations were made earlier. Although certainly it is an ansatz at these higher energies, our assumption that one can rely solely upon the on-shell amplitudes in the Faddeev approach gets a strong support from the results that we obtain in the present work.

4.3.1 Exploring the $\pi\pi N$ system through experimental amplitudes

We first study the $\pi\pi N$ system with total charge zero considering $\pi^0\pi^0 n$, $\pi^0\pi^- p$, $\pi^+\pi^- n$, $\pi^-\pi^+ n$ and $\pi^-\pi^0 p$ as coupled channels. We label them as particle 1, 2 and 3 in the order in which they are written above. We calculate the three-body T_R^{ij} matrices (Eqs. (1.41)) by using, for the πN interaction: (a) experimental amplitudes, i.e., Eq. (4.3) with the phase shifts and inelasticities shown in Fig. 4.5, when the invariant mass of πN system is above its threshold (b) and the t-matrix obtained from chiral Lagrangian [17] for those πN total energies which fall below threshold. For the $\pi\pi$ interaction we use the t-matrix obtained and studied thoroughly in [2], where the dynamical generation of the $\sigma(600)$, $f_0(980)$ and $a_0(980)$ resonances was found and the theoretical results for physical observables coincided well with the experimental ones. We take proper symmetrized amplitudes into account wherever necessary, for instance, for the $\pi^0\pi^0$ subsystem in the $\pi^0\pi^0 N$ channel.

In order to be consistent with the results of section 4.2, we

first check if we find an evidence for the $N^*(1710)$. For this, we obtain the amplitude for total isospin of the three particles $I=1/2$ and for the isospin of the $\pi\pi$ subsystem, denoted by $I_{\pi\pi}$, being equal to zero, i.e., we calculate $\langle I = 1/2, I_{\pi\pi} = 0|T_R(\sqrt{s}, \sqrt{s_{23}})|I = 1/2, I_{\pi\pi} = 0\rangle$ (see the definition of the $|I = 1/2, I_{\pi\pi} = 0\rangle$ state in the previous section).

We find exactly the same peak at 1704 MeV in the squared amplitude as obtained in Fig.s 4.1 -4.4. In this way, we ensure that we reproduce our previous results by using the experimental data for the πN interaction above the πN threshold. With this assurance, we now look for resonances in the higher energy region in same or other isospin configurations.

We now study the $\pi\pi N$ amplitudes for the case in which the isospin of the subsystem of particle 2 and 3, i.e., pion nucleon (and its coupled channels) is $1/2$ in the initial as well as the final state. To obtain this amplitude we write the $\pi\pi N$ states in the isospin base as

$$
\begin{aligned}
| \pi^0 \pi^0 n \rangle =& | 1,0\rangle \otimes | 1,0\rangle \otimes | 1/2, -1/2\rangle \\
=& | 1,0\rangle \otimes \left\{ \sqrt{\frac{2}{3}} \, | I_{\pi N} = 3/2, I_{\pi N}^z = -1/2\rangle \right. \\
& \left. + \sqrt{\frac{1}{3}} \, | I_{\pi N} = 1/2, I_{\pi N}^z = -1/2\rangle \right\} \\
=& \sqrt{\frac{2}{5}} \, | I = 5/2, I_{\pi N} = 3/2\rangle \\
& + \frac{1}{3}\sqrt{\frac{2}{5}} \, | I = 3/2, I_{\pi N} = 3/2\rangle \\
& - \frac{\sqrt{2}}{3} \, | I = 1/2, I_{\pi N} = 3/2\rangle \\
& + \frac{\sqrt{2}}{3} \, | I = 3/2, I_{\pi N} = 1/2\rangle \\
& + \frac{1}{3} \, | I = 1/2, I_{\pi N} = 1/2\rangle.
\end{aligned}
$$

Similarly, by omitting the label I and $I_{\pi N}$ to simplify,

$$| \pi^+ \pi^- n \rangle = -\sqrt{\frac{1}{10}} | 5/2, 3/2 \rangle - \sqrt{\frac{2}{5}} | 3/2, 3/2 \rangle$$
$$- \sqrt{\frac{1}{2}} | 1/2, 3/2 \rangle$$

$$| \pi^- \pi^+ n \rangle = -\sqrt{\frac{1}{10}} | 5/2, 3/2 \rangle + \frac{2}{3}\sqrt{\frac{2}{5}} | 3/2, 3/2 \rangle$$
$$- \frac{1}{3\sqrt{2}} | 1/2, 3/2 \rangle - \frac{\sqrt{2}}{3} | 3/2, 1/2 \rangle$$
$$+ \frac{2}{3} | 1/2, 1/2 \rangle \tag{4.6}$$

$$| \pi^- \pi^0 p \rangle = \sqrt{\frac{1}{5}} | 5/2, 3/2 \rangle - \frac{4}{3\sqrt{5}} | 3/2, 3/2 \rangle \rangle$$
$$+ \frac{1}{3} | 1/2, 3/2 - \frac{1}{3} | 3/2, 1/2 \rangle$$
$$+ \frac{\sqrt{2}}{3} | 1/2, 1/2 \rangle$$

$$| \pi^0 \pi^- p \rangle = \sqrt{\frac{1}{5}} | 5/2, 3/2 \rangle + \frac{1}{3\sqrt{5}} | 3/2, 3/2 \rangle$$
$$- \frac{1}{3} | 1/2, 3/2 \rangle - \frac{2}{3} | 3/2, 1/2 \rangle$$
$$- \frac{\sqrt{2}}{3} | 1/2, 1/2 \rangle.$$

Inverting the above equations we get, for example,

$$| 1/2, 1/2 \rangle = \frac{1}{3}\left(| \pi^0 \pi^0 n \rangle - \sqrt{2} | \pi^0 \pi^- p \rangle \right.$$
$$\left. + \sqrt{2} | \pi^- \pi^0 p \rangle + 2 | \pi^- \pi^+ n \rangle \right) \tag{4.7}$$

$$| 3/2, 1/2 \rangle = \frac{1}{3}\left(\sqrt{2} | \pi^0 \pi^0 n \rangle - 2 | \pi^0 \pi^- p \rangle \rangle \right.$$
$$\left. - | \pi^- \pi^0 p - \sqrt{2} | \pi^- \pi^+ n \rangle \right). \tag{4.8}$$

In Fig. 4.8 we show the squared T_R^* amplitude for $I = 1/2$ and $I_{\pi N} = 1/2$ in the initial and the final state versus the total energy of the three-body system and the invariant mass of the meson-baryon subsystem formed by the second and third particle (πN). A peak around an energy of 2100 MeV with a width of ~ 250 MeV appears when $\sqrt{s_{23}}$ is close to 1670 MeV, thus having a $\pi N^*(1650)$ structure. The peak position and the width of this peak are compatible with the findings of various partial wave analyzes indicated by the PDG [22] about the $N^*(2100)$, for which the peak position is found in the range 1855 - 2200 MeV and the width in the range of 69-360 MeV. Thus we identify this peak with the $N^*(2100)$.
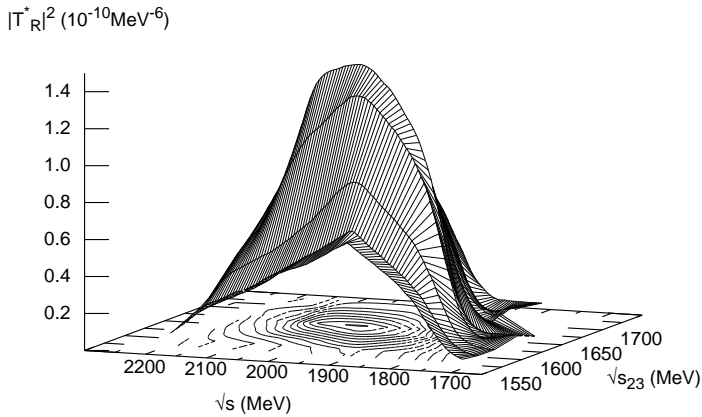

Figure 4.8: The $N^*(2100)$ in the $\pi\pi N$ system with five coupled channels.

Since this peak appears when $\sqrt{s_{23}}$ is close to the mass of
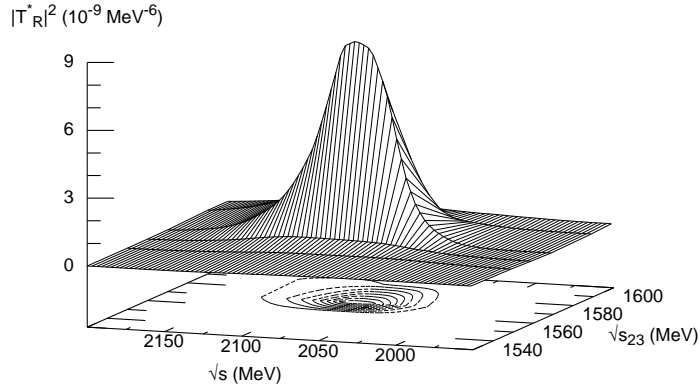
Figure 4.9: The $N^*(2100)$ in the $\pi\pi N$ system including 14 coupled channels.

the N^* (1650) and has been obtained using as input that πN t-matrix which contains the information on the $N^*(1650)$, we conclude that the inclusion of the $N^*(1650)$ in the πN subsystem is essential to generate a resonance at 2100 MeV.

In this former study, we do not find evidence for any resonance in the isospin 3/2 configuration, but the situation is different when we introduce coupled channels, as we discuss below.

4.3.2   Inclusion of the $\pi K\Sigma$, $\pi K\Lambda$ and $\pi\eta N$ channels

Next, we solve the Faddeev equations with fourteen coupled channels: $\pi^0\pi^0 n$, $\pi^0\pi^- p$, $\pi^0 K^+\Sigma^-$, $\pi^0 K^0\Sigma^0$, $\pi^0 K^0\Lambda$, $\pi^0\eta n$, $\pi^+\pi^- n$, $\pi^+ K^0\Sigma^-$, $\pi^-\pi^+ n$, $\pi^-\pi^0 p$, $\pi^- K^+\Sigma^0$, $\pi^- K^0\Sigma^+$, $\pi^- K^+\Lambda$ and $\pi^-\eta p$. Again, we label them as particles 1, 2 and 3 in the order in which they are written above. As there are no data for $K\Sigma \to K\Sigma$, $K\Lambda \to K\Lambda$, etc., we use the model of [17] to calcu-

late the corresponding amplitudes. The πN interaction below threshold is determined using the same model as for $K\Sigma$ and $K\Lambda$ and above the threshold we use the experimental results.

We continue to study those amplitudes where the isospin of the subsystem of particle 2 and 3, i.e., pion nucleon (and its coupled channels), is $1/2$ in the initial as well as the final state. In Fig. 4.9 we show the $\pi\pi N$ amplitude for total isospin $I = 1/2$ for such a case, i.e., $|\langle I = 1/2, I_{\pi N} = 1/2 | T_R^* | I = 1/2, I_{\pi N} = 1/2 \rangle|^2$.

As shown in Fig. 4.9 we obtain a peak at an energy of 2080 MeV with a width of 54 MeV for a $\sqrt{s_{23}}$ near 1570 MeV, which we identify with the $N^*(2100)$ listed in the PDG [22]. Comparison of the Figs. 4.8 and 4.9 shows that the inclusion of the $\pi K \Sigma$, $\pi K \Lambda$ and $\pi \eta N$ channels makes the resonance more pronounced (by an order of magnitude in the squared T_R^*-matrix) and much narrower. These changes in the results can be easily understood with respect to the previous ones obtained with only five coupled channels by noticing that now the wave function of the resonance contains extra components which have smaller phase space in the decay of the resonance. At the same time, the $\pi\pi N$ component becomes smaller due to the normalization of the wave function and, hence, the decay into $\pi\pi N$ is also reduced.

In Fig. 4.10 we plot now the T_R^*-matrix for the $\pi K \Lambda$ channel for total isospin $I = 3/2$ with $I_{K\Lambda} = 1/2$ in the initial and the final state. This amplitude has been calculated by using the relation

$$| I = 3/2, I_{K\Lambda} = 1/2 \rangle = \frac{1}{\sqrt{3}} \left(\sqrt{2} \, | \, \pi^0 K^0 \Lambda \rangle + | \, \pi^- K^+ \Lambda \rangle \right),$$

(4.9)

which has been obtained by writing the $\pi K \Lambda$ states in isospin base analogously to Eqs. (4.6,4.7).

A peak is found in the $\langle I = 3/2, I_{K\Lambda} = 1/2 \, | \, T_R^*(\sqrt{s}, \sqrt{s_{23}}) \, | \, I = 3/2, I_{K\Lambda} = 1/2 \rangle$ amplitude at a total energy of ~ 2126 MeV with ~ 42 MeV of width. In this case, the invariant mass $\sqrt{s_{23}}$, at which the peak appears, is around 1590 MeV. This

peak can be identified with the $\Delta(1910)$ listed in [22], whose position, given by different partial wave analyzes, ranges up to 2070 MeV and the width varies from 190-500 MeV.
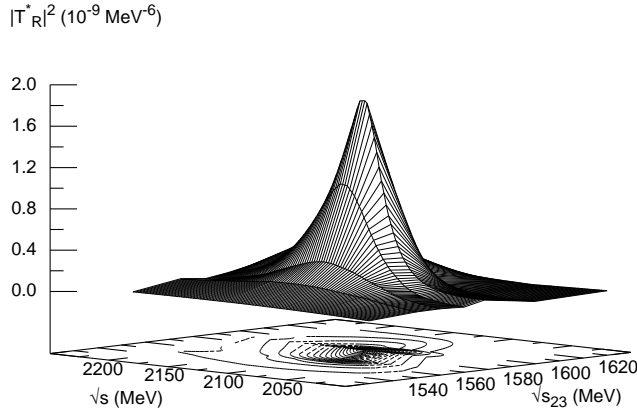
Figure 4.10: The $\Delta(1910)$ in the $\pi K \Lambda$ system including 14 coupled channels.

Thus the introduction of the $\pi K \Sigma$, $\pi K \Lambda$ and $\pi \eta N$ channels, together with the inclusion of the $N^*(1650)$ in the πN t-matrix, is important to get this resonance. One should note that we get smaller widths than the experimental ones. The πN decay channels are not considered in our approach and they should contribute to increase the widths. Note that this can be done even with a small πN component, as implicitly assumed here, since there is more phase space for decay into the πN channel.

We do not find any evidence of the $\Delta(1750)$, which could indicate a different structure for this state than the one studied in this work.

4.4 Exploring the Nf_0 and Na_0 systems

Until now, we have investigated possible resonant states in the $\pi\pi N$ system and its coupled channels which have been obtained by adding a pion to pseudoscalar-baryon systems which couple strongly in $J^\pi = 1/2^-$ and isospin $1/2$ configuration, i.e., πN, $K\Sigma$, $K\Lambda$ and ηN. The invariant mass of this pseudoscalar-baryon subsystem has been varied around that of the $N^*(1535)$ and $N^*(1650)$, hence, treating the three-body system as a πN^* system with $1500 < M_{N^*} < 1760$ MeV, although within the three-body Faddeev equations. There are other configurations of this three-body system, like $Na_0(980)$ and $Nf_0(980)$, which we have not discussed so far.

In order to study such a system, we must take $NK\bar{K}$, $N\pi\pi$ and $N\pi\eta$ as coupled channels, such that the $\pi\pi$ and $K\bar{K}$ subsystem dynamically generate the $f_0(980)$ and the $\pi\eta$ subsystem along with $K\bar{K}$ generates the $a_0(980)$ resonance. In this way, we can study the $Nf_0(980)$ and $Na_0(980)$ systems simultaneously. Concretely, we take the following coupled channels into account: $n\pi^0\pi^0$, $p\pi^0\pi^-$, $n\pi^0\eta$, $n\pi^+\pi^-$, $n\pi^-\pi^+$, $p\pi^-\pi^0$, $p\pi^-\eta$, nK^+K^-, $nK^0\bar{K}^0$, pK^0K^-. We label the particles as 1, 2, 3 in the order in which they are written above. This means that the subsystem of particles 2 and 3 consists of two pseudoscalar mesons whose invariant mass, $\sqrt{s_{23}}$, is varied around 980 MeV. With these channels we solve the Eqs. (1.41) in the same formalism which we have explained in the previous sections. In this case we find that the $NK\bar{K}$ amplitude is bigger in magnitude as compared to those of the other coupled channels. We thus make isospin combinations of the $NK\bar{K}$ channels, similarly to Eqs. (4.6, 4.7) and obtain the amplitude for total isospin $I = 1/2$ and the isospin of the $K\bar{K}$ system, $I_{K\bar{K}}$, equal to 0 or 1.

In the case of total isospin of the $NK\bar{K}$ system equal to $1/2$ with the isospin of the $K\bar{K}$ subsystem equal to one the amplitude

$$\langle I = 1/2, I_{K\bar{K}} = 1 \mid T_R^*(\sqrt{s}, \sqrt{s_{23}}) \mid I = 1/2, I_{K\bar{K}} = 1\rangle, \quad (4.10)$$

shows a peak around 2080 MeV , with a width of 51 MeV (which

we do not show here), which we relate as the $Na_0(980)$ partner
of the peaks shown in Figs. 4.8 and 4.9. Thus the peak corre-
sponding to the $N^*(2100)$ has been seen in $\pi\pi N$ system as well
as in the $NK\bar{K}$ system.

Interestingly, along with this $N^*(2100)$ state, we find an-
other peak with even larger magnitude of the squared three-
body amplitude at $\sqrt{s} = 1924$ MeV with a width of 20 MeV.
We show this peak in Fig. 4.11 for the $NK\bar{K}$ channel.
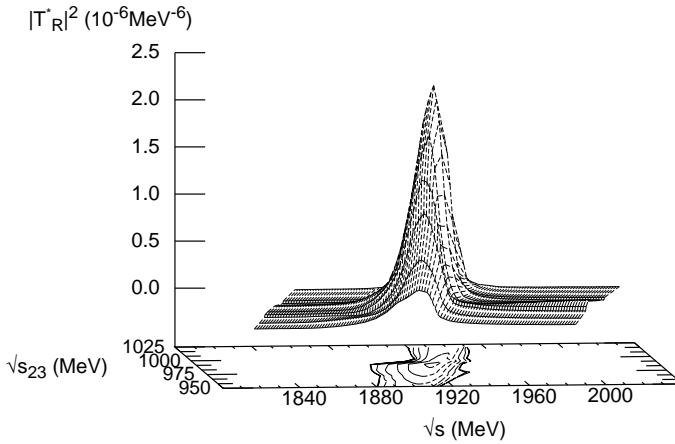
Figure 4.11: A possible $N^*(1910)$ in the $NK\bar{K}$ channels.

This state is about 7 MeV below the $NK\bar{K}$ threshold (as-
suming an average mass for the kaons of 496 MeV and 939
MeV for the nucleon). Therefore, this result indicates that the
$Na_0(980)$ system gets bound at around 1920 MeV. This pos-
sibility has been already suggested by the authors in [71], in
which they study the $NK\bar{K}$ channel using effective two-body
potentials to describe the $\bar{K}N$, $\bar{K}K$, KN interactions. They
find that the $NK\bar{K}$ system can get bound while the $K\bar{K}$ sub-

system acts like the a_0. Our result is, thus, in agreement with the suggestions in [71]. Interestingly, the existence of a $1/2^+$ N^* resonance around 1935 MeV has also been proposed earlier [90] on the basis of a study of the data on the $\gamma p \to K^+\Lambda$ reaction in an isobar model, although other theories [91] which include explicitly resonances up to 1855 MeV can reproduce these data (further work along these lines to include higher mass resonances is under way [92]).

Since this peak found at 1920 MeV is below the three-body threshold and, in the two-body problem, the poles for the $f_0(980)$ and $a_0(980)$ appear below the $K\bar{K}$ threshold, the three particles in the system have associated complex momenta in the momentum representation. To avoid the use of unphysical complex momenta in the three-body system, which will lead to imaginary energies in the real plane, we give a minimum value, around 50 MeV, to the momentum of the particles as explained in section 2.1. We have checked the sensitivity of our results to the mentioned choice by changing the minimum momentum from 50 MeV to 100 MeV and we find the peak and width to remain almost unchanged.

We also made the total isospin $1/2$ combination of the $NK\bar{K}$ system by considering the $K\bar{K}$ subsystem in isospin 0 in the initial and the final state, i.e., considering the $Nf_0(980)$ component of the $NK\bar{K}$ channel. In this case too, just as in the amplitude for $Na_0(980)$, we find a peak around 1923 MeV with a width of 30 MeV and another one around 2052 MeV with a width of 60 MeV. The magnitude of the $Nf_0(980)$ amplitude around 1920 MeV is very similar to the one of the $Na_0(980)$ amplitude (i.e., the one shown in Fig. 4.11), but the magnitude of $Nf_0(980)$ amplitude around 2050 MeV is bigger than the magnitude of the $Na_0(980)$ amplitude.

From the whole study we would conclude that there are two N^*'s with $J^\pi = 1/2^+$ in the energy region $1800 < \sqrt{s} < 2200$ MeV.

4.5   Conclusions

We can summarize the results of this study as follows:

1. We have first studied the $\pi\pi N$ system in s-wave, thus in
   $J^\pi = 1/2^+$ configuration, using unitary chiral amplitudes.
   We find a resonance at 1704 MeV, which can be associated
   with the $N^*(1710)$ [22]. The peak has a full width $\Gamma =$
   375 MeV to be compared with that of the $N^*(1710)$ which
   ranges from 90-500 MeV [22]. We find that the invariant
   mass of the $\pi\pi$ subsystem falls in the region of the mass
   of the σ (500 -i 200 MeV) when the $\pi\pi N$ amplitude peaks
   at $\sqrt{s} = 1704$ MeV, which means that the large width of
   the $N^*(1710)$ could be related to that of the σ resonance
   formed in the $\pi\pi$ subsystem. We do not find other N^*
   or Δ resonances with $J^P = 1/2^+$. The Roper resonance,
   although it has an important coupling to $\sigma(500 - i200)N$,
   does not show up in our approach. This should not be seen
   as a negative result, but as an evidence that the structure
   of the Roper is far more complex than that envisaged by
   the $\pi\pi N$ interaction in s-wave, which is what we have
   investigated in the present work. No evidence for states
   with $I = 3/2$ and $I = 5/2$ is found in this work

2. After studying the $\pi\pi N$ system using chiral amplitudes
   for the description of the πN interaction, we have ex-
   tended the study of the $\pi\pi N$ system to higher energies
   by using the experimental data for the πN interaction,
   which contains the information on excitation of both the
   $N^*(1535)$ and the $N^*(1650)$. The latter N^* was absent
   within the chiral πN t-matrix. Here, apart from confirm-
   ing the $N^*(1710)$, we find evidence for the other $1/2^+$
   N^*, i.e., the $N^*(2100)$, and also for the $1/2^+$ $\Delta(1910)$
   resonance. The findings reported here indicate that the
   inclusion of the $N^*(1650)$ in the interaction of the πN
   subsystem is essential to generate these higher mass $1/2^+$
   resonances.

- We have first made a search taking only the $\pi\pi N$ channels where a resonance having the properties of $N^*(2100)$ was found.

- No isospin 3/2 resonances is found in the study of the $\pi\pi N$ channels alone.

- On including the $\pi K\Sigma$, $\pi K\Lambda$ and $\pi\eta\Sigma$ channels, the same resonance around 2100 MeV is produced but with larger magnitude and narrower width, indicating the addition of more channels to which the resonance couples strongly.

- The $\Delta(1910)$ is found on inclusion of the $\pi K\Sigma$, $\pi K\Lambda$ and $\pi\eta\Sigma$ channels in the isospin $I = 3/2$ amplitude.

- Further, we have investigated the $NK\bar{K}$, $N\pi\pi$ and $N\pi\eta$ channels where the $K\bar{K} - \pi\pi$ subsystem rearranges itself as a $f_0(980)$ resonance, while $K\bar{K} - \pi\eta$ acts like the $a_0(980)$. We obtain a new peak at ~ 1924 MeV, apart from the one corresponding to the $N^*(2100)$, with a strong coupling to $Na_0(980)$ and $Nf_0(980)$.

3. Finally the resonances found here show that the three-body component is large and dominant in the wave function of these resonances. Though this does not exclude contributions from πN or genuine three quarks components, they must be relatively suppressed. One could aim at including such additional components in a coupled channel formalism. The realization of the important role of the two meson cloud in the structure of the resonance is a very novel result to which one should pay attention when exploring other static or dynamical properties of the resonance.

We conclude this chapter by stating that the study of three-body systems, for the cases where a complete theoretical two-body input is not available, is also possible in our formalism using on-shell experimental amplitudes.

Clues for a new N^* state around 1920 MeV

In the last chapter, we have obtained a bound state of $NK\bar{K}$ around 1920 MeV with $J^P = 1/2^+$ when the $K\bar{K}$ system is resonating like the $f_0(980)$ or the $a_0(980)$. In this chapter, we provide a series of arguments which support the idea that the peak seen in the $\gamma p \to K^+\Lambda$ reaction around 1920 MeV should correspond to the mentioned state. At the same time we propose polarization experiments for this reaction as a further test of the prediction, as well as a study of the total cross section for the $\gamma p \to K^+K^-p$ reaction at energies close to threshold and the mass distribution of the two kaons.

5.1 Introduction

The theoretical interest in three-hadron systems other than the traditional three-nucleon states is old. In [93] a study of a possible system of $K\pi N$ was made, based only on symmetries. More recently, a possible $\bar{K}NN$ bound state has been the object of intense study [59–64]. However, our efforts have proved to be a qualitative step forward in this topic, which has been made possible by combining elements of unitarized chiral perturbation theory $U\chi PT$ [2–4,9,94–96], with Faddeev equations in coupled

channels. In chapter 3 systems of two mesons and one baryon with strangeness $S = -1$ were studied, finding resonant states which could be identified with the existing low-lying baryonic $J^P = 1/2^+$ resonances, two Λ and four Σ states. Similarly, in the case of the $S = 0$ sector the $N^*(1710)$ appears neatly as a resonance of the $\pi\pi N$ system, as well as including the channels coupled to $\pi\pi N$ within SU(3). Further studies, including a realistic πN amplitude beyond the $N^*(1535)$ region to which the chiral theories are limited, give rise to other $S = 0$, $J^P = 1/2^+$ states, more precisely, the $N^*(2100)$ and the $\Delta(1910)$ (all this has been discussed in the previous chapter).

Independently, interesting studies based on variational methods have been made [71, 97]. In particular, in Ref. [71] a bound state of $K\bar{K}N$ with $I = 1/2, J^P = 1/2^+$ was found around 1910 MeV in the configuration $a_0(980)N$, suggesting a bound state of the $a_0(980)$ and a nucleon. Since the $K\bar{K}$ system couples to $\pi\pi$ and $\eta\pi$ channels to generate the $f_0(980)$ and $a_0(980)$ resonances, a more complete coupled channel study using Faddeev equations was called for, and this was done within our formalism, as discussed in section 4.3.1, where it was concluded that a state appears indeed around this energy, mostly made of $K\bar{K}N$ but as a mixture of $a_0(980)N$ and $f_0(980)N$.

A N^* state with these characteristics is not catalogued in the PDG [22]. However, there is a peak in the $\gamma p \to K^+\Lambda$ reaction at around 1920 MeV, clearly visible in the integrated cross section and also at all angles from forward to backward [98–100]. The $\gamma p \to K^+\Lambda$ reaction has been the object of intense theoretical study [90, 101–104] (see [105] for a recent review). With respect to our present investigation, the possible signal for a new resonance from the peak of the cross section around 1920 MeV was already suggested in [90]. However, no spin and parity assignment were given, since there were several candidates in this region related to the missing resonances of the quark models. Other theoretical studies do not make use of this extra state, as in [101], although in this latter work only resonances with mass

up to 1855 MeV were included[1]. In a recent combined analysis of the $\gamma p \to K^+\Lambda$ reaction with other reactions [106], a claim for a N^* resonance around 1900 MeV was made, however, the resonance was assumed to have $J^P = 3/2^+$. Note in this respect that the PDG quotes in its latest edition that there is no evidence for this resonance in the latest analysis of the GWU group [107]. The state around this energy found in [8, 108] has instead $J^P = 1/2^+$ quantum numbers.

As one can see, the situation concerning this state and its possible nature is far from settled. In this chapter we collect several arguments to make a case in favor of the state predicted in [71] with $J^P = 1/2^+$ and confirmed by us.

5.2 Comparison of the $\gamma p \to K^+\Lambda$ and $\gamma p \to K^+\Sigma^0$ reactions

A peak of moderate strength on top of a large background is clearly seen for the $\gamma p \to K^+\Lambda$ reaction around 1920 MeV at all angles (see Fig. 18 of [99]). One can induce qualitatively a width for this peak of about 100 MeV or less. On the other hand, if one looks at the $\gamma p \to K^+\Sigma^0$ reaction, one finds that starting from the threshold a big large and broad structure develops, also visible at all angles (see Fig. 19 of [99]). The width of this structure is about 200-300 MeV. One can argue qualitatively that the relatively narrow peak of the $\gamma p \to K^+\Lambda$ reaction around 1920 MeV on top of a large background has nothing to do with the broad structure of $\gamma p \to K^+\Sigma^0$ around 1900 MeV. A more quantitative argument can be provided by recalling that in [109] the broad structure of the $\gamma p \to K^+\Sigma^0$ is associated to two broad Δ resonances in their model, which obviously can not produce any peak in the $\gamma p \to K^+\Lambda$ reaction, which filters isospin 1/2 in the final state. Certainly, part of the structure is background, which is already obtained in chiral unitary theories at the low energies of the reaction [104].

---

[1]Work to include more resonances in the approach of [101] is underway [92]
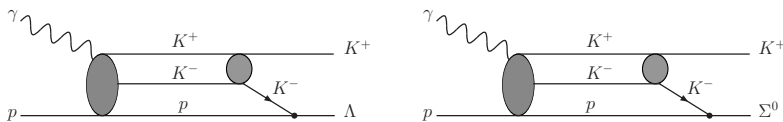
Figure 5.1: Diagrams depicting the $\gamma p \to K^+\Lambda$, $\gamma p \to K^+\Sigma^0$ processes through the $1/2^+$ N^* K^+K^-N resonance of [71, 108].

We believe that the peak in the $\gamma p \to K^+\Lambda$ reaction is a genuine isospin $1/2$ contribution which does not show up in the $\gamma p \to K^+\Sigma^0$ reaction. This feature would find a natural interpretation in the picture of the state proposed in [71, 108]. Indeed, in those works the state at 1920 MeV is a $K\bar{K}N$ system in relative s-waves for all pairs. The $\gamma p \to K^+\Lambda$ and $\gamma p \to K^+\Sigma^0$ reactions proceeding through the excitation of this resonance are depicted in Fig. 5.1. The two reactions are identical in this picture, the only difference being the Yukawa coupling of the K^- to the proton to generate either a Λ or a Σ^0.

The Yukawa couplings in SU(3) are well known and given in terms of the F and D coefficients [76], with $D + F = 1.26$ and $D - F = 0.33$ [104, 110]. The particular couplings for $K^-p \to \Lambda$ and $K^-p \to \Sigma^0$ are e.g. given in [111].

$$
\begin{aligned}
V_{K^-p\to\Lambda} &= -\frac{2}{\sqrt{3}}\frac{D+F}{2f} + \frac{1}{\sqrt{3}}\frac{D-F}{2f} \\
\\
V_{K^-p\to\Sigma^0} &= \frac{D-F}{2f}
\end{aligned}
\tag{5.1}
$$

with f the pion decay constant. Hence, the couplings are proportional to -1.26 and 0.33 for the $K^-p \to \Lambda$ and $K^-p \to \Sigma^0$ vertices, respectively. Therefore, it is clear that in this picture the signal of the resonance in the $\gamma p \to K^+\Lambda$ reaction is far larger than in the $\gamma p \to K^+\Sigma^0$ one, by as much as an order of magnitude in the case that the resonance and background contributions sum incoherently. The $3/2^+$ resonance used in the analysis of the $\gamma p \to K^+\Lambda$ reaction in [106] is also used for

the $\gamma p \to K^+ \Sigma^0$ reaction in that work and also gives a smaller contribution in this latter case. In the picture of [71, 108] the $1/2^+$ resonance also appears in the $\gamma p \to K^+ \Sigma^0$ reaction but with a smaller intensity than in the $\gamma p \to K^+ \Lambda$ one, as we have mentioned.

5.3   Pion induced reactions

The fact that a N^* resonance around 1900 MeV is not reported in the PDG tables finds a natural interpretation from our work and that of [71]. Indeed, since most of the information about resonances is obtained from πN reactions, it is easy to understand why this resonance did not appear in these reactions. Once again, in our framework and in that of [71], the pion induced reactions going through the resonance would proceed as shown in Fig. 5.2a.
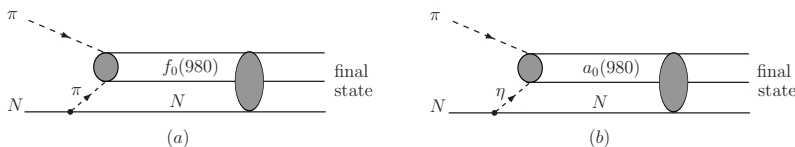
Figure 5.2: Diagrams for π induced reactions exciting the $1/2^+$ resonance of [8, 108].

As we can see from Fig. 5.2, the fact that the $f_0(980)$ has a small coupling to the $\pi\pi$ channels [2], as reflected by its small decay width, necessarily weakens the strength of the pion induced reactions producing the resonance, compared to other processes. Since the wave function of the state has also an $a_0(980)N$ component, in this case the mechanism would be the one of Fig. 5.2b, since the $a_0(980)$ has also a small coupling to $\eta\pi$. This, and also the small ηNN coupling (see e.g. Ref. [112]), make again the mechanism of production very weak.

It is also possible to devise some indirect method to create the $N f_0(980)/a_0(980)$ intermediate states. One can devise the mechanisms of Fig. 5.3. The diagram of Fig. 5.3a involves the

Figure 5.3: Possible indirect mechanism for the $\pi N \to N f_0(980)/a_0(980)$.

$\pi N \to K\Lambda(1405)$ transition while the one of Fig. 5.3b involves the $\pi N \to K\Lambda$ one. The strength of the former amplitude is much weaker than that of the second one as one can induce from experimental cross sections [113, 114] and the associated amplitudes [17, 46]. However, the s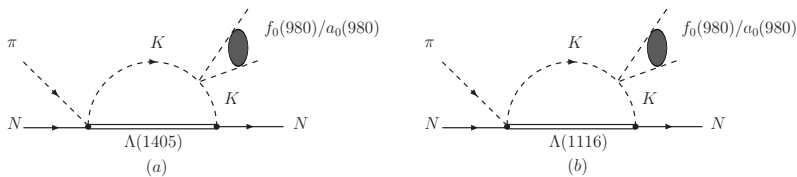econd one is penalized by the p-wave coupling $KN\Lambda$ in the loop, where the two other vertices are in s-wave. As a general rule, loops are reduced with respect to tree level amplitudes, but in the present case the structure of these loops, with a meson-meson $\to$ meson-meson vertex, makes the contribution very small as a direct evaluation of the diagrams shows [13].

In this respect it is also very illustrative to see that in [106] a large set of reactions was analyzed, and in Table 1 of the paper it was shown that the resonance around 1900 MeV had a weight bigger than 1 % only in the $\gamma p \to K^+\Lambda$ and $\gamma p \to K^+\Sigma^0$ reactions. This means that the weight of this resonance in the $\gamma p \to \pi N$, $\gamma p \to \eta N$, $\gamma p \to \pi\pi N$, $\gamma p \to \pi\eta N$ and $\pi N \to \pi\pi N$, analyzed there, is negligible. This would again find a natural explanation along the lines discussed above if one looks at the mechanisms for these reactions depicted in Fig. 5.4 which are all suppressed, since they always involve the coupling of the $f_0(980)$ to $\pi\pi$ or the $a_0(980)$ to $\pi\eta$.

5.4   Angular distributions

In this section we give a different argument in favor of the existence of a N^* at 1920 MeV with $J^P = 1/2^+$. We study the
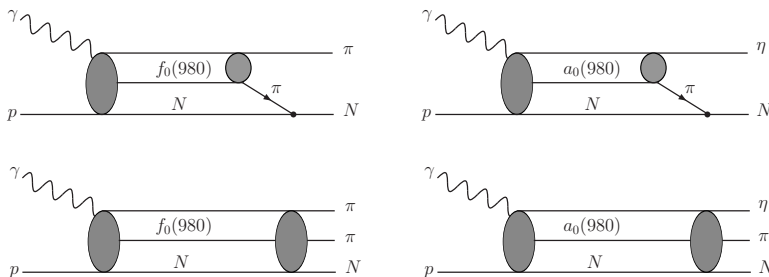
Figure 5.4: Diagrammatic representation of the γ induced reactions through the $1/2^+$ N^* resonance of [71, 108] with πN, ηN, $\pi\pi N$ or $\eta\pi N$ in the final state.

angular dependence of the $\gamma p \to K^+\Lambda$ proceeding through the resonance excitation. In order to get the basic structure of the amplitude with the quantum numbers of the resonance we take a typical mechanism compatible with the nature of the resonance as having $K\bar{K}$ in s-wave and in relative s-wave with the nucleon. This is shown in Fig. 5.5

The structure of the amplitude, close to K^+K^-p threshold, is given by

$$t^{(1/2)} \propto \vec{\sigma}\vec{q}\left(\frac{\vec{\sigma}\times\vec{k}}{2M_N}\right)\vec{\epsilon}, \tag{5.2}$$

where q $(\vec{q} = -\vec{q}_{K+})$ and k are depicted in Fig. 5.5, M_N is the nucleon mass an $\vec{\epsilon}$ is the photon polarization vector. The amplitude can be rewritten as

$$t^{(1/2)} \propto \vec{\epsilon}(\vec{q}\times\vec{k}) + i\vec{\epsilon}\vec{q}\vec{\sigma}\vec{k} - i\vec{\epsilon}\vec{\sigma}\vec{k}\vec{q} \tag{5.3}$$

Summing the modulus squared of the amplitude over initial and final polarizations of the nucleons and the photons one obtains

$$\overline{\sum}\sum|t^{(1/2)}|^2 \propto 2\vec{q}^{\,2}\,\vec{k}^{\,2} \tag{5.4}$$

and we see that there is no angular dependence.

Next we assume that we have a $J^P = 3/2^+$ state and we show in Fig. 5.6 the equivalent diagram to that in Fig. 5.5, but
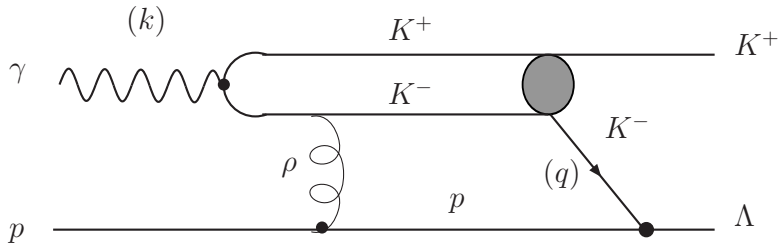
Figure 5.5: Schematic amplitude for $\gamma p \to K^+ \Lambda$ exciting the $1/2^+$ N^* resonance of [8, 108].
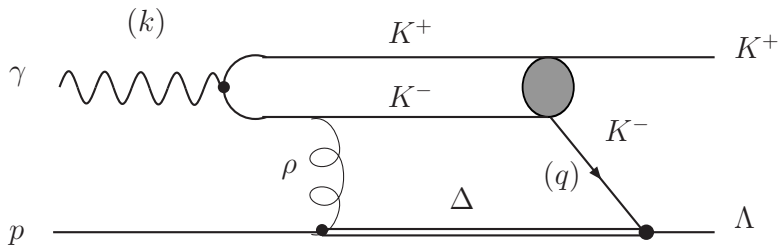
Figure 5.6: Schematic amplitude for $\gamma p \to K^+ \Lambda$ exciting a $3/2^+$ Δ intermediate state.

assuming a $J^P = 3/2^+$ baryonic intermediate state coupled to $K\bar{K}$. The amplitude has now the structure

$$t^{(3/2)} \propto \vec{S}\vec{q}\left(\frac{\vec{S}^\dagger \times \vec{k}}{2M_N}\right)\vec{\epsilon} \qquad (5.5)$$

with $\vec{S}$ the spin transition operator from spin 3/2 to spin 1/2. We can rewrite the amplitude taking into account the relation-

ship

$$\sum_{M_S} S_i |M_S\rangle \langle M_S| S_j^\dagger = \frac{2}{3} \delta_{ij} - \frac{i}{3} \epsilon_{ijk} \sigma_k \qquad (5.6)$$

and find

$$t^{(3/2)} \propto \frac{2}{3} \vec{\epsilon}(\vec{q} \times \vec{k}) - \frac{i}{3} \vec{\epsilon}\,\vec{q}\,\vec{\sigma}\vec{k} + \frac{i}{3} \vec{\epsilon}\,\vec{\sigma}\,\vec{k}\,\vec{q}. \qquad (5.7)$$

Upon summing the modulus square of the amplitudes over initial and final spins we find now

$$\overline{\sum}\sum |t^{(3/2)}|^2 \propto \frac{1}{9}\vec{k}^2\,\vec{q}^2(3\,sin^2\theta + 2). \qquad (5.8)$$

We see that now we have a strong angular dependence and the biggest strength is expected for $\theta = 90$ degrees.

Although we have extracted the angular dependence from the particular model of Figs. 5.5, 5.6, the results are general for $\gamma N \to R \to K\Lambda$ with R a $1/2^+$ or a $3/2^+$ resonance, as one would get from the tree level amplitudes of Fig. 5.7 using the standard γNN, PNN, γNR, PNR vertices, where P stands for a pseudoscalar meson [115].
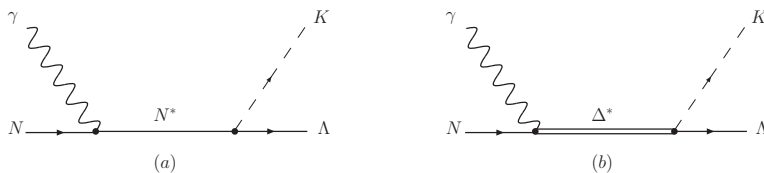
Figure 5.7: Diagrams for the process $\gamma N \to N^* \to K\Lambda$ (a) and $\gamma N \to \Delta^* \to K\Lambda$ (b).

Next we would like to recall what happens experimentally. As one can see in Ref. [99], the signal around 1920 MeV is present at all angles and one finds roughly a contribution of the peak around 1920 MeV over a smooth background of the order of $0.5\,\mu b$ for $d\sigma/dcos\theta$ at all angles. This would disfavor the association of the peak to a $3/2^+$ resonance, since in this case at 90 degrees one would expect the maximum signal of

the resonance, with a strength about 5/2 the size of the one at forward or backward angles. The argument assumes that signal and background will sum incoherently in the reaction, which does not have to be necessarily correct, but one does not expect much coherence either in view of the many mechanisms contributing to the background in the theoretical models.

We have also given some thought to the possible use of the asymmetries already measured for this reaction [100, 116]. It is easy to see that the asymmetry, Σ, for the amplitude of our $1/2^+$ state given by Eq. (5.2) is $\Sigma = 0$. With this value of Σ, and assuming the contribution of the peak of the state over the background of about 20%, we find that adding the contribution of the $1/2^+$ signal Σ is reduced by about 20%. Considering that the values measured for Σ in [100, 116] have less precision than the cross sections, $\Sigma \simeq 0.25 \pm 0.15$, the changes induced in Σ by the $1/2^+$ signal are not of much help.

5.5   Test with polarization experiments

In case the $J^P = 1/2^+$ assignment was correct, an easy test can be carried out to rule out the $3/2^+$ state. The experiment consists in performing the $\gamma p \to K^+ \Lambda$ reaction with a circularly polarized photon with helicity 1, thus $S_z = 1$ with the z-axis defined along the photon direction, together with a polarized proton of the target with $S_z = 1/2$ along the same direction. With this set up, the total spin has $S_z^{tot} = 3/2$. Since L_z is zero with that choice of the z direction, then $J_z^{tot} = 3/2$ and J must be equal or bigger than 3/2. Should the resonant state be $J^P = 1/2^+$, the peak signal would disappear for this polarization selection, while it would remain if the resonance was a $J^P = 3/2^+$ state (unless the amplitude becomes zero for some reason). Thus, the disappearance of the signal with this polarization set up would rule out the $J^P = 3/2^+$ assignment.

Such type of polarization set ups have been done and are common in facilities like ELSA at Bonn, MAMI B at Mainz or CEBAF at Jefferson Lab, where spin-3/2 and 1/2 cross sections,

which play a crucial role in the GDH sum rule, see e.g. Ref. [117], were measured in the two-pion photoproduction [118,119] reaction. The theoretical analysis of [120] shows indeed that the separation of the amplitudes in the spin channels provides information on the resonances excited in the reaction.

5.6 Analysis of the reaction $\gamma p \to K^+ K^- p$ close to threshold

An ideal test of the nature of the resonance predicted around 1920 MeV is the study of the process $\gamma p \to K^+ K^- p$ close to threshold. This reaction has received relatively good experimental attention [121–124], stimulated recently by the search of a possible pentaquark state of strangeness S=1. Theoretically it has also been studied in [15,16,125–127], also motivated by the search of the pentaquark of strangeness $S = 1$, or to study the nature of the $\Lambda(1520)$ and other resonances. Yet, the emphasis here is different and the measurements required are very close to threshold, in the region below the ϕ production to avoid unnecessary complications in the analysis. Indeed, as we mentioned, the resonance has all the $K^+ K^- p$ components in s-wave and the energy is just a bit below the threshold of the reaction. The effect of this resonance should be seen as an accumulation of strength in the cross section close to threshold compared with phase space. Such effects are common in many reactions [128–130]. In order to see the effects expected for this case we again draw in Fig. 5.8 a typical diagram which would contribute to the $\gamma p \to K^+ K^- p$ close to threshold through the intermediate resonance excitation.

In Fig. 5.8, the shaded blob represents all the interactions of $K^+ K^- p \to K^+ K^- p$, which one encounters in a full Faddeev calculation. Hence, the amplitude for $\gamma p \to K^+ K^- p$ can be written as

$$t_{prod} \propto T_{K^+ K^- p \to K^+ K^- p} \qquad (5.9)$$

The $T_{K^+ K^- p \to K^+ K^- p}$ amplitude was evaluated using Faddeev equations in coupled channels [108]. We are assuming that this
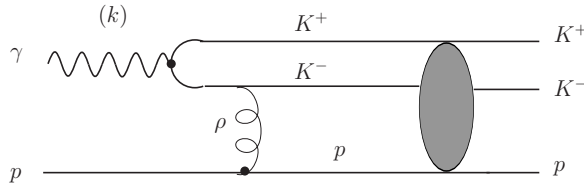
Figure 5.8: Schematic amplitude for $\gamma p \to K^+ K^- p$ exciting the $1/2^+$ N^* resonance of [8, 108].

term, which exhibits the peak due to the $1/2^+$ N^* resonance, dominates over a possible background term close to threshold (for instance, a tree level diagram like the one of Fig. 5.8 omitting the interaction of the particles symbolized by the shaded blob or diagrams with two-particle final-state interactions). The scheme of the latter work is very rewarding for experimental tests. Indeed, what one evaluates there is the T-matrix as a function of two variables. These are $\sqrt{s}$, the total energy, and $\sqrt{s_{23}}$, the invariant mass of the subsystem of two particles that one expects to be highly correlated. This is the case here, where the $K^+ K^-$ is correlated to the $a_0(980)$ and $f_0(980)$ resonances below the $K^+ K^-$ threshold, hence $\sqrt{s_{23}}$ is taken for the $K^+ K^-$ pair. Since the T amplitude of [108] does not have any angular dependence, and for a fixed total energy only depends on $\sqrt{s_{23}}$, the differential cross section for the $\gamma p \to K^+ K^- p$ reaction is readily found to be

$$\frac{d\sigma}{dM_{inv}} = C \frac{1}{s - M_N^2} \frac{1}{\sqrt{s}} p \, \tilde{q} |T_{K^+ K^- p \to K^+ K^- p}|^2 \qquad (5.10)$$

$$p = \frac{\lambda^{1/2}(s, M_{inv}^2, M_N^2)}{2\sqrt{s}}, \quad \tilde{q} = \frac{\lambda^{1/2}(M_{inv}^2, m_K^2, m_K^2)}{2M_{inv}}$$

where C is a constant and we have written M_{inv} for the invariant mass of the two-kaon system, the $\sqrt{s_{23}}$ variable in our
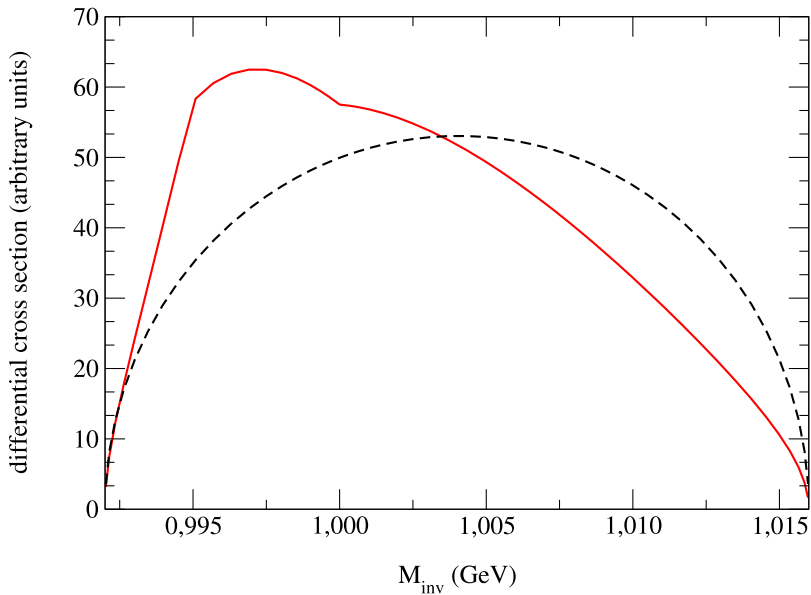
Figure 5.9: $d\sigma/dM_{inv}$ with phase space (dashed line) and using the $K^+ K^- p \to K^+ K^- p$ amplitude of [108] (solid line). The curves have been normalized to have the same integrated cross section.

formalism.

In order to show the effects of the resonance below threshold and the correlations of M_{inv} we show two plots in Figs. 5.9 and 5.10.

In Fig. 5.9 we take a fixed energy, just below ϕN production with $\sqrt{s} = 1955$ MeV and plot $d\sigma/dM_{inv}$ as a function of M_{inv} for phase space (dashed line) and for Eq. (5.10) (solid line). As we can see, there is a big asymmetry of the mass distribution with respect to phase space, with a clear accumulation of strength close to $M_{inv} = 2m_K$ as a consequence of the presence of the $f_0(980)$ or $a_0(980)$ below threshold. The results have been normalized by multiplying an arbitrary factor in order to obtain the same integrated cross sections.

In Fig. 5.10, we have instead represented the integrated cross
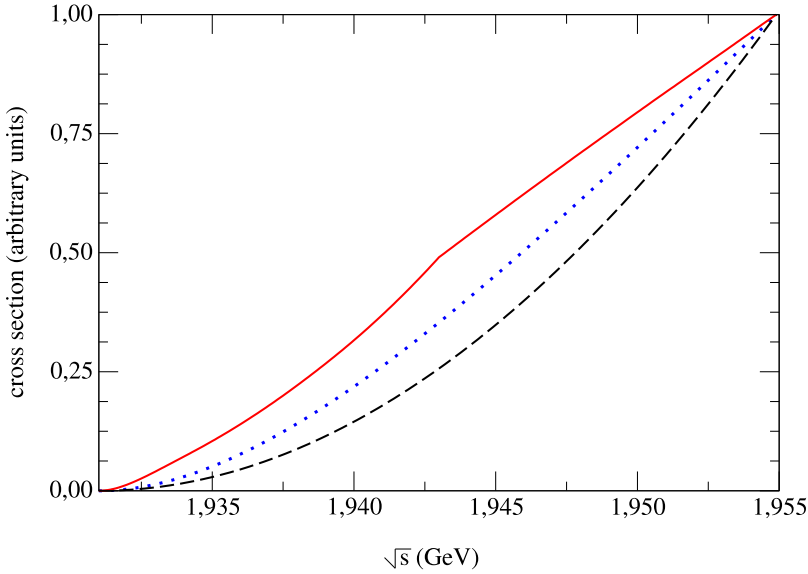
Figure 5.10: Integrated cross sections. Dashed line: phase space. Dotted line: using the amplitude of Eq. (5.11) accounting for K^+K^- final-state interaction. Solid line: results obtained using the $K^+K^-p \rightarrow K^+K^-p$ amplitude of [108]. The curves have been normalized to unity at 1955 MeV.

section of $\gamma p \rightarrow K^+K^-p$ as a function of the energy from threshold up to $\sqrt{s} = 1955$ MeV evaluated with Eq. (5.10) (solid line) and we compare the results with phase space (dashed line). The cross section have been normalized to one at $\sqrt{s} = 1955$ MeV for comparison. What we observe here is that the cross section is also more pronounced at lower energies as a consequence of the presence of the three particle resonance below threshold.

We should also take into account that the shape of $d\sigma/dM_{inv}$ in Fig. 5.9 should be expected from final-state interactions of the K^+K^- pair close to threshold, even if the $N^*(1920)$ resonance were not present [128–130]. This means that instead of phase space we should already consider a T matrix element accounting for the K^+K^- final-state interaction incorporating the pole of the $f_0(980)$ or $a_0(980)$. Thus we perform the evaluation of the

cross section with an empirical amplitude

$$t_{prod} \propto \frac{1}{M_{inv}^2 - M_{f_0}^2 + i\Gamma_{f_0} M_{f_0}} \tag{5.11}$$

with $M_{f_0} = 980$ MeV and $\Gamma_{f_0} = 30$ MeV. We note that using this amplitude we obtain a distribution $d\sigma/dM_{inv}$ very similar to the one obtained in Fig. 5.9 using the amplitude of [108]. The results for the integrated cross section with the amplitude of Eq. (5.11) can be seen as the dotted line in Fig. 5.10. We can still see deviations from the new curve incorporating the $K^+ K^-$ final-state interaction with respect to the curve accounting for the $N^*(1920)$ resonance in addition (solid curve in Fig. 5.10).

In our work the width obtained, of around 20 MeV, should be smaller than the one of the real state because we only have three-body states and the decay into two particles is not included in our formalism. As discussed in the previous chapters, even if the building blocks are three particles, one can obtain a larger width for the decay into two-body systems because there is more phase space for it. Because of that, in order to estimate possible uncertainties from this deficiency, we show what we would observe if we just had a resonance below threshold with a typical Breit-Wigner amplitude with mass $M_R = 1924$ MeV and width of about 60 MeV,

$$t_{prod} \propto \frac{1}{\sqrt{s} - M_R + i\frac{\Gamma}{2}} \frac{1}{M_{inv}^2 - M_{f_0}^2 + i\Gamma_{f_0} M_{f_0}} \tag{5.12}$$

The problem in this case is that the span of energies chosen in Fig. 5.10 from threshold to 1955 MeV is only of about 25 MeV, smaller than the width, such that one can not see the resonance structure in such a narrow range any more. Going to higher energies has the problem that we should face the ϕ production which has a large cross section. A way out of this problem could be found by eliminating from the experimental cross section the very narrow peak for the ϕ production. Assuming then that there is no contribution from ϕ production we compare the result obtained with the amplitude of Eq. (5.11) and the one
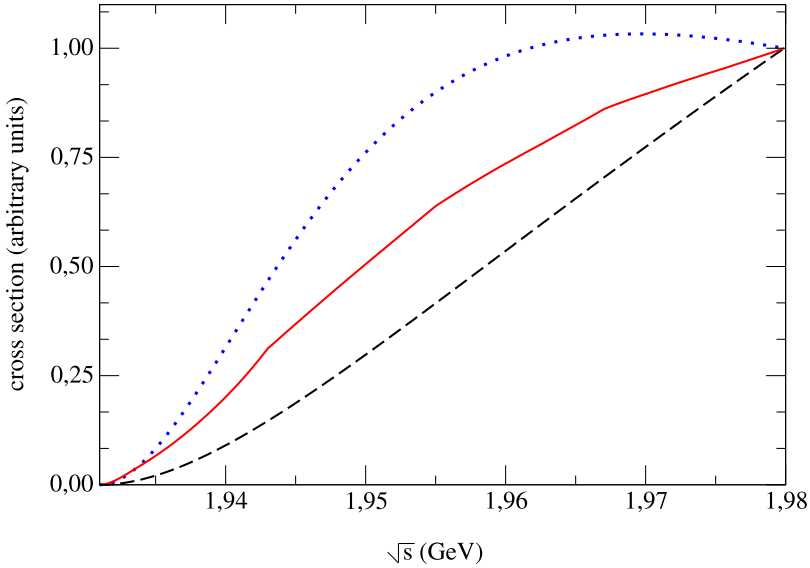
Figure 5.11: Integrated cross sections. Dashed line: using the amplitude of Eq. (5.11) which accounts for the K^+K^- final-state interaction. Solid line: results using the K^+K^-p amplitude of [108]. Dotted line: results using the empirical amplitude of Eq. (5.12) accounting for the K^+K^- final-state interaction plus a resonant pole at 1924 MeV with a width of 60 MeV.

with Eq. (5.12) which accounts also for the $N^*(1920)$ resonant pole. We show the results in Fig. 5.11, where the cross sections have been normalized to one at $\sqrt{s} = 1980$ MeV.

We observe that the effect of the $N^*(1920)$ resonance is clearly visible, with an enhanced cross section at lower energies compared with the curve that has only the K^+K^- final state. We also include in the figure the results obtained using the amplitude of Eq. (5.9) (solid line). The region between the two upper curves can indicate the theoretical uncertainties but we can see that, in any case, a clear enhancement due to the N^* resonance is seen.

The effects observed in this calculation call for an experimental test which could verify, or eventually refute the find-

ings obtained above, which are based on the nature of the predicted $1/2^+$ state around 1920 MeV. This analysis is underway at Spring8/Osaka [131].

5.7 Conclusions

The independent prediction, also using different methods, of a $1/2^+$ state around 1920 MeV as a bound state of $K\bar{K}N$, which appears in the $a_0(980)N$ and $f_0(980)N$ configurations, stimulated us to suggest that this state may have already been seen in the peak observed in the $\gamma p \to K^+\Lambda$ reaction around this energy. Based on the structure found in [71] and in our work, we could explain why a relatively narrow peak appears in the $\gamma p \to K^+\Lambda$ reaction on top of a large background and it does not show up on top of the broader structure around these energies in the $\gamma p \to K^+\Sigma^0$ reaction. We could also find an easy interpretation on why the state does not show up in pion induced reactions, or in reactions with πN or ηN in the final states, because of the small coupling of the $f_0(980)N$ to $\pi\pi$ or of the $a_0(980)N$ to $\eta\pi$. In order to find extra support for the idea we suggested two experiments. One of them is the separation of the $S_z = 3/2$ and $S_z = 1/2$ parts of the $\gamma p \to K^+\Lambda$ cross section, which would rule out the $3/2^+$ assignment if there is no cross section in the $S_z = 3/2$ channel. The other one is the investigation of the cross section close to threshold and the invariant mass distributions close to the two kaon mass, which should show enhancements close to both thresholds, indicating a bound state below the $K\bar{K}N$ mass with the two kaons strongly correlated to form the $a_0(980)N$ and $f_0(980)N$ states. Both experiments are feasible in existing laboratories and we hope that the present work encourages their implementation.

$S = 1$, $1/2^+$ states in the $N\pi K$ system

6.1 Introduction

The observation of a peak in the K^+n invariant mass for the $\gamma n \to K^+ K^- n$ reaction on a ^{12}C target at Spring8/Osaka [35] raised great hopes that for the first time a strangeness S=1 narrow exotic baryon could be found. The peak was thus associated to a pentaquark, since the standard $3q$ states cannot produce S=1. Subsequently, many experiments were done, some which reproduced this peak and others which did not, and the issue stimulated a large number of theoretical works that gave a huge impetus to the field of hadron structure (see the extensive list of references, for example, in [132, 133]). Waters calmed down, a thorough experimental review was written in [134] and a period of rest followed till a new experimental analysis was done at LEPS confirming the original peak, now on a deuteron target and with more statistics [135]. Although one cannot rule out an interpretation of the peak as a consequence of the particular set up of LEPS, no alternative conventional explanation for this peak has been provided.

On the theoretical side most of the works concentrated on finding possible states of five quarks (pentaquark). From the

perspective of the meson-baryon interaction the situation does not look encouraging, since the KN interaction obtained from chiral Lagrangians is basically repulsive in nature [76], and one does not expect to find a narrow (long lived) resonance, as the one claimed in [35], in this system. This is why very early there were suggestions that if the peak represented a new state it could be a bound state of three hadrons, $K\pi N$, with the pion acting as a glue between the nucleon and the K, which would only be bound by about 30 MeV. However, investigations along this line, weakly concluded the difficulty to have this system as a bound state [83, 136].

The purpose of this chapter is to perform a thorough calculation of the $K\pi N$ system using Faddeev equations to see the possibility to find bound states or resonances. The interest in the three hadron systems is old. In [93] there was already a study of such possible systems based only on symmetries. In chapter 3 systems of two mesons and one baryon with strangeness $S = -1$ were studied, finding resonant states which could be identified with two Λ and four Σ known low-lying resonances with $J^P = 1/2^+$. Similarly, in the case of the $S = 0$ sector (chapter 4) the $N^*(1710)$ appears neatly as a resonance of the $\pi\pi N$ system, as well as including the channels coupled to $\pi\pi N$ within SU(3) [57]. The study in $S = 0$ sector was further extended by using the experimental data on the πN scattering and by adding more coupled channels in section 4.3, the outcome of which was the dynamical generation of three resonances, one with quantum numbers of the N^* (2100), another with those of the Δ (1910), plus a new N^* at $\sim$ 1920 MeV (also predicted by Jido et. al. [71]).

The achievements obtained in the former studies and especially the finding of several low-lying $S =$-1 resonances with two meson-one baryon structure motivates us to have a fresh look at the πKN system using our formalism and to make a thorough investigation of the possibility to have the system bound. This is the purpose of the present chapter. As we will show in the following section, we do not get the system bound in

the region of the possible S=1 state of [35]. At higher energies
a bump appears which, however, does not have the ordinary
shape of the resonances that we have found in other channels.
This could correspond to some of the bumps seen using the time
delay method in the analysis of the KN system in [137].

6.2   Formalism and Results

We solve the Faddeev equations for the $N\pi K$ system following
the formalism developed chapters 1 and 2. We study the $N\pi K$
system for total charge +1 taking into account four channels to
solve Eqs. (1.112): $p\pi^0 K^0$, $n\pi^0 K^+$, $p\pi^- K^+$, $n\pi^+ K^0$. In this
case, the coupled channels appearing for the calculation of the
two-body t-matrices are listed below:

- $K^+\Sigma^0$, $K^0\Sigma^+$, $K^+\Lambda$, $\pi^0 p$, $\pi^+ n$, ηp for the πN interaction
  with charge +1.

- $K^+\Sigma^-$, $K^0\Sigma^0$, $K^0\Lambda$, $\pi^- p$, $\pi^0 n$, ηn for the πN interaction
  with null charge.

- $\pi^+ K^0$, $\pi^0 K^+$ for πK interaction with charge +1.

- $\pi^- K^+$, $\pi^0 K^0$ for πK interaction with charge 0.

- And $K^0 p$, $K^+ n$ for KN interaction with charge +1,
  $K^0 n$ for charge 0 and $K^+ p$ for charge +2.

The meson-baryon potential obtained with chiral Lagrangians
has the general form, after projecting in S-wave, of Eq. (1.6).
For the πN system and its coupled channels for total charge
zero, which dynamically generate the N^* (1535), the coefficients
C_{ij} in Eq. (1.6) can be found in [17], while for the KN system
in [5]. The coefficients for the πN system for total charge +1
are given in Table 6.1 .

The potential for the πK system can be obtained from [3],
in which the $\kappa(800)$ gets dynamically generated.

Table 6.1: C_{ij} coefficients for the πN interaction with charge $+1$

	$K^+\Sigma^0$	$K^0\Sigma^+$	$K^+\Lambda$	$\pi^0 p$	$\pi^+ n$	ηp
$K^+\Sigma^0$	0	$\sqrt{2}$	0	$-\frac{1}{2}$	$\frac{1}{\sqrt{2}}$	$-\frac{\sqrt{3}}{2}$
$K^0\Sigma^+$		1	0	$\frac{1}{\sqrt{2}}$	0	$-\sqrt{\frac{3}{2}}$
$K^+\Lambda$			0	$-\frac{\sqrt{3}}{2}$	$-\sqrt{\frac{3}{2}}$	$-\frac{3}{2}$
$\pi^0 p$				0	$\sqrt{2}$	0
$\pi^+ n$					1	0
ηp						0

The T_R^* matrix for different possible total isospins has been obtained using the following relations:

$$|N\pi K; I = 0, I_{\pi K} = 1/2\rangle = \frac{1}{\sqrt{6}}\Big[|p\pi^0 K^0\rangle - \sqrt{2}|p\pi^- K^+\rangle$$
$$+ \sqrt{2}|n\pi^+ K^0\rangle + |n\pi^0 K^+\rangle\Big]$$

$$|N\pi K; I = 1, I_{\pi K} = 1/2\rangle = \frac{1}{\sqrt{6}}\Big[|p\pi^0 K^0\rangle - \sqrt{2}|p\pi^- K^+\rangle$$
$$- \sqrt{2}|n\pi^+ K^0\rangle - |n\pi^0 K^+\rangle\Big] \quad (6.1)$$

$$|N\pi K; I = 1, I_{\pi K} = 3/2\rangle = \frac{1}{\sqrt{6}}\Big[\sqrt{2}|p\pi^0 K^0\rangle$$
$$+ |p\pi^- K^+\rangle + |n\pi^+ K^0\rangle - \sqrt{2}|n\pi^0 K^+\rangle\Big]$$

$$|N\pi K; I = 2, I_{\pi K} = 3/2\rangle = \frac{1}{\sqrt{6}}\Big[\sqrt{2}|p\pi^0 K^0\rangle + |p\pi^- K^+\rangle$$
$$- |n\pi^+ K^0\rangle + \sqrt{2}|n\pi^0 K^+\rangle\Big]$$

with the phase convention $|\pi^+\rangle = -|I_\pi = 1, I_{\pi z} = 1\rangle$. The I and $I_{\pi K}$ in the above equations represent the total isospin of the three-body system and that of the πK system, respectively.

We calculate Eqs. (1.112) as a function of the total energy and the invariant mass of the subsystem of particles 2 and 3. The invariant masses of the other two subsystems can be written in terms of $\sqrt{s}$ and $\sqrt{s_{23}}$ as explained in section 2.1. We have calculated the T_R matrices for the energy range 1500 MeV $< \sqrt{s} <$ 2100 MeV, with the motivation to find some structure around 1540 MeV, and for $600 < \sqrt{s_{23}} < 1100$ MeV to generate dynamically the κ (800) in the KN subsystem in order to have some attractive interaction in the three-body system.

We do not find any resonance in the isospin 1 and 2 configurations. We obtain one peak with a broad structure in the squared amplitude in isospin zero (i.e., when the πK subsystem is in isospin 1/2 configuration) around 1720 MeV. The full width at half maximum of the peak is of the order of 200 MeV. These features have nothing in common with the resonance claimed in [35]. The value of $\sqrt{s_{23}}$, for which the bump is found, is around the mass of the κ (800) resonance. We show this peak in Fig. 6.1, where we plot the squared amplitude for the total isospin zero. As is evident from Fig. 6.1, the structure of the peak is far from a Breit-Wigner. Though the strength of this amplitude is similar to that of the corresponding $S =$ -1 case [56], its shape is different from those of the clear resonances found in the latter. Its unconventional peaking behavior cast doubts whether this peak could have a pole associated in the complex plane, the accepted criterium to define a peak as a resonance. The technique to extrapolate the amplitudes to the complex plane with the two variables that we have is not available and looks nontrivial, since it involves working with complex momenta for some particles and real for others. Yet, independently from whether the structure found deserves or not to be called a resonance, the fact remains that the chiral dynamics of this coupled channel three-body system leads to such a bump in the cross section in a region where the system clusters like a

κ and a nucleon. This peak should be visible in KN scattering with the quantum numbers $I = 0$, $J^P = 1/2^+$, but even better in the $KN \to \pi KN$ reaction, since the peak appears well above the πKN threshold, or in any reaction producing πKN in $I = 0$ in the final state.
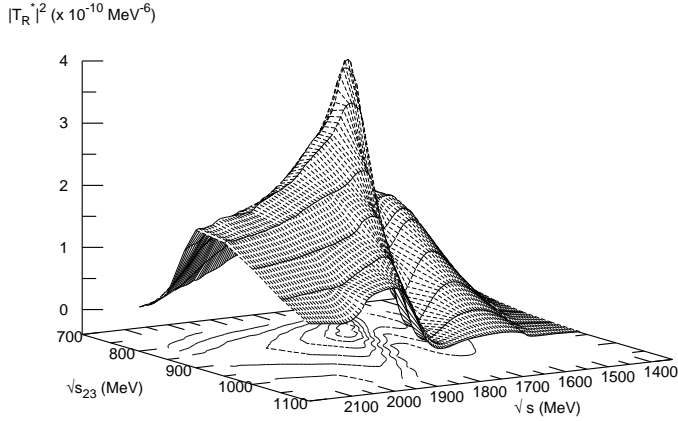
Figure 6.1: The isospin zero amplitude squared for the $N\pi K$ system as a function of the total energy and the invariant mass of the πK subsystem.

Interestingly, a broad structure at around 1800 MeV seems to be present in the data [138] of K^+N scattering in the P_{01} partial wave and in the time delay analysis of these data [137], which could correspond to the peak shown in Fig. 6.1.

6.3 Summary

The possibility of existence of strangeness $+1$ baryon with a strong coupling to the $N\pi K$ system has been investigated by

solving Faddeev equations in the formalism which has gener-
ated dynamically many strange and non strange resonances in
three-body systems. We do not find any structure in the en-
ergy region close to 1542 MeV, therefore, the interpretation of a
possible Θ^+ as a $N\pi K$ bound state, with all the interactions in
s-wave, is ruled out. A bump is found around 1720 MeV with
about 200 MeV of width and with isospin zero, which reveals
the underlying chiral dynamics of the three-body system, and
that we hope can be seen in K^+N scattering, but much better
in reactions producing πKN in $I = 0$ in the final state. Our
study should stimulate experimental work in this direction.

CHAPTER 7

The X(2175) as a $\phi K \bar{K}$ molecular state

So far we have discussed only meson-meson-baryon systems studied with our formalism. In this chapter we will focus on investigations of three meson systems consisting of two pseudoscalars and one vector meson, $\phi K \bar{K}$ and $\phi\pi\pi$. The study results in finding of a resonance which supports the recently 1^{--} $X(2175)$ state found at BABAR and BES facilities.

7.1 Introduction

The discovery of the X(2175) 1^{--} resonance in $e^+e^- \to \phi f_0(980)$ with initial state radiation at BABAR [47,48], also confirmed at BES in $J/\Psi \to \eta\phi f_0(980)$ [49], has stimulated research around its nontrivial nature in terms of quark components. The possibility of it being a tetraquark $s\bar{s}s\bar{s}$ is investigated within QCD sum rules in [50], and as a gluon hybrid $s\bar{s}g$ state has been discussed in [51, 52]. A recent review on this issue can be seen in [53], where the basic problem of the expected large decay widths into two mesons of the states of these models, contrary to what is experimentally observed, is discussed. The basic data on this resonance from [47, 48] are $M_X = 2175 \pm 10$ MeV and $\Gamma = 58 \pm 16 \pm 20$ MeV, which are consistent with the numbers

quoted from BES $M_X = 2186 \pm 10 \pm 6$ MeV and $\Gamma = 65 \pm 25 \pm 17$ MeV. In Ref. [48] an indication of this resonance is seen as an increase of the $K^+ K^- K^+ K^-$ cross section around 2150 MeV. A detailed theoretical study of the $e^+ e^- \to \phi f_0(980)$ reaction was done in Ref. [54] by means of loop diagrams involving kaons and K^*, using chiral amplitudes for the $K\bar{K} \to \pi\pi$ channel which contains the $f_0(980)$ pole generated dynamically by the theory. The study revealed that the loop mechanisms reproduced the background but failed to produce the peak around 2175 MeV, thus reinforcing the claims for a new resonance around this mass (see Fig. 7.1).
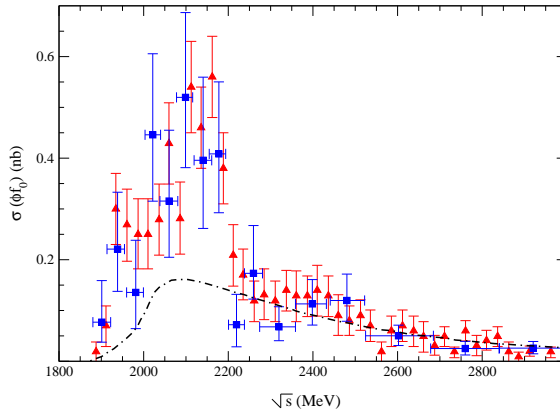
Figure 7.1: The cross section for the $e^+ e^- \to \phi f_0$ reaction. The dashed-dotted line shows the result of the calculation of the cross section in the plane wave approximation [54]. The data, which corresponds to the $e^+ e^- \to \phi (\pi\pi)_{I=0}$ reaction (triangles for charged pions and boxes for neutral pions), have been taken from [47, 48].

We wish to advocate a very different picture for the X(2175) resonance for which a reliable calculation can be made and which could lead naturally to a very narrow width and no coupling to two pseudoscalar mesons. The picture is that the X(2175) is an ordinary resonant state of $\phi f_0(980)$ generated

by their interaction. The $f_0(980)$ resonance is dynamically generated from the interaction of $\pi\pi$ and $K\bar{K}$ treated as coupled channels within the chiral unitary approach of [2,139,140], qualifying as a kind of molecule with $\pi\pi$ and $K\bar{K}$ as its components, with a large coupling to $K\bar{K}$ and a weaker one to $\pi\pi$ [hence, the small width compared to that of the $\sigma(600)$]. The vector-pseudoscalar interaction has also been studied using chiral dynamics in [79, 141], which lead to the dynamical generation of the low-lying axial vectors. We shall follow the approach of Ref. [79] to obtain the ϕK and $\phi\pi$ amplitudes and that of [2] to calculate the $K\bar{K}$ and $\pi\pi$ ones .

To study the $\phi f_0(980)$ interaction, we are thus forced to investigate the three-body system $\phi K\bar{K}$. For this purpose we have solved the Faddeev equations with coupled channels $\phi K^+ K^-$ and $\phi K^0 \bar{K}^0$. The picture is later complemented with the addition of the $\phi\pi\pi$ state as a coupled channel.

7.2   Formalism

To study the $\phi K\bar{K}$ system, it is required to solve Eqs. (1.112). The procedure followed is (1) we solve coupled-channel Bethe-Salpeter equations for pseudoscalar - pseudoscalar meson (PP) interaction as done in [2]; and for pseudoscalar-vector mesons (PV) interaction as in [79]; (2) then we solve the Faddeev equations for the three-body, i.e., vector-pseudoscalar-pseudoscalar (VPP) mesons, system using the model developed in chapters 1 and 2. We revise the input and the formalism for this study in this section.

We label ϕ as particle 1 and K and $\bar{K}$ as particle 2 and 3, respectively. The invariant mass of the $K\bar{K}$ system $\sqrt{s_{23}}$ is taken as an input in the three-body calculations and is varied around the mass of the f_0. The $K\bar{K}$ interaction t^1 in this region contains the pole of the $f_0(980)$ [2, 139]. The other invariant masses s_{12} and s_{13} can be then calculated in terms of $\sqrt{s_{23}}$ and the total energy (Eq. (2.1)). Thus, there are two variables of the calculations, i.e., the total energy and the invariant mass of

the $K\bar{K}$ system.

To obtain the input the two-body t matrices for the PP interaction we solve the Bethe-Salpeter equation

$$t = V + V\tilde{G}t \qquad (7.1)$$

for five coupled channels, i.e., K^+K^-, $K^0\bar{K}^0$, $\pi^+\pi^-$, $\pi^0\pi^0$, and $\pi^0\eta$. The potentials V are calculated from the lowest order chiral Lagrangian and the loops $\tilde{G}$ have been calculated using dimensional regularization as in [2]. The authors of [2, 139, 140] found poles in the t matrices, in the isospin 0 sector, corresponding to the σ and the f_0 resonances, and also the one corresponding to the $a_0(980)$ for the isospin 1 case. It was also found that the f_0 resonance is dominated by the $K\bar{K}$ channel and the pole for the f_0 appears at ~ 973 MeV even when the $\pi\pi$ channel is eliminated. The matrix element corresponding to the $K\bar{K} \rightarrow K\bar{K}$ scattering is used as an input to solve Eqs.(1.112) and (1.114). In the two-body problem, the $f_0(980)$ pole appears below the $K\bar{K}$ threshold. It corresponds to total energies of the $K\bar{K}$ system below $2m_k$ and in the momentum representation to purely imaginary kaon momenta if we take $p_K^2 = m_K^2$ (which is not the case in a bound state). To avoid using unphysical complex momenta in the three-body system, we give a minimum value of about 50 MeV/c to the kaon momentum in the $K\bar{K}$ center of mass system, as discussed in section 2.1. It should be mentioned that the results are almost insensitive to this choice of the minimum momentum. For example, a change in this momentum by about 40% changes the position of the peak merely by ~ 5 MeV.

For the VP meson interaction, Eq. (7.1) is calculated with $\phi K, \omega K, \rho K, K^*\eta$, and $K^*\pi$ as coupled channels. The potential for the VP meson-meson interaction has been obtained from the lowest order chiral Lagrangian and projected in the s wave [79], and then the $\phi K \rightarrow \phi K$ element of the resulting coupled-channel t matrix is used as an input in Eq. (1.112)

Coming back to the three-body problem, our interest is to check the possibility of existence of a resonance or a bound state

with isospin zero in the $\phi K \bar{K}$ system; thus the full T_R matrix [Eq. (1.114)] is to be projected to total isospin 0. When adding the $\phi \pi \pi$ channel, we must deal with the $\pi \pi$ and $\phi \pi$ interactions which are part of the coupled-channel study of the scalar and axial vector resonances, respectively.

7.3 A discussion on possible three-body coupled channels

In the construction of the $K \bar{K}$ and ϕK two-body t matrices we consider all coupled channels as indicated in section 7.2. We shall argue here that in the three-body case we can omit some states. The ϕK system couples to ωK, ρK, $K^* \pi$, and $K^* \eta$. We shall bear in mind that we are looking for a state with total $I = 0$ and with $\sqrt{s_{23}} \simeq 980$ MeV, as found in the experiment [47, 48]. When adding the $\bar{K}$ of the three-body $\phi K \bar{K}$ system to the coupled channels of the ϕK, we obtain the following states: $\omega K \bar{K}$, $\rho K \bar{K}$, $K^* \pi \bar{K}$, and $K^* \eta \bar{K}$. If we want the subsystem of two pseudoscalar mesons to build up the f_0 (980), which is dynamically generated in the $K \bar{K}$ and $\pi \pi$ interaction, we must exclude the $K^* \pi \bar{K}$ and $K^* \eta \bar{K}$ states. The $\rho K \bar{K}$ state is also excluded because when $K \bar{K}$ couples to the f_0 (980) the total isospin of the state is $I = 1$. Only the $\omega K \bar{K}$ state is left over. We could consider this channel as a coupled channel of $\phi K \bar{K}$, but the $\omega K \bar{K}$ channel lies ~ 400 MeV below the X (2175) resonance mass and hence is not expected to have much influence in that region. In more technical words, a channel which lies far away from the energy region under investigation would only bring a small and smooth energy-independent contribution to the final amplitude because of the large off-shellness of the propagators.

Thus the introduction of the $\omega K \bar{K}$ channel can only influence mildly the results obtained with the $\phi K \bar{K}$ system alone, and thus we neglect it in the study. Furthermore we have also seen that the $\phi K \to \omega K$ and $\omega K \to \omega K$ amplitudes are weaker than the $\phi K \to \phi K$ one.

Even though we argue above that $\bar{K}^* \pi K$ and $\bar{K}^* \eta K$ chan-

nels should be neglected, we have also investigated the effect of
including the $\bar{K}^* \pi K$ channel, as an example. This is a channel
where the πK interaction (together with the ηK channel) leads
to the scalar κ resonance, and actually there are works which
hint towards a possibility of $\bar{K}^* \kappa$ forming a molecule with mass
around 1576 MeV [142]. What we find can be summarized as
follows:

- In the energy region of our interest, we find a small tran-
  sition amplitude from $\phi K \to K^* \pi$ as compared to $\phi K \to$
  ϕK, indicating a small mixture of the $\phi K \bar{K}$, and $\bar{K}^* \pi K$
  components.

- Studying the $\bar{K}^* \pi K$ system alone, we find that the corre-
  sponding amplitudes are much smaller in size than those
  found in the $\phi K \bar{K}$ system in the energy region around
  2150 MeV.

- Around 1600 MeV, the $\bar{K}^* \pi K$ amplitudes can be bigger
  than around 2150 MeV, but they are still smaller than the
  $\phi K \bar{K}$ amplitude at 2150 MeV.

From these findings we conclude that, although more de-
tailed work needs to be done at energies around 1600 MeV
to check the suggestion of [142], the amplitude of the $\bar{K}^* \pi K$
channel in this energy region seems too weak to support bound
states. On the other hand, we can be more assertive by stat-
ing that the effect of the $\bar{K}^* \pi K$ channel around 2150 MeV is
negligible.

We can now stick to having the ϕ as the vector meson and
$K \bar{K}$ as the main PP channel. Yet, $K \bar{K}$ and $\pi \pi$ couple strongly
in $I=0$, both the $K \bar{K} \to K \bar{K}$ and $\pi \pi \to \pi \pi$ amplitudes are
strong, and it is only the intricate nonlinear dynamics of coupled
channels of the Bethe-Salpeter equations that produces at the
end two states, the σ that couples strongly to the $\pi \pi$ channel
and the f_0 (980) that couple strongly to $K \bar{K}$. Hence, we find
advisable to include $\phi \pi \pi$ as a coupled channel.

7.4 Results

In Fig. 7.2, we show the squared amplitude $\mid T_R \mid^2$ and its projection, as a function of the total energy ($\sqrt{s}$) and the invariant mass of the $K\bar{K}$ system ($\sqrt{s_{23}}$), in the isospin zero configuration. We have made the isospin projection of the amplitude of Eq. (1.114) using the phase convention $\mid K^- \rangle = - \mid 1/2, -1/2 \rangle$ as

$$\mid \phi K\bar{K}; I = 0, I_{K\bar{K}} = 0 \rangle = \frac{1}{\sqrt{2}} \Big[\mid \phi K^+ K^- \rangle + \mid \phi K^0 \bar{K}^0 \rangle \Big].$$

A clear sharp peak of $\mid T_R \mid^2$ can be seen at 2150 MeV, with a full width at half maximum ~ 16 MeV. In order to make a meaningful comparison of this width with the experimental results, we have folded the theoretical distribution with the experimental resolution of about 10 MeV and then we find an appropriate Breit-Wigner distribution with a width $\Gamma \sim 27$ MeV. The peak in $\mid T_R \mid^2$ appears for the $\sqrt{s_{23}} \sim 970$ MeV which is very close to the pole of the f_0 resonance [2].

The total mass, the invariant mass of the $K\bar{K}$ subsystem and the quantum numbers I^G, $J^{PC} = 0^-$, 1^{--} of the resonance found here are all in agreement with those found experimentally for the $X(2175)$ [47, 48]. These findings strongly suggest that this resonance can be identified with the $X(2175)$.

Yet, our approach can go further and we can make an evaluation of the production cross section and compare it with the experimental results of [47, 48]. For this we make use of the theoretical evaluation of the $\phi f_0(980)$ production in the $e^+ e^-$ reaction studied in [54]. The authors in [54] studied the production of the ϕ and $f_0(980)$ as plane waves (pw) in the final state and could reproduce the background but not the peak structure around $X(2175)$ mass. Since our resonance develops from the interaction of the ϕ and f_0, the consideration of the final state interaction (fsi), in addition to the uncorrelated ϕf_0 production amplitude (T_{pw}^{PR}) of [54], could explain the experimental data in the peak region. We show here that this is indeed the case. We implement the ϕf_0 fsi by multiplying T_{pw}^{PR} by the
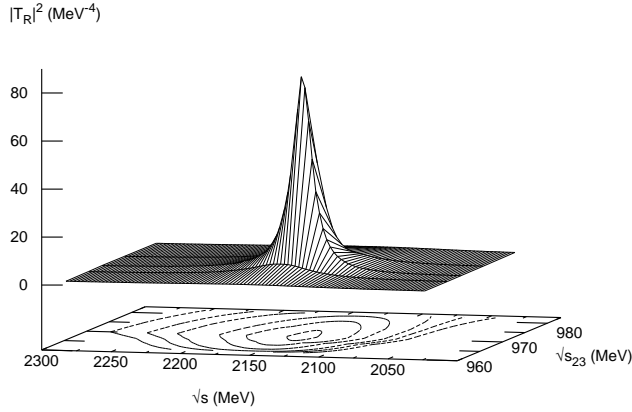
Figure 7.2: The $\phi K\bar{K}$ squared amplitude in the isospin 0 configuration.

factor

$$F_{fsi} = [1 + \tilde{G}_{PR}(s)t_{PR}(s)], \qquad (7.2)$$

where t_{PR} is the scattering matrix for ϕ and f_0 and $\tilde{G}_{PR}(s)$ is the loop function of the ϕ and f_0 propagators. For $\tilde{G}_{PR}$ we use the standard formula for two mesons [2] with a cut-off (Λ) of the order of the sum of the two meson masses, as was the case in [2], and hence $\Lambda \sim 2$ GeV here. We do not have the t_{PR}, but in the vicinity of the resonance it must be proportional to the three-body T_R [Eq. (1.114)], implying $T_{PR} = \alpha T_R$. The proportionality coefficient α is readily obtained using a relation based on unitarity, $Im\{T_{PR}^{-1}\} = -Im\{\tilde{G}_{PR}\}$, implicit in Eq. (7.1). Assuming the ϕf_0 channel to be the main source of $Im\{T_R\}$, as the experimental study suggests [47, 48], we have

$$Im\{T_{PR}^{-1}\} = \alpha^{-1}Im\{T_R^{-1}\} = -Im\{\tilde{G}_{PR}\} = \frac{k_\phi}{8\pi\sqrt{s}}, \qquad (7.3)$$

which determines α. In Eq. (7.3), k_ϕ is the ϕ momentum in the ϕf_0 center of mass system.
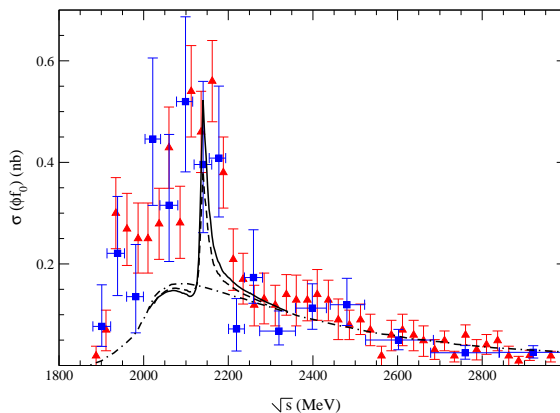
Figure 7.3: The cross section for the $e^+ e^- \rightarrow \phi f_0$ reaction. The dashed-dotted line shows the result of the calculation of the cross section in the plane wave approximation [54]. The dashed (solid) line shows the result of multiplying the amplitude from Ref. [54] by the final state interaction factor [Eq. (7.2)] calculated using a cutoff of 2 (2.5) GeV for the $\tilde{G}_{PR}(s)$. The data, which corresponds to the $e^+ e^- \rightarrow \phi (\pi\pi)_{I=0}$ reaction (triangles for charged pions and boxes for neutral pions), have been taken from [47, 48].

With this information we evaluate the $e^+ e^- \rightarrow \phi f_0$ production cross section taking the results for the ϕf_0 production in the plane wave approximation from [54], and by multiplying the final state interaction factor of Eq. (7.2) calculated with our three-body amplitude. We show the results in Fig.7.3. We can see that taking a cut-off of the order of 2-2.5 GeV for the $\tilde{G}_{PR}$, we obtain results for the production cross section which are in fair agreement with the experimental ones.

We would like now to comment on the effects of including the $\phi\pi\pi$ channel, as discussed in Sec. 7.3 . We observe a similar peak as in Fig. 7.2 (see Fig. 7.4); however, the position of the
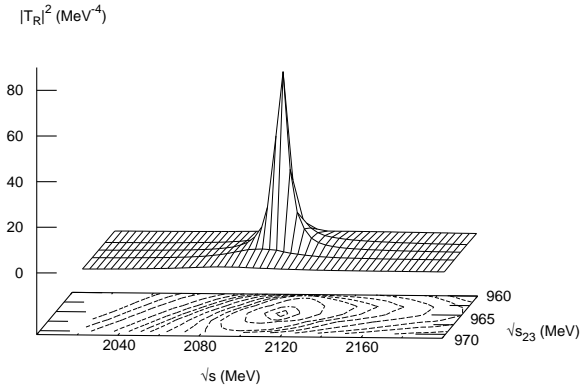
Figure 7.4: The squared amplitude in the isospin 0 configuration including the $\phi\pi\pi$ channel.

peak in the total energy has been displaced by about 38 MeV downwards to an energy of 2112 MeV. At the same time, the peak shows up around $\sqrt{s_{23}} \simeq 965$ MeV, about 15 MeV below the nominal energy of the f_0 (980). These differences with the nominal values of the masses of the resonances are typical of any hadronic model of resonances and, thus, the association of the resonance found to the X (2175), which has the same quantum numbers as the resonance found, is the most reasonable conclusion. In any case, the different checks made in our work, have always led to a clean peak around the same position, and the difference found could give us an idea of the theoretical uncertainties.

We have checked the sensitivity of the resonance found to the change in the cut-off ($\Lambda \sim 1000$ MeV) used in the calculation of the input two-body t matrices [Eq. (7.1)], which gives the same results as dimensional regularization. There is not

much freedom to change the Λ in our case, because it has been constrained by reproducing the data on the respective two-body scattering. We thus change Λ by ~ 20 MeV for calculating Eq. (7.1), which still guarantees a reasonable agreement with the two-body cross sections, and find that it gives rise to a change in the peak position (in Fig.7.2) in $\sqrt{s}$ by ~ 8 MeV. The cutoff is also needed to evaluate the G functions of Eq. (1.102), and we use the same cut-off of about 1 GeV. Since this function involves loops with three-meson propagators, it is very insensitive to the cutoff. The same change of ~ 20 MeV (or more) in Λ leads to negligible changes in the results in this case.

Finally, it should be mentioned that the T_R matrix for isospin 1 does not show any structure.

7.5   Off-shell effects and three-body forces

As discussed in section 1.3.1, our approach makes use of the explicit cancellation of the off-shell parts of the two-body t matrices in the three-body diagrams with the genuine three-body forces, which arise from the same chiral Lagrangians. This makes sense since the off-shell part of a scattering matrix is unphysical and can be changed arbitrarily by performing a unitary transformation of the fields.

As we explained in section 1.3.1, inside the loops, the off-shell part of the chiral amplitudes, which behaves as $p^2 - m^2$ (where p is the four vector of the off-shell particle) for each of the meson legs, cancels a propagator leading to a diagram with the topology of a three-body force. It is also a peculiar feature of the chiral Lagrangians that there is a cancellation of these three-body forces with those arising from the $PPV \to PPV$ contact terms of the theory. Examples of similar cancellations are well known in chiral theories [18, 143]. The detailed derivation of the cancellation of the off-shell part of the t matrices and the three-body force arising from the chiral Lagrangian can be seen in section 1.3.1. However, in the $\phi K \to \phi K$ case, the potential is zero. In this case, the t matrix is generated by rescattering

through $K^* \pi$ and $K^* \eta$ states, and the cancellation is found in the transition potentials.

We find also instructive to see what one gets if the off-shell part of the two-body t matrices is retained. Following Refs. [2, 79] we find, for the s wave,

$$V_{K\bar{K}}(I = 0) = -\frac{1}{4f^2}(3s_{23} - \sum_i (p_i^2 - m_i^2)) \qquad (7.4)$$

$$V_{\phi K} \simeq \frac{3}{2}s_{12} - \frac{1}{2}\sum m_i^2 - \frac{1}{2}\sum_i (p_i^2 - m_i^2). \qquad (7.5)$$

The $(p_i^2 - m_i^2)$ terms in Eq. (7.4) are ineffective in the loops of the two-body t matrix [Eq. (7.1)] [2] but will show up in the external legs of the two-body t matrix used as an input in the Faddeev equations. Hence

$$t_{K\bar{K}}(I = 0) = t_{on}\left(1 - \frac{\sum_i (p_i^2 - m_i^2)}{3s_{23}}\right) \qquad (7.6)$$

$$t_{\phi K} = t_{on}\left(1 - \frac{\sum_i (p_i^2 - m_i^2)}{3s_{12} - \sum_i m_i^2}\right), \qquad (7.7)$$

where t_{on} denotes the corresponding on-shell t-matrix. If we use these amplitudes to study the $\phi K \bar{K}$ system, instead of the on-shell ones we find a very similar result to that depicted in Fig.7.2, with the amplitude peaking at $\sqrt{s} = 2110$ MeV and $\sqrt{s_{23}} = 975$ MeV. Thus, the $K\bar{K}$ still appears very correlated around the $f_0(980)$, but the total energy has been shifted by 40 MeV. This is the result we obtain by using the off-shell t matrices and neglecting the effect of the $PPV \to PPV$ contact term of the theory, which as discussed in section 1.3.1.2 cancels the effect of the off-shell part of the t matrix. In other words, we could say that the three-body forces of the chiral Lagrangian are responsible for a shift of the resonance mass from 2110 to $\sim$ 2150 MeV, thus leading to a better agreement with the mass of the $X(2175)$, but, of course, the result holds for the particular choice of fields of the ordinary chiral Lagrangians.

7.6 Summary

In summary, the interaction of the $\phi K\bar{K}$ system studied with the Faddeev equations leads to a rearrangement of the $K\bar{K}$ subsystem as the $f_0(980)(0^{++})$ resonance. Then, the $f_0(980)$ together with the ϕ forms a narrow resonant 1^{--} state with a mass bigger than $m_\phi + 2m_K$, which decays into $\phi f_0(980)$ and hence is most naturally associated to the recently discovered $X(2175)$ resonance. The narrow width of around 27 MeV obtained here is compatible within errors with the experimental width $58\pm16\pm20$ MeV. We have also included $\phi\pi\pi$ as a coupled channel of $\phi K\bar{K}$ and find a peak very similar to the one found with the $\phi K\bar{K}$ channel alone, except that the peak is displaced by 38 MeV down to smaller masses. We also noted that the theoretical uncertainties are of this order of magnitude.

The typical differences of our results with the experimental ones are in the range of 50 MeV for the mass and the width are roughly compatible. These are typical differences found in successful models of hadron spectroscopy. The theory also shows that there is no resonance in $\phi a_0(980)$. Although a complete study of this state would require the addition of the $\phi\eta\pi$ channel, we found that the strength of the $\phi K\bar{K}$ amplitude in $I = 1$ is much smaller in magnitude than that of the $\phi K\bar{K}$ in $I = 0$, far away from developing a pole upon reasonable changes of the input variables. It would be most interesting to test experimentally this prediction.

The $\phi(1020)f_0(980)$ s-wave scattering has also been studied later in [144] employing chiral Lagrangians coupled to vector mesons through a minimal coupling. The $X(2175)$ resonance is generated in that approach by the self-interactions between the $\phi(1020)$ and the $f_0(980)$ resonances. The authors of [144] are able to describe the $e^+e^- \to \phi(1020)f_0(980)$ scattering data, concluding that the $X(2175)$ resonance has a large $\phi(1020)f_0(980)$ meson-meson component and, thus, confirming the results shown in this chapter.

Yet another work, with completely different model but similar conclusions like ours, has been reported recently [145].

CHAPTER 8

The $Y(4260)$ as a $J/\psi K\bar{K}$ system

We have studied another three meson system where a new charmonium like resonance has recently been found. It has been named as the $Y(4260)$ and it appears in the $J/\psi\pi\pi$ invariant mass. In many ways this state resembles the $X(2175)$ resonance which has been discussed in the previous chapter. As we will show in this chapter, the $Y(4260)$ also gets generated due to the dynamics of three mesons: $J/\psi\pi\pi$ and $J/\psi K\bar{K}$.

8.1 Introduction

An enhancement in the data for the $\pi^+\pi^- J/\psi$ invariant mass spectrum was found near 4.26 GeV by the BABAR collaboration in a study of the $e^+e^- \rightarrow \gamma_{ISR}\pi^+\pi^- J/\psi$ process [146]. A fit to this data set was made by assuming a resonance with 4.26 GeV of mass and 50 to 90 MeV of width [146]. The resonance was named as the $Y(4260)$ and it was found to be of $J^{PC} = 1^{--}$ nature. Later on, an accumulation of events with similar characteristics in the $\pi^+\pi^- J/\psi$, $\pi^0\pi^0 J/\psi$ and the $K^+K^- J/\psi$ mass spectra was reported by the CLEO collaboration [147, 148], thus confirming the results from BABAR. Following these works, the BELLE collaboration obtained the cross sections for

the $e^+e^- \to \pi^+\pi^- J/\psi$ reaction in the 3.8 to 5.5 GeV region [149], by keeping all the interactions in the final state in S-wave, and found a peak at 4.26 GeV and a bump around 4.05 GeV.

Although the $Y(4260)$ does not seem to fit in to the charmonium spectrum of the particle data group [22] known up to ~ 4.4 GeV, a proposal to accommodate it as a $4s$ state has been made in [150]. Several other suggestions have been made for the interpretation of this state, for example, the authors of [151] propose it to be a tetra-quark state, others propose a hadronic molecule of $D_1 D$, $D_0 D^*$ [152,153], $\chi_{c1}\omega$ [154], $\chi_{c1}\rho$ [155] and yet another idea is that it is a hybrid charmonium [156] or charm baryonium [157], etc. Within the available experimental information, none of these suggestions can be completely ruled out and it is not clear if the $Y(4260)$ possesses any of these structures dominantly or is a mixture of all of them. In Refs. [158–160] the authors call the attention of the readers to the presence of the opening of the $D_s^* \bar{D}_s^*$ channel very close to the peak position of the $Y(4260)$ in the updated data from BABAR [161] and associate the peak corresponding to $Y(4260)$ to a $D_s^* \bar{D}_s^*$ cusp. A fit to the data from [146, 161] has been made in [159] and the additional presence of a rather broad bump around 4.35 GeV has been proposed.

There are some peculiarities in the experimental findings which motivate us to carry out a study of the $J/\psi\pi\pi$ system. There is no enhancement found around 4.26 GeV in the process with the $D^* \bar{D}^*$ [162] or other hadron final states [22] and it is concluded that $Y(4260)$ has an unusually strong coupling to the $\pi\pi J/\psi$ final state [146–149]. Further, the data on the invariant mass of the $\pi\pi$ subsystem obtained by the Belle collaboration [149], for total energy range, 3.8-4.2 GeV, 4.2-4.4 GeV and 4.4-4.6 GeV, have curious features. The $\pi\pi$ mass distribution data in 3.8-4.2 GeV and 4.4-4.6 GeV seem to follow the phase space, however, that corresponding to the 4.2-4.4 GeV total energy differs significantly from the phase space and shows an enhancement near $m_{\pi\pi} = 1$ GeV. Do these findings indicate

that the $Y(4260)$ has a strong coupling to $f_0(980)J/\psi$, similar to the $X(2175)$ to the $\phi f_0(980)$ [47, 49]? It is interesting to recall that the $X(2175)$ was found as a dynamically generated resonance in the $\phi K\bar{K}$ system [58, 144] with the $K\bar{K}$ subsystem possessing the characteristics of the $f_0(980)$. Similarly, the $Y(4660)$ [163] has been suggested as a $\psi' f_0(980)$ resonance [164].

In order to find an answer to this question, we have solved the Faddeev equations for the $J/\psi\pi\pi$ and $J/\psi K\bar{K}$ coupled channels and we discuss the formalism and results of our study in this chapter.

8.2 Formalism

In the previous chapter the $\phi K\bar{K}$ system was investigated and we found the dynamical generation of the $X(2175)$ resonance [58]. The study was carried out by solving the Faddeev equations for the three-meson system using chiral Lagrangians for interaction of the constituent mesons. There are some similarities between the $X(2175)$ and the $Y(4260)$. Both resonances are of $J^{PC} = 1^{--}$ nature. The $X(2175)$ was found in the $\phi f_0(980)$ cross sections [47–49] and a study of this system using chiral dynamics required calculations for the $\phi K\bar{K}$ system since the $f_0(980)$ is basically a $K\bar{K}$ molecule in such a formalism. The $Y(4260)$ has been found in a system of a vector and two pseudoscalar mesons, with the two pseudoscalars interacting in s-wave and with their invariant mass showing a dominant peak around 1 GeV in the $Y(4260)$ region. This hints towards a possibility of clustering of the two pions to form the $f_0(980)$. If the two pions rearranged themselves to form the $f_0(980)$ resonance, the $Y(4260)$ would be about 200 MeV above the $J/\psi f_0$ threshold just as in case of the $X(2175)$ which is about 200 MeV above the $\phi f_0(980)$ threshold. Besides, the diagonal term of the potential obtained from chiral Lagrangian for $J/\psi\pi$ is zero just as the one for the ϕK (or $\phi\pi$) interaction. However, the $\phi\pi$ (or ϕK) scattering matrix is non-zero due to loops of the non-diagonal (coupled channel) $\phi\pi \to \bar{K}K^*(K\bar{K}^*)$ terms.

Similarly, the $J/\psi\pi \to J/\psi\pi$ at the lowest order is null but the scattering matrix is formed through iterations of the potential involving non diagonal transitions within the coupled channels, like $J/\psi\pi \to \bar{D}D^* \to J/\psi\pi$. This would give rise to three-body diagrams of the kind shown in Figs. 8.1 and 8.2. All these mentioned similarities between the $X(2175)$ and the $Y(4260)$, and the experimental findings of $Y(4260)$ with seemingly strong coupling to the $J/\psi\pi\pi$ channel motivate us to carry out a three-body calculation of the $J/\psi\pi\pi$ system. Then, by analogy to the study of the $\phi K\bar{K}$ system made in chapter 7, we study the $J/\psi\pi\pi$ and $J/\psi K\bar{K}$ systems as coupled channels in the isospin 0 base and by considering all the interactions in S-wave. In order to do that, we first have to calculate the two-body amplitudes for the pseudoscalar-vector and the pseudoscalar-pseudoscalar pairs.
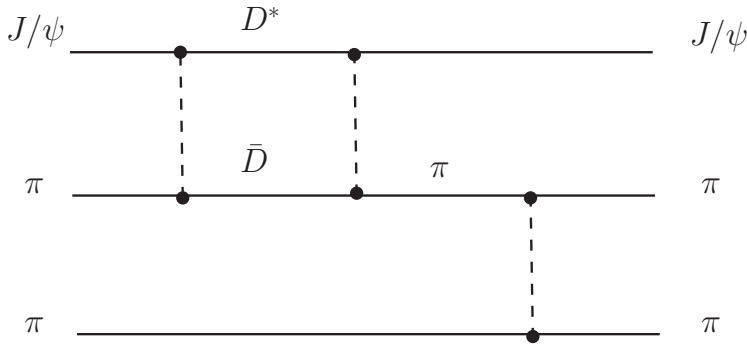
Figure 8.1: A three-body interaction diagram where the $J/\psi\pi$ interaction proceeds through $\bar{D}D^*$ coupled channel.

8.2.1 The t-matrix for the pseudoscalar-vector meson interaction.

For constructing the pseudoscalar-vector interaction Lagrangian we follow the works in [165, 166]. The starting point for the con-
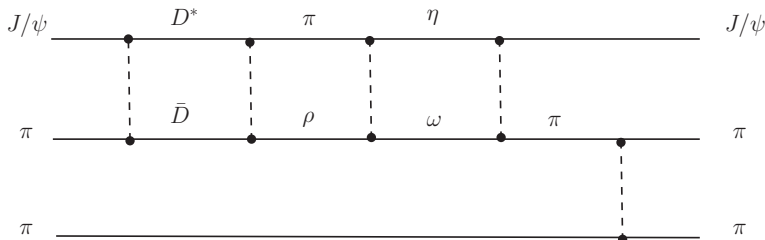
Figure 8.2: Another possible contribution of the $J/\psi\pi$ amplitude, through loops of other coupled channels, to the three-body interaction.

struction of the Lagrangian are fields containing all pseudoscalar and vector mesons from a 15-plet of $SU(4)$ plus a singlet. In the physical basis these fields read:

$$
\Phi = \begin{pmatrix}
\frac{\eta}{\sqrt{3}} + \frac{\pi^0}{\sqrt{2}} + \frac{\eta'}{\sqrt{6}} & \pi^+ & K^+ & \overline{D}^0 \\
\pi^- & \frac{\eta}{\sqrt{3}} - \frac{\pi^0}{\sqrt{2}} + \frac{\eta'}{\sqrt{6}} & K^0 & D^- \\
K^- & \overline{K}^0 & \sqrt{\frac{2}{3}}\eta' - \frac{\eta}{\sqrt{3}} & D_s^{\,-} \\
D^0 & D^+ & D_s^{\,+} & \eta_c
\end{pmatrix}
$$

$$
\mathcal{V}_\mu = \begin{pmatrix}
\frac{\rho_\mu^0}{\sqrt{2}} + \frac{\omega_\mu}{\sqrt{2}} & \rho_\mu^+ & K_\mu^{*+} & \bar{D}_\mu^{*0} \\
\rho_\mu^{*-} & \frac{-\rho_\mu^0}{\sqrt{2}} + \frac{\omega_\mu}{\sqrt{2}} & K_\mu^{*0} & D_\mu^{*-} \\
K_\mu^{*-} & \bar{K}_\mu^{*0} & \phi_\mu & D_{s\mu}^{*-} \\
D_\mu^{*0} & D_\mu^{*+} & D_{s\mu}^{*+} & J/\psi_\mu
\end{pmatrix}.
$$

These two fields differ from those used in [165, 166] because of the inclusion of a $SU(4)$ singlet in order to take into account the

η-η' and ω-ϕ mixing, which was not considered in these previous works.

For each one of these fields a current is defined:

$$J_\mu = (\partial_\mu \Phi)\Phi - \Phi \partial_\mu \Phi \tag{8.1}$$

$$\mathcal{J}_\mu = (\partial_\mu \mathcal{V}_\nu)\mathcal{V}^\nu - \mathcal{V}_\nu \partial_\mu \mathcal{V}^\nu. \tag{8.2}$$

and the Lagrangian is constructed by coupling these currents:

$$\mathcal{L}_{PPVV} = -\frac{1}{4f^2} Tr\left(J_\mu \mathcal{J}^\mu\right). \tag{8.3}$$

The Lagrangian in Eq. (8.3) is $SU(4)$ symmetric by construction. We know, though, that $SU(4)$ symmetry is badly broken in nature, because of the heavy charmed quark mass. The first step to break the $SU(4)$ symmetry in the Lagrangian is to recognize that the interaction behind the coupling of the two currents in Eq. (8.3) is the exchange of a vector meson, which can be formally visualized within the hidden gauge approach of [167–170]. In this way we suppress these terms in the Lagrangian where a heavy meson is exchanged by the factor $\gamma = m_L^2/m_H^2$ where m_L is the value of a light vector-meson mass (800 MeV) and m_H the value of the heavy vector-meson mass (2050 MeV). In the interaction of only heavy mesons ($D^*\bar{D}_s$, $\bar{D}_s D^*$) the vector meson exchanged is the J/ψ and we suppress it by the factor $\psi = m_L^2/m_{J/\psi}^2$. We also consider different values for the f appearing in the coupling of Eq. (8.3), for light mesons we use $f = f_\pi = 93$ MeV but for heavy ones $f = f_D = 165$ MeV.

With our phenomenological Lagrangian we can obtain the potential for a given process $(P(p)V(k))_i \rightarrow (P'(p')V'(k'))_j$:

$$v_{ij}(s,t,u) = -\frac{\xi_{ij}}{4f_i f_j}(s-u)\epsilon.\epsilon', \tag{8.4}$$

where s and u are the usual Mandelstam variables, f_k is the decay constant of the pseudoscalar meson k, ϵ's are the vector-meson polarization vectors and i, j refer to the initial and final

channels in the coupled channel space. The matrix of coefficients ξ_{ij} can be directly calculated from the Lagrangian of Eq. (8.3). Eq. (8.4) should be projected into s-wave, which is the only partial wave that we study. We come back to technical details in the results section.

We take the following coupled channels for the strangeness S=1 case: $K^*\pi$, ρK, $K^*\eta$, $K^*\eta\prime$, ωK, ϕK, $D_s^*\bar{D}$, $\bar{D}^*D_s$, $J/\psi K$ and $K^*\eta_c$. And the coefficient matrix ξ_{ij} for these channels in isospin $I = \frac{1}{2}$ is given below

$$
\xi = \begin{pmatrix}
2 & -\frac{1}{2} & 0 & 0 & -\frac{\sqrt{3}}{2} & \sqrt{\frac{3}{2}} & \sqrt{\frac{3}{2}}\gamma & 0 & 0 & 0 \\
-\frac{1}{2} & 2 & \sqrt{2} & -\frac{1}{2} & 0 & 0 & 0 & -\sqrt{\frac{3}{2}}\gamma & 0 & 0 \\
0 & \sqrt{2} & 0 & 0 & -\sqrt{\frac{2}{3}} & \frac{2}{\sqrt{3}} & \frac{\gamma}{\sqrt{3}} & -\frac{\gamma}{\sqrt{3}} & 0 & 0 \\
0 & -\frac{1}{2} & 0 & 0 & \frac{1}{2\sqrt{3}} & -\frac{1}{\sqrt{6}} & \frac{\gamma}{\sqrt{6}} & \sqrt{\frac{2}{3}}\gamma & 0 & 0 \\
-\frac{\sqrt{3}}{2} & 0 & -\sqrt{\frac{2}{3}} & \frac{1}{2\sqrt{3}} & 0 & 0 & 0 & \frac{\gamma}{\sqrt{2}} & 0 & 0 \\
\sqrt{\frac{3}{2}} & 0 & \frac{2}{\sqrt{3}} & -\frac{1}{\sqrt{6}} & 0 & 0 & \gamma & 0 & 0 & 0 \\
\sqrt{\frac{3}{2}}\gamma & 0 & \frac{\gamma}{\sqrt{3}} & \frac{\gamma}{\sqrt{6}} & 0 & \gamma & \psi & 0 & -\gamma & -\gamma \\
0 & -\sqrt{\frac{3}{2}}\gamma & -\frac{\gamma}{\sqrt{3}} & \sqrt{\frac{2}{3}}\gamma & \frac{\gamma}{\sqrt{2}} & 0 & 0 & \psi & -\gamma & -\gamma \\
0 & 0 & 0 & 0 & 0 & 0 & -\gamma & -\gamma & 0 & 0 \\
0 & 0 & 0 & 0 & 0 & 0 & -\gamma & -\gamma & 0 & 0
\end{pmatrix}
$$

For strangeness S=-1 the coupled channels considered are $\bar{K}^*\pi$, $\rho\bar{K}$, $\bar{K}^*\eta$, $\bar{K}^*\eta\prime$, $\omega\bar{K}$, $\phi\bar{K}$, $\bar{D}_s^*D$, $D^*\bar{D}_s$, $J/\psi\bar{K}$ and $\bar{K}^*\eta_c$ and the coefficients for these channels are the same as for their corresponding S=1 channels above.

For strangeness S=0, one can find the coupled channels and the coefficient matrix in [171].

To obtain the t-matrix we project in s-wave the potentials of Eq. (8.4) (removing $-\epsilon \cdot \epsilon'$) and plug them into the scattering equation for the coupled channels:

$$t = v + vg't. \tag{8.5}$$

In this equation g' is a diagonal matrix with each one of its elements given by the loop function for each channel in the coupled channel space. For channel i with mesons of masses m_1 and m_2, g'_{ii} is given by:

$$g'_{ii} = \frac{1}{16\pi^2} \left(\alpha_i + Log\frac{m_1^2}{\mu^2} + \frac{m_2^2 - m_1^2 + s}{2s} Log\frac{m_2^2}{m_1^2} \right.$$
$$+ \frac{p}{\sqrt{s}} \left(Log\frac{s - m_2^2 + m_1^2 + 2p\sqrt{s}}{-s + m_2^2 - m_1^2 + 2p\sqrt{s}} \right.$$
$$\left. \left. + Log\frac{s + m_2^2 - m_1^2 + 2p\sqrt{s}}{-s - m_2^2 + m_1^2 + 2p\sqrt{s}} \right) \right), \tag{8.6}$$

where p is the three momentum of the two mesons in their center of mass frame. The two parameters μ and α are not independent, we fix μ=1500 MeV and use for α the same values used in [166]. These values of α are obtained from moderate changes from their natural size [6] in order to fit the spectrum for most of the known light and charmed axial resonances.

8.2.2 The t-matrix for the pseudoscalar-pseudoscalar meson interaction.

As discussed earlier, the Lagrangian for the $\pi\pi$, $K\bar{K}$ diagonal and non-diagonal potential is obtained from the lowest order

chiral Lagrangian [2]

$$\mathcal{L} = \frac{1}{12f^2} Tr\left((\partial_\mu \Phi \Phi - \Phi \partial_\mu \Phi)^2 + M\Phi^4\right), \qquad (8.7)$$

where,

$$\Phi = \begin{pmatrix} \frac{\pi^0}{\sqrt{2}} + \frac{\eta_8}{\sqrt{6}} & \pi^+ & K^+ \\ \pi^- & -\frac{\pi^0}{\sqrt{2}} + \frac{\eta_8}{\sqrt{6}} & K^0 \\ K^- & \overline{K}^0 & -\frac{2}{\sqrt{6}}\eta_8 \end{pmatrix} \qquad (8.8)$$

and

$$M = \begin{pmatrix} m_\pi^2 & 0 & 0 \\ 0 & m_\pi^2 & 0 \\ 0 & 0 & 2m_K^2 - m_\pi^2 \end{pmatrix}. \qquad (8.9)$$

The on-shell part of the potential obtained from the Lagrangian Eq. (8.7) in S-wave, for total isospin of the two pseudoscalars equal to 0, is [2]

$$V_{K\bar{K}\to K\bar{K}} = -\frac{3}{4f^2}\, s_{23}$$

$$V_{\pi\pi\to K\bar{K}} = -\frac{\sqrt{3}}{4f^2} s_{23} \qquad (8.10)$$

$$V_{\pi\pi\to\pi\pi} = -\frac{1}{f^2}\left(s_{23} - \frac{m_\pi^2}{2}\right).$$

These potentials are used to solve the Bethe-Salpeter equations for $\pi\pi$ and $K\bar{K}$ coupled channels using the same subtraction constants as the ones used in [2]. We would like to mention that we have taken care of the symmetrization of the $\pi\pi$ states. The dynamical generation of the σ and $f_0(980)$ scalar resonances in these systems was found using the potentials Eq. (8.10) in [2].

Thus, we obtain the t-matrices for the scattering of two pseudoscalars and of the vector-pseudoscalar mesons which reproduce the experimental data in the corresponding cases. With these inputs we solve the Faddeev equations Eqs. (1.112). We shall now discuss the results of our calculations.

8.3   Results and conclusions

Using the t-matrices explained in the above section as input, we solve Eqs. (1.112) for the $J/\psi\pi\pi$ and $J/\psi K\bar{K}$ channels in total isospin 0, varying the total energy $\sqrt{s}$ between 4 and 5 GeV and the invariant mass of the two pseudoscalars, $\sqrt{s_{23}}$, between 400 to 1100 MeV. As explained above, the $J/\psi\pi$ and $J/\psi K$ interaction is null at the lowest order but it is non-zero when the loops of the coupled channels are considered in the iteration of the potential leading to the t-matrix. A diagram for the lowest order non-zero contribution to the $J/\psi\pi$ interaction has been shown in Fig. 8.1, and its contribution is written mathematically as

$$v_{\pi\pi\to\pi\pi}\ g^{13}\ v_{J/\psi\pi\to D^*\bar{D}}\ g'_{D^*\bar{D}}\ v_{D^*\bar{D}\to J/\psi\pi}. \tag{8.11}$$

The potential in Eq. (8.4) has been obtained by assuming that the momentum transfer, i.e., the Mandelstam variable t, in $J/\psi\pi \to D^*\bar{D}$ amplitude is negligibly small compared to the vector mass. However for the energies and channels considered here, such an approximation is not good and we need to take the effect of large momentum transfer into account. In order to do this, we consider the D^*-exchange in the $J/\psi\pi \to D^*\bar{D}$ potential (following [17]) to get

$$v_{J/\psi\pi\to D^*\bar{D}} \to \int \frac{d\hat{k}'}{4\pi} v_{J/\psi\pi\to D^*\bar{D}} \frac{-m_{D^*}^2}{(k'-k)^2 - m_{D^*}^2}, \tag{8.12}$$

where k' and k are the four vectors of the D^* and the J/ψ, respectively. This would mean that the $J/\psi\pi \to J/\psi\pi$ amplitude implicit in Eq. (8.11) would be as shown in Fig.8.3. Similarly,
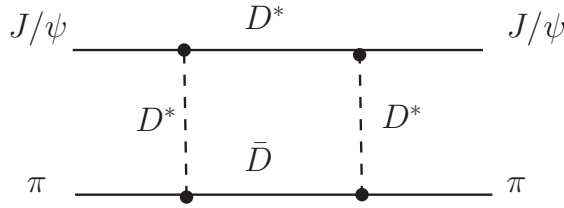
Figure 8.3: The $J/\psi\pi \to J/\psi\pi$ amplitude proceeding through the intermediate $D^*\bar{D}$ channel in the loop with a D^* exchange at the $J/\psi\pi \to D^*\bar{D}$ vertex.

we take into account this correction for the $J/\psi K$ and the $J/\psi\bar{K}$ amplitudes also.

With these new potentials we calculate the t-matrix for the J/ψ-pseudoscalar interaction and carry out the calculations for the $J/\psi\pi\pi$ and the $J/\psi K\bar{K}$ systems. We find a resonance in both systems at $\sqrt{s} = 4150$ MeV with a full width at half maximum of 90 MeV. The peak appears when the invariant mass of two pseudoscalars is around that of the $f_0(980)$, indicating that the resonance has a strong coupling to the $J/\psi f_0(980)$ channel. Both the $J/\psi\pi\pi$ and the $J/\psi K\bar{K}$ amplitudes are similar in this energy region, though they have quite different magnitudes. We find the $J/\psi K\bar{K}$ amplitude to be much larger in magnitude as compared to that of the $J/\psi\pi\pi$ system. This reveals the strong coupling of the three-body resonance to $J/\psi f_0(980)$, since the $f_0(980)$ couples most strongly to $K\bar{K}$ [3, 139, 172].

In Fig. 8.4 we show the $J/\psi K\bar{K}$ squared amplitude as a function of the total energy of the three body system and the invariant mass of the $K\bar{K}$ system. We have also studied the invariant mass spectrum of the two pions at $\sqrt{s} = 4$ GeV, 4.3 GeV and 4.5 GeV, i.e., in the energy region of the resonance and below and above it. To do that we take the three-body

$|T_R^*|^2$ (10^{-3}MeV^{-4})
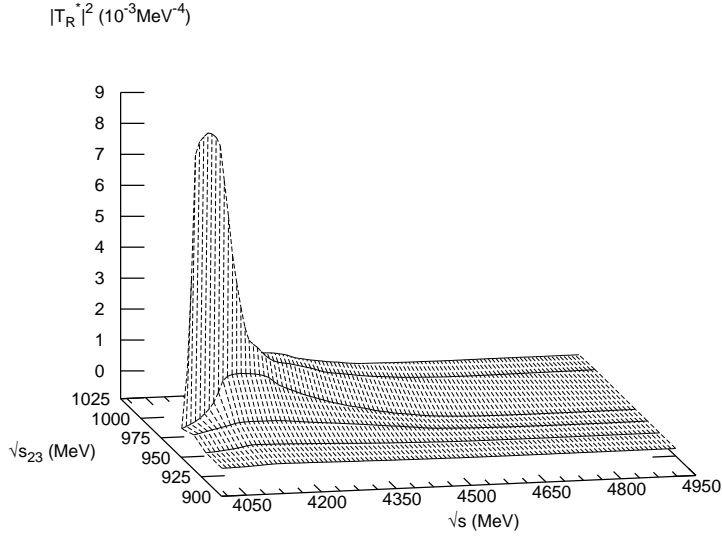
Figure 8.4: $|T_R^*|^2$ for the $J/\psi K\bar{K}$ system in total isospin $I = 0$ as a function of the total energy, $\sqrt{s}$, and the invariant mass of the $K\bar{K}$ subsystem, $\sqrt{s_{23}}$.

$|T_R^*|^2$-matrix and multiply it by the phase space factor

$$\frac{\tilde{p} \cdot \tilde{q}}{\sqrt{s}} \qquad (8.13)$$

where

$$\tilde{p} = \frac{\lambda^{1/2}(s, m_{J/\psi}^2, M_{inv}^2)}{2\sqrt{s}} \qquad (8.14)$$

is the momentum of the J/ψ in the global center of mass system and

$$\tilde{q} = \frac{\lambda^{1/2}(M_{inv}^2, m_\pi^2, m_\pi^2)}{2M_{inv}} \qquad (8.15)$$

the momentum of the pion in the corresponding two-body center of mass system (M_{inv} is the invariant mass of the two pions).

As shown in Figs. 8.5, the invariant mass spectrum at $\sqrt{s} = 4$ GeV shows a phase space like behavior and the one at $\sqrt{s} = 4.3$ GeV shows a dominant peak of the $f_0(980)$ resonance. At 4.5 GeV, we still see the presence of the $f_0(980)$ in the two pion mass spectrum but the magnitude of this peak is much smaller as compared to the one seen at $\sqrt{s} = 4.3$ GeV, and we find that it gradually fades away at higher energies.

The features described above and depicted in Fig. 8.5 agree qualitatively with those found for the $M_{\pi\pi}$ spectrum in [149]. One should note that the peak of the $|T|^2$ matrix is found around 4150 MeV rather than the nominal 4260 MeV. While 100 MeV difference is not a big difference for a hadronic model where no parameters have been fitted to the resonance data, the fact remains that this difference is the largest one found so far for all the three-body states that we have studied in the earlier chapters of this Thesis. This should not be surprising and we would like to attribute it to uncertainties in $SU(4)$ and the fact that, unlike other cases, here we have no data to tune our $J/\psi\pi$ and $J/\psi K$ ($\bar{K}$) interaction with our limited freedom in the subtraction constants.

In order to have some rough estimate of uncertainties we have varied the SU(4) symmetry breaking parameter, γ, which enters the evaluation of the $J/\psi\pi \rightarrow J/\psi\pi$ or $J/\psi K(\bar{K}) \rightarrow J/\psi K(\bar{K})$ amplitudes, which proceed as shown in Fig. 8.3 and involve necessarily this parameter. We summarize the results here: if we increase γ in 15 % we find that the strength of the peak of Fig. 8.4 is also increased in about 50 %. The magnitud of the peaks in Fig. 8.5 are also changed in a similar amount. However, we see that the position of the peaks and their widths are affected much less and the changes found are of the order of 5 MeV for both.

To summarize the results, the quantum numbers of the state obtained, the proximity in the mass to the experimental one and particularly the decay mode of the resonance give us strong

reasons to associate the state found to the $Y(4260)$ resonance.

With the end of the summary of this chapter we are close to the end of this Thesis. This is the last of the three-hadron systems we have studied so far. All our results are definitely encouraging and motivate us to scrutinize many more such systems. In the next and last chapter of this Thesis we will make a summary of our work along with a list of future plans.
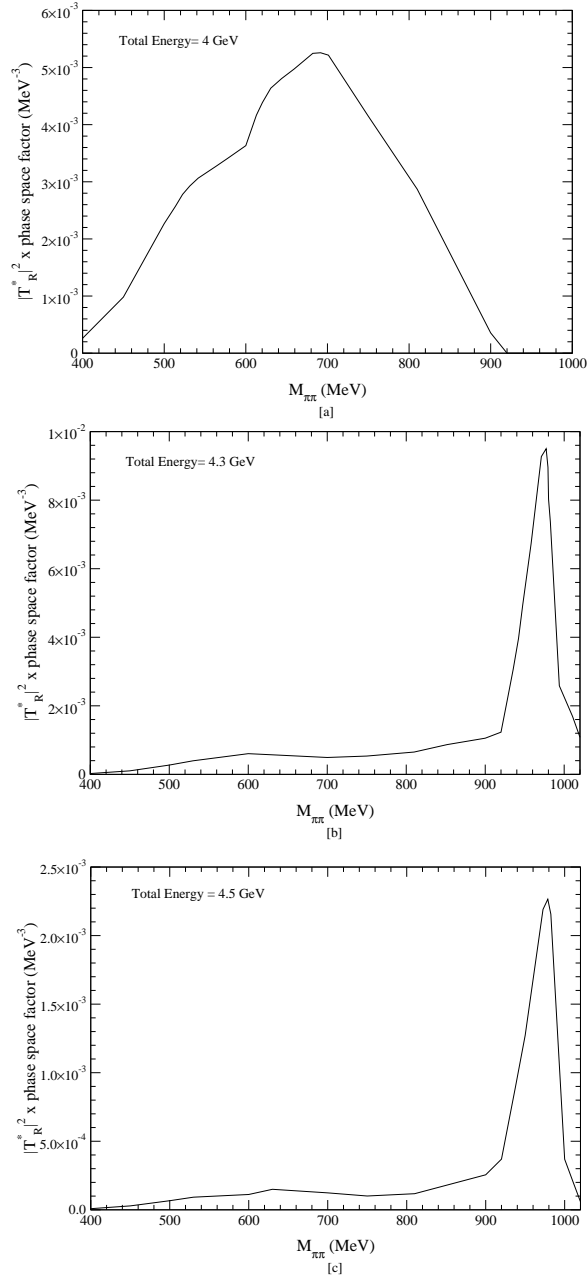
Figure 8.5: $|T_R^*|^2$ times the phase space factor for $J/\psi\pi\pi$ plotted as a function of the invariant mass $M_{\pi\pi}$ of the two pions system for three different total energies: a) 4 GeV; b) 4.3 GeV; c) 4.5 GeV.

CHAPTER 9

Summary and future outlook

In this Thesis we have formulated a general formalism to solve the Faddeev equations in the coupled channel approach by using unitary chiral dynamics to calculate the input two-body amplitudes for the different pairs of the system and its coupled channels. The off-shell contributions of the two-body t-matrices to the Faddeev equations has been found to give rise to three-body forces, apart from those arising directly from the chiral Lagrangian. However, the total sum of all these forces has been found to be zero in the $SU(3)$ limit. In a realistic case, this sum is only 5 % of the total on-shell contribution of the t-matrices to the Faddeev equations. Hence, the on-shell t-matrices have been used for the solution of the Faddeev equations, while at the same time neglecting three-body forces generated by the same chiral Lagrangian. This fact allowed us to reformulate the integral Faddeev equations into a set of algebraic equations.

We have applied this scheme to study several three-hadron systems. In chapter 3 we have explained our investigation of the $\pi \bar{K} N$ system and its coupled channels for $S = -1$, $Q = 0$ and $J^P = 1/2^+$ quantum numbers. The calculations result into dynamical generation of the following four Σ and two Λ resonances: $\Sigma(1560)$, $\Sigma(1620)$, $\Sigma(1660)$, $\Sigma(1770)$, $\Lambda(1600)$ and

$\Lambda(1810)$. The spin-parity for $\Sigma(1560)$ is unknown and our work predicts it to be $1/2^+$. The Σ's and Λ's found in our work correspond to all the $1/2^+$ resonances in the energy region scanned, i.e., $1500 - 1800$ MeV.

A study of the $\pi\pi N$ system and its coupled channels has been exposed in chapter 4. The calculated three-body T-matrix reveals dynamical generation of four resonances: (1) One with mass around 1704 MeV and 375 MeV of width, which we obtain when the two pions interact for an invariant mass close to 600 MeV in isospin zero, thus, in the $\sigma(600)$ region. This is in perfect agreement with the feature of the $N^*(1710)$ listed by the PDG [22]. (2) Another one with mass around that of the $N^*(2100)$, with one of the πN pairs simultaneously resonating as the $N^*(1650)$, implying a $\pi N^*(1650)$ structure. (3) Another one with mass and quantum numbers of the $\Delta(1910)$. (4) And yet another peak around 1920 MeV shows up in the T-matrix for the $K\bar{K}N$ channel with total isospin 1/2, $J^\pi = 1/2^+$, when the $K\bar{K}$ system clusters to generate the $f_0(980)$ and the $a_0(980)$ resonances. This state is not listed in the PDG and it was already suggested by the authors of [71]. In fact, there are many experimental findings which favor the existence of a N^* with spin-parity $1/2^+$ at an energy close to 1910 MeV, although better experimental studies are needed to confirm this state.

In chapter 5 we provide a series of arguments which support the idea that the peak seen in the $\gamma p \to K^+\Lambda$ reaction around 1920 MeV should correspond to the above mentioned state. At the same time we propose polarization experiments in that reaction as a further test of the prediction, as well as a study of the total cross section for $\gamma p \to K^+K^-p$ at energies close to threshold and of $d\sigma/dM_{inv}$ for invariant masses close to the two kaon threshold. These experiments are already going on at Spring8.

We have also looked for exotic states in two meson-one baryon systems. In chapter 6 we have considered the $N\pi K$ system with total strangeness +1 in order to investigate the possibility that the Θ^+ could be interpreted as a $N\pi K$ bound state. We do not

find any structure in the energy region 1530-1540 MeV, therefore the Θ^+ can not be considered as a $N\pi K$ bound state, with all the interactions in s-wave. However, a signal is found around 1720 MeV with about 200 MeV of width and with isospin zero, which reveals the underlying chiral dynamics of the three-body system, and that we hope can be seen in K^+N scattering, but much better in reactions producing $\pi K N$ in $I = 0$ in the final state. Our study should stimulate experimental work in this direction.

Recently, the $X(2175)$ resonance has been predicted in the $e^+e^- \to X \to \phi f_0(980)$ reaction. Since in the chiral models the $f_0(980)$ resonance appears in the $K\bar{K}$ interaction with a strong coupling to that channel, a study of the $\phi K\bar{K}$ system could explain the experimental results. We solved the few-body equations for the $\phi K\bar{K}$ and $\phi\pi\pi$ system and found the dynamical generation of the $X(2175)$ state when the $K\bar{K}$, $\pi\pi$ subsystem is resonating close to the $f_0(980)$, exactly as it was found experimentally. We further implement the final state interaction to the $e^+e^- \to \phi f_0(980)$ amplitude with our three-body T matrix and we are able to find the peak in the cross section around 2175 MeV. This has been elaborated in chapter 7.

In chapter 8, the model was also used to investigate the formation of the $Y(4260)$ resonance in the $J/\psi\pi\pi$ and $J/\psi K\bar{K}$ system, arriving to the conclusion that this state is dynamically generated when the three-body system clusters like a J/ψ and the $f_0(980)$.

The success obtained in the study of the $\pi\bar{K}N$, $\pi\pi N$, $\pi K N$, $\phi K\bar{K}$, and $J/\psi K\bar{K}$ systems and their respective coupled channels encourage us to extend the formalism to other systems.

The work developed in this Thesis opens a new research line in hadron physics and there are still many systems to be explored and whose properties can be understood as a consequence of having dynamical generation of three-body hadron resonances . Some examples of the systems which we plan to study are listed below.

Two baryon- One meson systems

Recently, several investigations have been made to check the possibility of existence of a bound state in the $\bar{K}NN$ system [59–65]. All these works arrive to the conclusion that there is a bound state in the $\bar{K}NN$ system, however, they have discrepancies about the value of the binding energy and the width of the bound state. We find a series of works based on Faddeev equations which lead to relatively large binding, of the order of 50-70 MeV [59–62], while other works based on variational methods lead to smaller bindings of the order of 20-30 MeV [63–65]. The widths also vary from 50-100 MeV. We believe that the origin of such discrepancies may lie in the fact that these models work with off-shell amplitudes: it is well known that given a certain physical amplitude, on shell in nature, there are infinite number of potentials that give this amplitude upon solving the Schrödinger equation. The differences between the different potentials will only show up in the off shell extrapolation of the amplitude. However, this information enters as an input while solving the Faddeev equation as well as in the variational calculations. Therefore, different potentials leading to the same on shell amplitude will provide different results upon solution of the respective equations.

Thus our formalism which does not depend on the off-shell part of the amplitudes can be very important in order to clarify the value of the width and binding energy of the bound state found in the $\bar{K}NN$.

It is also interesting to study systems like ηNN, ωNN, etc. The possibility of existence of η-nucleus bound states/resonances has been discussed since almost two decades ago [173] and the issue is still not settled. Many theoretical investigations suggest the existence of such states with deuteron or two nucleons. Also, a search of ω nucleus bound states is being made both experimentally and theoretically [174]. A study of such systems with our formalism could shed some light on these issues.

Two pseudoscalar and one vector meson systems

Analogous to the study we made of the $\phi K \bar{K}$, $\phi\pi\pi$ systems at high energies, it is also interesting to study systems like $\rho\pi\pi$, $\omega\pi\pi$, $K^*\pi\bar{K}$, etc., at lower energies since many of the low-lying vector states, like, for example, $\omega(1450)$, $\omega(1650)$ can couple strongly to these channels and, therefore, could be dynamically generated in those systems. Very recently a new resonance, namely the X(1576), has been found in the $K^*K\pi$ system [175] which would be also interesting to study.

Three-body systems with two vector mesons

Inspired by the success of the unitary chiral approach, a further extension has recently been made to study the interaction between two vector mesons and between one vector meson and one baryon [15,176–179]. The novelty is that instead of using interaction kernels provided by ChPT, one uses the transition amplitudes provided by the hidden-gauge Lagrangians [167], which lead to a suitable description of the interaction of vector mesons among themselves and of vector mesons with other mesons or baryons. Coupled-channel unitarity works in the same way as in the unitary chiral approach, but now the dynamics is provided by the hidden-gauge Lagrangians [167,168]. As shown by several recent works [176–181], this combination seems to work very well.

We can use these vector-vector and vector meson-baryon amplitudes as input in our formalism and, then, we can investigate the possibility of dynamical generation of states in systems formed by, for example, three vector mesons, two vector mesons and one baryon, two vector mesons and one pseudoscalar meson, etc.

Three pseudoscalar systems

There are several states listed in the Particle Data Book, for example, $\eta(1295)$, $\eta(1475)$, which have large branching ratios

for the $\eta\pi\pi$ decay channel. This indicates that the interaction of the $\eta\pi\pi$ and coupled channels might lead to such resonances. Therefore, investigation of these kind of systems could play an important role in understanding the properties of these states.

Resumen de la Tesis

Introducción

La Cromodinámica Cuántica (QCD) es la teoría de la interacción fuerte basada en una fuerza de color que describe la interacción entre quarks y gluones. Es bien conocido que el desarrollo perturbativo de QCD tiene gran éxito en la región de altas energías debido al fenómeno de la libertad asintótica (a altas energías los quarks que constituyen el hadrón interaccionan muy débilmente, tanto, que pueden cosiderarse como partículas libres), pero la teoría se convierte en no perturbativa a bajas e intermedias energías y es imposible utilizar métodos perturbativos para extraer información de los Lagrangianos de QCD. Existen progresos en esa línea (QCD en el retículo) pero todavía existen serios problemas por resolver.

Una de las teorías que han permitido describir con éxito la interacción fuerte a bajas e intermedias energías es la teoría chiral unitaria ($U\chi PT$), cuyo radio de convergencia es del ordern de 2 GeV. La teoría chiral unitaria ha permitido describir exitosamente la interacción hadrón-hadrón dando lugar a la explicación de muchos estados como resonancias generadas dinámicamente, hecho que pone de manifiesto la existencia de diversos estados cuyas propiedades no pueden explicarse como sistemas

187

de tres quarks o de pares quark-anti-quark.

Sin embargo, existen todavía muchos estados que parecen
poseer una estructura interna más compleja, como, por ejemplo,
dos mesones y un barión, o tres mesones. A pesar de que existe
una larga tradición en el estudio de sistemas de tres bariones,
como por ejemplo, sistemas formados por tres nucleones, un
estudio de sistemas formados por dos mesones y un barión, como
$\pi\pi\Sigma$, $\pi\pi\Lambda$, o tres mesones, como, por ejemplo, $\phi K\bar{K}$, $\phi\pi\pi$, etc.
no ha sido realizado nunca. El estudio de este tipo de sistemas
constituye un paso importante hacia un mayor conocimiento de
la interacción fuerte a energías intermedias y la estructura de
los hadrones.

En esta Tesis hemos realizado un estudio de sistemas for-
mados por tres hadrones, concretamente, dos mesones pseu-
doscalares y un barión del octete $1/2^{+}$, y un mesón vectorial
y dos mesones pseudoscalares, con el fin de explorar la posible
formación de resonancias e investigar los efectos de la inter-
acción de estas partículas en la sección eficaz de reacciones que
involucran un estado final de tres partículas.

Metodología

Para estudiar sistemas de tres cuerpos es necesario resolver
las ecuaciones de Faddeev. Tradicionalmente, las ecuaciones
de Faddeev han sido resueltas mediante el uso de potenciales
separables y considerando pocos canales acoplados. Sin em-
bargo, nosotros hemos utilizado la teoría chiral unitaria para
resolver dichas ecuaciones. Este hecho requiere la incorporación
de un gran número de canales acoplados a fin de implemen-
tar la simetría SU(3) en la dinámica chiral unitaria. El uso de
las amplitudes chirales nos ha permitido demostrar que existe
una cancelación entre la parte off-shell de esas amplitudes y las
fuerzas de tres cuerpos procedentes de los propios Lagrangianos
quirales, siendo por tanto la parte on-shell de las amplitudes la
única relevante a la hora de resolver las ecuaciones. Este he-
cho es de especial importancia, puesto que a diferencia de los

métodos utilizados usualmente que asumen una determinada
parte off-shell en los potenciales, los resultados obtenidos no
dependen de la extrapolación off-shell de las amplitudes, la cual
es no física, y permiten convertir las ecuaciones de Faddeev,
que son ecuaciones integrales, en un sistema algebraico de ecua-
ciones acopladas.

La resolución de las ecuaciones de Faddeev nos permite obtener
la matriz T del sistema de tres cuerpos y, por tanto, buscar reso-
nancias que puedan asociarse con estados que hayan sido obser-
vados experimentalmente. Para obtener la matriz T, tal y como
hemos explicado en el capítulo 1, reescribimos las ecuaciones de
Faddeev de la siguiente manera:

$$T^i = t^i \delta^3(\vec{k}'_i - \vec{k}_i) + \sum_{j \neq i = 1}^{3} T_R^{ij}, \quad i = 1, 2, 3 \qquad (9.1)$$

con $\vec{k}_i$ ($\vec{k}'_i$) el momento inicial (final) de la partícula i, tal que
las particiones T_R^{ij} satisfacen el siguiente sistema de ecuaciones
algebraicas

$$
\begin{aligned}
T_R^{12} &= t^1 g^{12} t^2 + t^1 \Big[G^{121} T_R^{21} + G^{123} T_R^{23} \Big] \\
T_R^{13} &= t^1 g^{13} t^3 + t^1 \Big[G^{131} T_R^{31} + G^{132} T_R^{32} \Big] \\
T_R^{21} &= t^2 g^{21} t^1 + t^2 \Big[G^{212} T_R^{12} + G^{213} T_R^{13} \Big] \\
T_R^{23} &= t^2 g^{23} t^3 + t^2 \Big[G^{231} T_R^{31} + G^{232} T_R^{32} \Big] \qquad (9.2) \\
T_R^{31} &= t^3 g^{31} t^1 + t^3 \Big[G^{312} T_R^{12} + G^{313} T_R^{13} \Big] \\
T_R^{32} &= t^3 g^{32} t^2 + t^3 \Big[G^{321} T_R^{21} + G^{323} T_R^{23} \Big]
\end{aligned}
$$

Las particiones T_R^{ij} contienen la contribución de todos los di-
agramas en los que las últimas interacciones vienen dadas en
términos de las matrices de dos cuerpos t^j y t^i, respectivamente.
g^{ij} es la función de Green del sistema y G^{ijk} es una función loop
(para más detalles véase capítulo 1).

De esta forma, la matriz T viene dada por

$$T = \sum_{i=1}^{3} T^i = \sum_{i=1}^{3} t^i \delta^3(\vec{k}_i' - \vec{k}_i) + T_R$$

$$T_R \equiv \sum_{i=1}^{3} \sum_{j \neq i=1}^{3} T_R^{ij} \qquad (9.3)$$

Todas las matrices que aparecen en la Eq. (9.2) están proyectadas en onda S, por lo tanto dando lugar a $J^\pi = 1/2^+$ para los sitemas de dos mesones y un barión estudiados y $J^\pi = 1^-$ para los sistemas de tres mesones analizados.

Este sistema de ecuaciones ha sido resuelto para diversos sistemas:

1. **Sistema Mesón-Mesón-Barión con extrañeza -1**

   Utilizando el formalismo desarrollado a lo largo de esta Tesis hemos estudiado el sistema $\pi\bar{K}N$ y sus 22 canales acoplados para carga total nula. Tal y como hemos mostrado en el capítulo 3, hemos obtenido la generación dinámica de todas las resonancias Σ y Λ de espín-paridad $1/2^+$ contenidas en la Tabla de Partículas en la región de energías 1500-1800 MeV.

2. **Estados de extrañeza nula y $J^P = 1/2^+$ como resonancias en el sistema $\pi\pi N$**

   Los resultados obtenidos en el estudio del sistema $\pi\bar{K}N$ nos hizo extender el modelo presentado en esta Tesis a sistemas formados por dos mesones y un barión para el caso de carga total nula y extrañeza cero.

   El análisis realizado en el capítulo 4 ha puesto de manifiesto que el estado $N^*(1710)$ puede interpretarse como un sistema resonante constituido por dos piones y un nucleón interaccionando en onda s. Además, también hemos obtenido que este estado tiene una importante componente $\sigma(600)N$ en su función de onda y que ningún otro

canal juega un papel importante en la generación de esa resonancia.

Sin embargo, tal y como vemos en la sección 4.3 de esta Tesis, a parte de este estado existen otras resonancias con espín-paridad $1/2^+$, como, por ejemplo, $N^*(2100)$ y $\Delta(1910)$ que no aparecen con las amplitudes procedentes de los Lagrangianos chirales al orden más bajo. Tal y como se pone de manifiesto en [17], sabemos que la teoría chiral unitaria utilizando los Lagrangianos a orden más bajo da lugar a una amplitud para la interacción πN que es capaz de reproducir los datos experimentales hasta una energía cercana a 1600 MeV, pero falla más allá de esa región de energía. De hecho, la resonancia $N^*(1650)$ no aparece con ese formalismo. Como consecuencia, cualquier estado formado por tres cuerpos en los que dos de sus partículas interaccionen para dar lugar a la resonancia $N^*(1650)$ no podríamos obtenerlo con el mismo modelo utilizado para el estudio del sistema $\pi\pi N$ y que da lugar al estado $N^*(1710)$.

En la sección 4.3 de esta Tesis realizamos un nuevo estudio del sistema $\pi\pi N$ y canales acoplados para extrañeza cero utilizando para describir la interacción del sistema πN: a) las amplitudes experimentales en lugar de las proporcionadas por la teoría chiral unitaria cuando estamos por encima del umbral del sistema πN ; b) Las amplitudes teóricas según el modelo desarrollado en [17] siempre que estemos por debajo del umbral de πN. A fin de comprobar este modelo, primero calculamos de nuevo la matriz T del sistema de tres cuerpos $\pi\pi N$ en la zona de energía cerca a 1700 MeV para ver si somos capaces de reproducir el estado $N^*(1710)$. La respuesta es que encontramos el mismo resultado que en el caso en el que utilizábamos las amplitudes chirales para el sistema πN. Confirmada la resonancia $N^*(1710)$, empezamos a ver si es posible generar también el resto de estados $1/2^+$ que se encuentran a energías más altas:

- En primer lugar realizamos un estudio del sistema $\pi\pi N$, considerando éste como único canal, utilizando la nueva amplitud πN que contiene información sobre la $N^*(1535)$ y $N^*(1650)$. Como resultado, a parte de obtener nuevamente el estado $N^*(1710)$, el estudio da lugar a otro estado sobre una energía total cercana a 2100 MeV y con una anchura alrededor de 250 MeV que puede identificarse con la resonancia $N^*(2100)$ que aparece en la Tabla de Partículas.

- Una vez hecho esto, consideramos los canales $\pi K\Sigma$, $\pi K\Lambda$, $\pi\eta N$ junto con el canal $\pi\pi N$ y recalculamos la amplitud. Esta vez, obtenemos un pico, de mayor magnitud, a una energía de 2080 MeV y con una anchura de 54 MeV. Los cambios surgidos como consecuencia de la adición de más canales pueden entenderse fácilmente si se considera que ahora la función de onda asociada a la resonancia contiene más componentes que en el caso de un solo canal, las cuáles tienen menor espacio de fases en el proceso de desintegración de la resonancia. Al mismo tiempo, la componente $\pi\pi N$ se ve reducida debido a la normalización de la función de onda y, por lo tanto, la anchura de desintegración a $\pi\pi N$ también se ve reducida. Además del estado $N^*(2100)$, obtenemos una resonancia con isospin $3/2$ con una masa cercana a 1910 que puede identificarse con el estado $\Delta(1910)$ de la Tabla de Partículas. Las dos resonancias, es decir, $N^*(2100)$ y $\Delta(1910)$, aparecen cuando la masa invariante del subsistema πN en isospin $1/2$ es cercana a 1650 MeV. Lo cual muestra que la presencia de la $N^*(1650)$ en la interacción πN juega un papel importante en la generación de estos dos estados y que la dinámica de todos los canales acoplados es esencial para el caso de la $\Delta(1910)$.

- A parte de estudiar la estructura σN y πN^* de estos sistemas, también hemos investigado la posibilidad

de obtener estados en los que los dos mesones puedan formar las resonancias $f_0(980)$ y $a_0(980)$. Para ello, hemos incluído el canal $K\bar{K}N$ ya que tanto la resonancia $f_0(980)$ como $a_0(980)$ se acoplan fuertemente a dicho canal. La resolución del sistema con este nuevo canal genera un pico sobre 2080 MeV con una anchura de 50 MeV que puede interpretarse como la componente $a_0(980)N$ del estado $N^*(2100)$. Además la matriz T para el sistema revela otro pico sobre 1920 MeV confirmando la predicción de D. Jido y Y. Kanada-En'yo [71] sobre la existencia de una resonancia N^* de espín-paridad $1/2^+$ sobre 1910 MeV. Este estado no aparece en la Tabla de Partículas, aunque especulaciones sobre su existencia existen desde hace casi 10 años.

Todos estos resultados se encuentran explicados con mayor detalle en el capítulo 4 de esta Tesis.

3. **Posible evidencia de una resonancia N^* constituida por tres hadrones en la reacción $\gamma p \to K^+ \Lambda$ reaction.**

   En el capítulo 4, tal y como hemos explicado, obtuvimos la generación dinámica de un nuevo estado N^* de espín-paridad $1/2^+$, de masa alrededor de 1920 MeV, como un estado constituido por dos mesones y un barión. Un estado de estas características, es decir, $I = 1/2$, $J^P = 1/2^+$ y masa cercana a 1920 MeV, fue predicho independientemente por los autores de [71] con un modelo basado en cálculos variacionales para el sistema $K\bar{K}N$. Un estado N^* de estas características no está catalogado en la Tabla de Partículas. Sin embargo, la sección eficaz para la reacción $\gamma p \to K^+ \Lambda$ muestra un pico sobre una energía de 1920 MeV [98, 99].

   La reacción $\gamma p \to K^+ \Lambda$ ha sido objeto de muchos estudios teóricos (véase las referencias del artículo arXiv:0902.3633

[nucl-th]) y, de hecho, los autores de [105] sugieren que la
señal observada alrededor de 1920 MeV en esa reacción
corresponde a una nueva resonancia N^*. Sin embargo,
no son capaces de identificar su espín y paridad, ya que
existen diversos estados con diferentes espín-paridad en
esa zona de energía asociados a los estados predichos por
los modelos de quarks. En el capítulo 5 hemos intentado
analizar si el estado observado con nuestro modelo y predi-
cho por los autores de [71] corresponde al pico observado
en la sección eficaz del proceso $\gamma p \rightarrow K^+ \Lambda$. Cabe destacar
que la sección eficaz para el proceso $\gamma p \rightarrow K^+ \Sigma^0$ no mues-
tra ningún pico en la región de energías cercana a 1920
MeV, así como en reacciones que involucren πN o ηN en
el estado final. Nosotros pensamos que la diferente intensi-
dad en las constantes de acoplo para los vértices $K^- p \rightarrow \Lambda$
y $K^- p \rightarrow \Sigma^0$ es la responsable de la aparición de un pico
relativamente estrecho en la reacción $\gamma p \rightarrow K^+ \Lambda$ y su
ausencia en el proceso $\gamma p \rightarrow K^+ \Sigma^0$.

También proponemos un razonamiento sencillo a través
del cuál somos capaces de explicar por qué el estado encon-
trado en el sistema $K\bar{K}N$ y canales acoplados no aparece
en reacciones inducidas por piones o procesos con πN o
ηN en el estado final, dado el pequeño acoplo de la res-
onancia $f_0(980)N$ a $\pi\pi$ o de la $a_0(980)$ a $\pi\eta$. Con tal
de observar estas propiedades hemos sugerido dos exper-
imentos. Uno de ellos consiste en la separación de las
componentes $S_z = 3/2$ y $S_z = 1/2$ en la sección eficaz
del proceso $\gamma p \rightarrow K^+ \Lambda$, lo cual permitirá descartar la
posibilidad de que el pico observado en esa sección efi-
caz corresponde a un estado de espín-paridad $3/2^+$ en
caso de que no se observe nada en el canal $S_z = 3/2$.
El otro experimento sugerido sería investigar la sección
eficaz del proceso $\gamma p \rightarrow K^+ K^- N$ cerca del umbral y la
distribución para la masa invariante para una energía cer-
cana a la suma de las masas de dos kaones, puesto que
si la sección eficaz mostrase un aumento cerca de ambos

umbrales indicaría la presencia de una resonancia debajo del umbral $K\bar{K}N$ donde los dos kaones estarán correlacionados para dar lugar a los estados $f_0(980)$ y $a_0(980)$. En el capítulo 5 hemos analizado la sección eficaz de estos procesos y hemos obtenido resultados que invitan a pensar que el pico observado en la reacción $\gamma p \rightarrow K^+\Lambda$ se corresponde con el estado predicho por los autores de [71] y confirmado por nosotros. Nuestro trabajo ha dado lugar a que se empiece a analizar nuestras propuestas para confirmar este estado en el laboratorio Spring8 en Osaka.

4. **Resonancias de $S = +1$ en el sistema $N\pi K$.**

La observación de un pico en la masa invariante K^+n para la reacción $\gamma n \rightarrow K^+K^-n$ en un blanco de ^{12}C en el laboratorio Spring8 en Osaka [35] generó grandes expectativas sobre el posible descubrimiento de un barión de extrañeza positiva, el cuál se denominó Θ^+. La señal observada fue asociada con un estado formado por cinco quarks, ya que con tres quarks no es posible obtener extrañeza $+1$. Después de este descubrimiento, se llevaron a cabo muchos experimentos con el afán de observar ese pico estimulando así la aparición de muchos trabajos teóricos con la finalidad de interpretar esa señal (véase la extensa lista de referencias, por ejemplo, en [132, 133]. Algunos experimentos observaron el estado, otros no y a pesar de que el pico fue confirmado en un nuevo análisis experimental realizado en LEPS, esta vez utilizando un blanco de deuterón y con más estadística, no se puede descartar que la señal que aparece sea consecuencia de las características particulares del LEPS. La situación actual es que todavía no existe ninguna explicación alternativa para la señal observada.

Desde el punto de vista teórico, la mayor parte de los trabajos realizados se concentraron en la búsqueda de un estado formado por cinco quarks. Sin embargo, desde el punto de vista de la interacción mesón-barión, la situación

no parece muy prometedora, ya que la interacción KN obtenida mediante Lagrangianos chirales es repulsiva [76]. Por lo tanto, no es de esperar que aparezca un estado estrecho como el observado en [35] en ese sistema. Por ese motivo, desde el principio, hubieron sugerencias de que si el pico observado representaba realmente una resonancia podría ser que pudiese explicarse como un estado ligado de $N\pi K$, con el pión actuando como una especie de pegamento entre el nucleón y el kaón. La energía de ligadura sería unos 30 MeV. No obstante, estudios realizados en esa línea pusieron de manifiesto la dificultad de formar un estado ligado en el sistema $N\pi K$ [83, 136].

En el capítulo 6 hemos investigado la posibilidad de la existencia de un estado de extrañeza positiva con un fuerte acoplamiento al sistema $N\pi K$ mediante el formalismo desarrollado en esta Tesis. El resultado de dicho estudio es que no encontramos ningún estado en la región de energías 1520-1540 MeV que pudiese asociarse con el Θ^+, pero observamos una estructura de unos 200 MeV de anchura sobre una energía de 1700 MeV para isospín total zero y en una zona de energía para el caso en el que el subsistema πK genera la resonancia $\kappa(700)$.

5. **Estudio de los mesones vectoriales** $X(2175)$ **e** $Y(4260)$**.** Recientemente se ha observado experimentalmente diversas resonancias mesónicas cuyas propiedades no pueden entenderse si se considera que están formadas por un par $q\bar{q}$. Estos estados reciben el nombre de X, Y, Z. Por ejemplo, la resonancia $X(2175)$ 1^{--} observada en BABAR [47, 48] en el proceso $e^+e^- \to \phi f_0(980)$ (también confirmada en BES en la reacción $J/\Psi \to \eta\phi f_0(980)$ [49]) ha generado diversos estudios intentando explicar sus propiedades considerando a ésta como un tetraquark o como un estado híbrido [50, 51]. Un estudio detallado de la reacción $e^+e^- \to \phi f_0(980)$ fue realizado en [54] utilizando diagramas con loops que involucran kaones y K^*, usando amplitudes chirales para el canal $K\bar{K} \to \pi\pi$ que contiene el polo

para el estado $f_0(980)$, el cual es generado dinámicamente por la teoría. Este estudio pone de manifiesto que el mecanismo utilizado es capaz de reproducir el fondo experimental observado para la reacción pero falla en reproducir la señal sobre 2175 MeV, por lo tanto, dando más fuerza a la posible existencia de un nuevo estado sobre esa energía.

Como en los modelos chirales la resonancia $f_0(980)$ se genera dinámicamente en el sistema $\pi\pi$, $K\bar{K}$, puede pensarse que el estado $X(2175)$ pudiera entenderse como un estado resonante en el sistema $\phi K\bar{K}$. En el capítulo 7 de esta Tesis hemos estudiado el sistema $\phi K\bar{K}$, $\phi\pi\pi$ considerando la interacción entre las tres partículas. Para ello hemos utilizado el formalismo desarrollado en los capítulos 1 y 2 encontrando que el estado $X(2175)$ se genera dinámicamente en el sistema de canales acoplados $\phi K\bar{K}$, $\phi\pi\pi$ cuando la masa invariante del subsistema $\pi\pi$, $K\bar{K}$ en isospín zero está cerca de la resonancia $f_0(980)$. Por lo tanto, indicando que la $X(2175)$ tiene un fuerte acoplo al sistema $\phi f_0(980)$, tal y como ha sido observado experimentalmente.

En el capítulo 8 de la Tesis hemos presentado un estudio del sistema formado por los canales $J/\psi K\bar{K}$, $J/\psi\pi\pi$ con tal de analizar la posible existencia de la resonancia $Y(4260)$, observada experimentalmente en la masa invariante $J/\psi\pi\pi$ para el proceso $e^+e^- \to \pi^+\pi^- J/\psi$ [147–149]. Nuestro trabajo muestra que este estado, análogamente a la $X(2175)$, puede interpretarse como un estado formado en el sistema $J/\psi K\bar{K}$, $J/\psi\pi\pi$ con el subsistema $K\bar{K}$, $\pi\pi$ resonando cerca de la $f_0(980)$.

Conclusiones

En esta Tesis hemos sentado las bases para la resolución de las ecuaciones de Faddeev con canales acoplados mediante el uso de la teoría quiral unitaria para calcular las matrices t que describen la interacción de los diferentes pares de partículas que

podemos tener en el sistema bajo consideración y sus respectivos canales acoplados. Tal y como hemos visto en la sección 1.3.1, la parte off-shell de las matrices t da lugar a una fuerza de tres cuerpos, además del término de contacto procedente del propio Lagrangiano chiral. Sin embargo, la suma de estas contribuciones resulta ser nula en el límite de $SU(3)$. En un caso más cercano a la realidad, esta suma es, aproximadamente, un 5% de la contributicón on-shell de las matrices t a las ecuaciones de Faddeev. Por lo tanto, para un modelo hadrónico, basta con considerar la parte on-shell de las matrices t para resolver las ecuaciones de Faddeev, despreciando al mismo tiempo las fuerzas de tres cuerpos procedentes del mismo Lagrangiano chiral. Este hecho permite convertir las ecuaciones integrales de Faddeev en unas algebraicas.

El formalismo desarrollado ha sido utilizado para el estudio de diferentes sistemas de tres cuerpos, dando lugar a la generación dinámica de muchos estados y explicando así las propiedades y la naturaleza de estos, que hasta el momento, en muchos casos, todavía era desconocida.

El trabajo llevado a cabo en esta Tesis abre una nueva línea de investigación en la Física Hadrónica y todavía existen muchos sistemas por explorar cuyas propiedades pueden ser debidas a la generación de resonancias formadas por la interacción de tres cuerpos. Algunos ejemplos de sistemas que tenemos en mente estudiar son:

1. **Sistemas formados por dos bariones y un mesón.**

   Recientemente, diversos trabajos teóricos han investigado la posibilidad de formar un estado ligado en el sistema $\bar{K}NN$ [59–65]. En todos ellos la conclusión es que existe un estado ligado en dicho sistema, sin embargo, existen discrepancias sobre el valor de la energía de ligadura y la anchura asociada al estado. De esta forma, aparecen una serie de artículos basados en las ecuaciones de Faddeev que dan lugar a una energía de ligadura relativamente grande, del orden de 50-70 MeV [59–62], mientras que otros trabajos basados en métodos variacionales generan una ligadura

menor, del orden de 20-30 MeV [63–65]. La anchura del estado ligado varía en el rango 50-100 MeV. En nuestra opinión el origen de tales discrepancias puede residir en el hecho de que estos modelos trabajan con la parte off-shell de las matrices t: es bien conocido que dada una cierta amplitud física, on-shell por naturaleza, existen infinitos potenciales que pueden dar lugar a esa amplitud después de resolver la ecuación de Schrödinger. La diferencia entre los potenciales radica en la extrapolación off-shell de estos. Esta información entra en juego tanto al resolver las ecuaciones de Faddeev como en los métodos variacionales. Por lo tanto, diferentes potenciales que dan lugar a la misma amplitud on-shell generarán diferentes resultados al resolver las correspondientes ecuaciones.

Con lo cual, un formalismo que no dependa de la parte off-shell de las amplitudes como el nuestro puede jugar un papel muy importante a la hora de clarificar el valor para la energía de ligadura y la anchura del estado ligado en el sistema $\bar{K}NN$.

También resulta interesante estudiar sistemas como, per ejemplo, ηNN, ωNN, etc. La posible existencia de estados ligados/resonancias de este tipo ha sido discutida desde hace casi dos décadas [173] y todavía no hay una respuesta clara. Muchos trabajos teóricos sugieren la existencia de tales estados con deuterón o dos nucleones. También, la búsqueda de estados ligados ωNN está llevándose a cabo en estos momentos teóricamente y experimentalmente [174]. Luego un estudio de tales sistemas con nuestro formalismo podría servir para confirmar teóricamente este tipo de estados.

2. **Sistemas de dos pseudoescalares y un mesón vectorial.**

Análogamente al estudio realizado del sistema $\phi K\bar{K}$, $\phi\pi\pi$ a altas energías, también sería interesante el estudio de sistemas como, por ejemplo, $\rho\pi\pi$, $\omega\pi\pi$, $K^*\pi\bar{K}$, etc., a en-

ergías más bajas ya que existen diversos estados, como, $\omega(1450)$, $\omega(1650)$ que pueden tener un fuerte acoplo a estos canales y, por lo tanto, podrían generarse dinámicamente en estos sistemas. Recientemente, un nuevo estado, $X(1576)$, ha sido observado experimentalmente en el sistema $K^*K\pi$ [175], luego sería interesante investigar este sistema.

3. **Sistemas de tres cuerpos que contienen dos mesones vectoriales.**

   Basado en el éxito de las teorías chirales unitarias, recientemente se ha llevado a cabo una generalización de éstas con tal de estudiar sistemas formados por dos mesones vectoriales y también un mesón vectorial y un barión [15, 176–179]. La novedad de estos trabajos es que en lugar de utilizar como potenciales en la ecuación de Bethe-Salpeter las amplitudes proporcionadas por las teorías chirales, se utilizan las proporcionadas por los Lagrangianos de la teoría del hidden-gauge [167]. Éstas permiten describir con éxito la interacción entre mesones vectoriales y también entre un mesón vectorial y otros mesones o bariones. La unitariedad en canles acoplados se implementa de la misma forma que en las teorías chirales, pero la dinámica viene dada ahora por los Lagrangianos de la teoría del hidden-gauge [167, 168]. Tal y como recientes trabajos apuntan [176–180] la combinación de unitariedad en canales acoplados y amplitudes proporcionadas por los Lagrangianos del hidden-gauge da lugar a buenos resultados en la descripción de los sistemas mencionados anteriormente.

   La extensión al caso de sistemas de tres cuerpos es inmediata, ya que bastaría con utilizar las amplitudes mesón vectorial- mesón vectorial y mesón vectorial-barión como input en nuestro formalismo. De esta forma podemos investigar la posibilidad de generar resonancias en sistemas formados, por ejemplo, por tres mesones vectoriales, dos mesones vectoriales y un barión, dos mesones vectoriales

y uno pseudoscalar, etc.

4. **Sistemas constituidos por tres mesones pseudoescalares.**

Existen diversos estados contenidos en la Tabla de Partículas, por ejemplo, $\eta(1295)$, $\eta(1475)$, que poseen una importante fracción de desintegración a sistemas de tres cuerpos como $\eta\pi\pi$. Este hecho pone de manifiesto que la interacción $\eta\pi\pi$ y canales acoplados podría dar lugar a la generación de esa resonancia. De este modo, el estudio de este tipo de sistemas puede desempeñar un papel importante a la hora de entender las propiedades de estos estados.

Bibliography

[1] D. Griffiths. Introduction to elementary particle physics. John Wiley & Sons, Inc., 1987.

[2] J. A. Oller and E. Oset. Chiral Symmetry Amplitudes in the S-Wave Isoscalar and Isovector Channels and the σ, $f_0(980)$, $a_0(980)$ Scalar Mesons. *Nucl. Phys.*, A620:438–456, 1997.

[3] J. A. Oller, E. Oset, and J. R. Pelaez. Meson-Meson interaction in a non-perturbative chiral approach. *Phys. Rev.*, D59:074001, 1999.

[4] J. A. Oller and E. Oset. N/D Description of Two Meson Amplitudes and Chiral Symmetry. *Phys. Rev.*, D60:074023, 1999.

[5] E. Oset and A. Ramos. Non perturbative chiral approach to s-wave $\bar{K}N$ interactions. *Nucl. Phys.*, A635:99–120, 1998.

[6] J. A. Oller and Ulf G. Meissner. Chiral dynamics in the presence of bound states: Kaon nucleon interactions revisited. *Phys. Lett.*, B500:263–272, 2001.

[7] E. Oset, A. Ramos, and C. Bennhold. Low lying S = -1 excited baryons and chiral symmetry. *Phys. Lett.*, B527:99–105, 2002.

[8] D. Jido, J. A. Oller, E. Oset, A. Ramos, and U. G. Meissner. Chiral dynamics of the two $\Lambda(1405)$ states. *Nucl. Phys.*, A725:181–200, 2003.

[9] C. Garcia-Recio, J. Nieves, E. Ruiz Arriola, and M. J. Vicente Vacas. $S = -1$ Meson-Baryon Unitarized Coupled Channel Chiral Perturbation Theory and the $S_{01}- \Lambda(1405)$ and $-\Lambda(1670)$ Resonances. *Phys. Rev.*, D67:076009, 2003.

[10] B. Borasoy, R. Nissler, and W. Weise. Chiral dynamics of kaon nucleon interactions, revisited. *Eur. Phys. J.*, A25:79–96, 2005.

[11] Jose A. Oller, Joaquim Prades, and Michela Verbeni. Surprises in threshold antikaon nucleon physics. *Phys. Rev. Lett.*, 95:172502, 2005.

[12] Jose A. Oller. On the strangeness -1 S-wave meson baryon scattering. *Eur. Phys. J.*, A28:63–82, 2006.

[13] V. K. Magas, E. Oset, and A. Ramos. Evidence for the two pole structure of the $\Lambda(1405)$ resonance. *Phys. Rev. Lett.*, 95:052301, 2005.

[14] B. Borasoy, U. G. Meissner, and R. Nissler. K^-p scattering length from scattering experiments. *Phys. Rev.*, C74:055201, 2006.

[15] L. Roca, Sourav Sarkar, V. K. Magas, and E. Oset. Unitary coupled channel analysis of the $\Lambda(1520)$ resonance. *Phys. Rev.*, C73:045208, 2006.

[16] L. Roca, E. Oset, and H. Toki. Testing the nature of the $\Lambda(1520)$ resonance through photoproduction. hep-ph/0411155, 2004.

[17] T. Inoue, E. Oset, and M. J. Vicente Vacas. Chiral unitary approach to S-wave meson baryon scattering in the strangeness S=0 sector. *Phys. Rev.*, C65:035204, 2002.

[18] C. Garcia-Recio, M. F. M. Lutz, and J. Nieves. Quark mass dependence of s-wave baryon resonances. *Phys. Lett.*, B582:49–54, 2004.

[19] E. van Beveren et al. A low-lying scalar meson nonet in a unitarized meson model. *Z. Phys.*, C30:615–620, 1986.

[20] Nils A. Tornqvist and Matts Roos. Resurrection of the Sigma Meson. *Phys. Rev. Lett.*, 76:1575–1578, 1996.

[21] A. Hosaka et al. Two-meson cloud contribution to the baryon antidecuplet binding. *Phys. Rev.*, C71:045205, 2005.

[22] C. Amsler et al. Review of particle physics. *Phys. Lett.*, B667:1, 2008.

[23] S. Prakhov et al. Reaction $K^- p \to \pi^0 \pi^0 \Lambda$ from $p(K^-) = $ 514-MeV/c to 750-MeV/c. *Phys. Rev.*, C69:042202, 2004.

[24] S. Prakhov et al. $K^- p \to \pi^0 \pi^0 \Sigma^0$ at $p(K^-) = $ 514-MeV/c to 750-MeV/c and comparison with other $\pi^0 \pi^0$ production. *Phys. Rev.*, C70:034605, 2004.

[25] Nathan Isgur and Gabriel Karl. P Wave Baryons in the Quark Model. *Phys. Rev.*, D18:4187, 1978.

[26] Nathan Isgur and Gabriel Karl. Positive Parity Excited Baryons in a Quark Model with Hyperfine Interactions. *Phys. Rev.*, D19:2653, 1979.

[27] L. Ya. Glozman and D. O. Riska. The Spectrum of the nucleons and the strange hyperons and chiral dynamics. *Phys. Rept.*, 268:263–303, 1996.

[28] R. A. Arndt, W. J. Briscoe, I. I. Strakovsky, R. L. Workman, and M. M. Pavan. Dispersion Relation Constrained Partial Wave Analysis of πN Elastic and $\pi N \rightarrow \eta N$ Scattering Data: The Baryon Spectrum. *Phys. Rev.*, C69:035213, 2004.

[29] R. A. Arndt, W. J. Briscoe, I. I. Strakovsky, and R. L. Workman. Extended Partial-Wave Analysis of πN Scattering Data. *Phys. Rev.*, C74:045205, 2006.

[30] R. E. Cutkosky, C. P. Forsyth, R. E. Hendrick, and R. L. Kelly. Pion - Nucleon Partial Wave Amplitudes. *Phys. Rev.*, D20:2839, 1979.

[31] D. M. Manley and E. M. Saleski. Multichannel resonance parametrization of πN scattering amplitudes. *Phys. Rev.*, D45:4002–4033, 1992.

[32] Wen-Tai Chiang, B. Saghai, F. Tabakin, and T. S. H. Lee. Dynamical coupled-channel model of kaon hyperon interactions. *Phys. Rev.*, C69:065208, 2004.

[33] Mijo Batinic, Ivo Slaus, Alfred Svarc, and B. M. K. Nefkens. pi N → eta N and eta N → eta N partial wave T matrices in a coupled, three channel model. *Phys. Rev.*, C51:2310–2325, 1995.

[34] S. Ceci, A. Svarc, and B. Zauner. The $\pi N \rightarrow \eta N$ data demand the existence of N(1710) P_{11} resonance reducing the 1700-MeV continuum ambiguity. *Phys. Rev. Lett.*, 97:062002, 2006.

[35] T. Nakano et al. Evidence for Narrow S=+1 Baryon Resonance in Photo- production from Neutron. *Phys. Rev. Lett.*, 91:012002, 2003.

[36] Dmitri Diakonov, Victor Petrov, and Maxim V. Polyakov. Exotic anti-decuplet of baryons: Prediction from chiral solitons. *Z. Phys.*, A359:305–314, 1997.

[37] Robert L. Jaffe and Frank Wilczek. Diquarks and exotic spectroscopy. *Phys. Rev. Lett.*, 91:232003, 2003.

[38] Sasa Ceci, Alfred Svarc, and Branimir Zauner. The re-analysis of the 1700-MeV structure of the P_{11} partial wave using the $\pi N \rightarrow K\Lambda$ production data. *Few Body Sys.*, 39:27–43, 2006.

[39] R. A. Arndt, Yakov I. Azimov, M. V. Polyakov, I. I. Strakovsky, and R. L. Workman. Nonstrange and other unitarity partners of the exotic Θ^+ baryon. *Phys. Rev.*, C69:035208, 2004.

[40] I. I. Strakovsky, R. A. Arndt, Yakov I. Azimov, M. V. Polyakov, and R. L. Workman. Present status of the non-strange and other flavor partners of the exotic Theta+ baryon. *J. Phys. Conf. Ser.*, 9:218, 2005.

[41] Kenneth H. Hicks. Experimental search for pentaquarks. *Prog. Part. Nucl. Phys.*, 55:647–676, 2005.

[42] Z. P. Li. Photoproduction signatures of hybrid baryons: An Application of the quark model with gluonic degrees of freedom. *Phys. Rev.*, D44:2841–2850, 1991.

[43] F. Cano, P. Gonzalez, S. Noguera, and B. Desplanques. Strong pionic decays of baryons from a spectroscopic quark model. *Nucl. Phys.*, A603:257–280, 1996.

[44] O. Krehl, C. Hanhart, S. Krewald, and J. Speth. What is the structure of the Roper resonance? *Phys. Rev.*, C62:025207, 2000.

[45] M. Dillig and M. Schott. Mesonic content of the nucleon and the Roper resonance. *Phys. Rev.*, C75:067001, 2007.

[46] T. Hyodo, A. Hosaka, E. Oset, A. Ramos, and M. J. Vicente Vacas. $\Lambda(1405)$ production in the $\pi^- p \rightarrow K^0 \pi\Sigma$ reaction. *Phys. Rev.*, C68:065203, 2003.

[47] B. Aubert et al. A Structure at 2175-MeV in $e^+e^- \to \phi$
     $f_0(980)$ Observed via Initial-State Radiation. *Phys. Rev.*,
     D74:091103, 2006.

[48] B. Aubert et al. The $e^+e^- \to K^+K^-\pi^+\pi^-$, $K^+K^-\pi^0\pi^0$
     and $K^+K^-K^+K^-$ Cross Sections Measured with Initial-
     State Radiation. *Phys. Rev.*, D76:012008, 2007.

[49] Medina Ablikim et al. Observation of $Y(2175)$ in $J/\psi \to$
     $\eta\phi f_0(980)$. *Phys. Rev. Lett.*, 100:102003, 2008.

[50] Zhi-Gang Wang. Analysis of Y(2175) as a tetraquark state
     with QCD sum rules. *Nucl. Phys.*, A791:106–116, 2007.

[51] Gui-Jun Ding and Mu-Lin Yan. Y(2175): Distinguish hy-
     brid state from higher quarkonium. *Phys. Lett.*, B657:49–
     54, 2007.

[52] F. E. Close. Rumsfeld Hadrons. 2007.

[53] Shi-Lin Zhu. New hadron states. *Int. J. Mod. Phys.*,
     E17:283–322, 2008.

[54] M. Napsuciale, E. Oset, K. Sasaki, and C. A. Vaquera-
     Araujo. Electron-positron annihilation into $\phi f_0(980)$ and
     clues for a new 1^{--} resonance. *Phys. Rev.*, D76:074012,
     2007.

[55] L. D. Faddeev. Scattering theory for a three particle sys-
     tem. *Sov. Phys. JETP*, 12:1014–1019, 1961.

[56] A. Martínez Torres, K. P. Khemchandani, and E. Oset.
     Three body resonances in two meson-one baryon systems.
     Phys. Rev., C77:042203, 2008.

[57] K. P. Khemchandani, A. Martínez Torres, and E. Oset.
     The $N^*(1710)$ as a resonance in the $\pi\pi N$ system. *Eur.
     Phys. J.*, A37:233–243, 2008.

[58] A. Martínez Torres, K. P. Khemchandani, L. S. Geng, M. Napsuciale, and E. Oset. The X(2175) as a resonant state of the $\phi K \bar{K}$ system. *Phys. Rev.*, D78:074031, 2008.

[59] N. V. Shevchenko, A. Gal, and J. Mares. Faddeev calculation of a $K^- pp$ quasi-bound state. *Phys. Rev. Lett.*, 98:082301, 2007.

[60] N. V. Shevchenko, A. Gal, J. Mares, and J. Revai. $\bar{K}NN$ quasi-bound state and the $\bar{K}N$ interaction: coupled-channel Faddeev calculations of the $\bar{K}NN - \pi \Sigma N$ system. *Phys. Rev.*, C76:044004, 2007.

[61] Toshimitsu Yamazaki and Yoshinori Akaishi. The basic K nuclear cluster $K^- pp$ and its enhanced formation in the $p + p \rightarrow K^+ + X$ reaction. *Phys. Rev.*, C76:045201, 2007.

[62] Y. Ikeda and T. Sato. Strange dibaryon resonance in the anti-K N N - pi Sigma N system. *Phys. Rev.*, C76:035203, 2007.

[63] Akinobu Dote and Wolfram Weise. Study of light kaonic nuclei with a chiral SU(3) - based $\bar{K}N$ interaction. *Prog. Theor. Phys. Suppl.*, 168:593–597, 2007.

[64] Akinobu Dote, Tetsuo Hyodo, and Wolfram Weise. $K^- pp$ system with chiral SU(3) effective interaction. *Nucl. Phys.*, A804:197–206, 2008.

[65] Akinobu Dote, Tetsuo Hyodo, and Wolfram Weise. Variational calculation of the ppK^- system based on chiral SU(3) dynamics. *Phys. Rev.*, C79:014003, 2009.

[66] E. Epelbaum et al. Few nucleon systems with two-nucleon forces from chiral effective field theory. *Eur. Phys. J.*, A15:543–563, 2002.

[67] V. Bernard, E. Epelbaum, H. Krebs, and Ulf-G. Meissner. Subleading contributions to the chiral three-nucleon force I: long-range terms. *Phys. Rev.*, C77:064004, 2008.

[68] C. Hanhart. private communication.

[69] C. Hanhart and A. Wirzba. Remarks on $NN \rightarrow NN\pi$ beyond leading order. *Phys. Lett.*, B650:354–361, 2007.

[70] E. Oset, H. Toki, M. Mizobe, and Toru T. Takahashi. sigma exchange in the N N interaction within the chiral unitary approach. *Prog. Theor. Phys.*, 103:351–365, 2000.

[71] Daisuke Jido and Yoshiko Kanada-En'yo. $K\bar{K}N$ molecule state with $I = 1/2$ and $J^P = 1/2^+$ studied with three-body calculation. *Phys. Rev.*, C78:035203, 2008.

[72] K. P. Khemchandani, A. Martínez Torres, and E. Oset. S = -1 resonances in two meson-one baryon systems. *Few Body Syst.*, 44:145–147, 2008.

[73] C. Lovelace. Strong Interactions and High Energy Physics. Edited by R. G. Moorhouse, Oliver & Boyd, 1964.

[74] J. Gasser and H. Leutwyler. Chiral Perturbation Theory: Expansions in the Mass of the Strange Quark. *Nucl. Phys.*, B250:465, 1985.

[75] Ulf G. Meissner. Recent developments in chiral perturbation theory. *Rept. Prog. Phys.*, 56:903–996, 1993.

[76] V. Bernard, Norbert Kaiser, and Ulf-G. Meissner. Chiral dynamics in nucleons and nuclei. *Int. J. Mod. Phys.*, E4:193–346, 1995.

[77] G. Ecker. Chiral perturbation theory. *Prog. Part. Nucl. Phys.*, 35:1–80, 1995.

[78] Elizabeth Ellen Jenkins and Aneesh V. Manohar. Baryon chiral perturbation theory using a heavy fermion Lagrangian. *Phys. Lett.*, B255:558–562, 1991.

[79] L. Roca, E. Oset, and J. Singh. Low lying axial-vector mesons as dynamically generated resonances. *Phys. Rev.*, D72:014002, 2005.

[80] Mandl and Shaw. Quantum field theory. John Wiley & Sons, 2002.

[81] C. Joachain. Quantum Collison theory. North-Holland, 1975.

[82] H. Pierre Noyes and E. D. Jones. Solution of a relativistic three body problem. *Few Body Syst.*, 27:123–139, 1999.

[83] Felipe J. Llanes-Estrada, E. Oset, and V. Mateu. On the possible nature of the Θ^+ as a $K\pi N$ bound state. *Phys. Rev.*, C69:055203, 2004.

[84] P. Fernandez de Cordoba et al. Projectile delta excitation in alpha - proton scattering. *Nucl. Phys.*, A586:586–606, 1995.

[85] E. Epelbaum et al. The three- and four-nucleon systems from chiral effective field theory. *Phys. Rev. Lett.*, 86:4787–4790, 2001.

[86] B. R. Martin, M. K. Pidcock, and R. G. Moorhouse. $\bar{K}n$ Interactions in the Resonance Region. 3. Resonance Spectra. *Nucl. Phys.*, B127:349, 1977.

[87] R. Armenteros et al. Energy-independent partial-wave analysis of $K^- n \rightarrow \Lambda\pi$ between 600 and 1200 mev/c. *Nucl. Phys.*, B8:183–194, 1968.

[88] E. Hernandez, E. Oset, and M. J. Vicente Vacas. The two pion decay of the Roper resonance. *Phys. Rev.*, C66:065201, 2002.

[89] Richard A. Arndt, Igor I. Strakovsky, Ron L. Workman, and Marcello M. Pavan. Updated analysis of πN elastic scattering data to 2.1- GeV: The Baryon spectrum. *Phys. Rev.*, C52:2120–2130, 1995.

[90] T. Mart and C. Bennhold. Evidence for a missing nucleon resonance in kaon photoproduction. *Phys. Rev.*, C61:012201, 2000.

[91] A. Usov and O. Scholten. K Lambda and K Sigma photo-production in a coupled channels framework. *Phys. Rev.*, C72:025205, 2005.

[92] O. Scholten. private communication.

[93] H. Harari and H. J. Lipkin. Three-Particle Baryon Resonances in Unitary Symmetry. *Phys. Rev. Lett.*, 13:345–348, 1964.

[94] Norbert Kaiser, P. B. Siegel, and W. Weise. Chiral dynamics and the low-energy kaon - nucleon interaction. *Nucl. Phys.*, A594:325–345, 1995.

[95] A. Dobado and J. R. Pelaez. The inverse amplitude method in Chiral Perturbation Theory. *Phys. Rev.*, D56:3057–3073, 1997.

[96] T. Hyodo, S. I. Nam, D. Jido, and A. Hosaka. Flavor $SU(3)$ breaking effects in the chiral unitary model for meson baryon scatterings. *Phys. Rev.*, C68:018201, 2003.

[97] Yoshiko Kanada-En'yo and Daisuke Jido. $\bar{K}\bar{K}N$ molecule state in three-body calculation. *Phys. Rev.*, C78:025212, 2008.

[98] K. H. Glander et al. Measurement of $\gamma p \rightarrow K^+\Lambda$ and $\gamma p \rightarrow > K^+\Sigma^0$ at photon energies up to 2.6 GeV. *Eur. Phys. J.*, A19:251–273, 2004.

[99] R. Bradford et al. Differential cross sections for $\gamma + p \rightarrow K^+ + Y$ for Λ and Σ^0 hyperons. *Phys. Rev.*, C73:035202, 2006.

[100] M. Sumihama et al. The $\gamma(\text{pol.}) \, p \rightarrow K^+\Lambda$ and $\gamma(\text{pol.}) \, p \rightarrow K^+\Sigma^0$ reactions at forward angles with photon energies from 1.5-GeV to 2.4-GeV. *Phys. Rev.*, C73:035214, 2006.

[101] A. Usov and O. Scholten. $K\Lambda$ and $K\Sigma$ photoproduction in a coupled channels framework. *Phys. Rev.*, C72:025205, 2005.

[102] V. Shklyar, H. Lenske, and U. Mosel. A coupled-channel analysis of $K\Lambda$ production in the nucleon resonance region. *Phys. Rev.*, C72:015210, 2005.

[103] B. Julia-Diaz, B. Saghai, T. S. H. Lee, and F. Tabakin. Dynamical coupled-channel approach to hadronic and electromagnetic production of kaon-hyperon on the proton. *Phys. Rev.*, C73:055204, 2006.

[104] B. Borasoy, P. C. Bruns, Ulf-G. Meissner, and R. Nissler. A gauge invariant chiral unitary framework for kaon photo- and electroproduction on the proton. *Eur. Phys. J.*, A34:161–183, 2007.

[105] T. Mart. Electromagnetic Productions of $K\Lambda$ and $K\Sigma$ on the Nucleons. *AIP Conf. Proc.*, 1056:31–38, 2008.

[106] V. A. Nikonov, A. V. Anisovich, E. Klempt, A. V. Sarantsev, and U. Thoma. Further evidence for $N(1900)$ P_{13} from photoproduction of hyperons. *Phys. Lett.*, B662:245–251, 2008.

[107] R. A. Arndt, W. J. Briscoe, I. I. Strakovsky, and R. L. Workman. Extended Partial-Wave Analysis of πN Scattering Data. *Phys. Rev.*, C74:045205, 2006.

[108] A. Martínez Torres, K. P. Khemchandani, and E. Oset. Solution to Faddeev equations with two-body experimental amplitudes as input and application to $J^P = 1/2^+$, S=0 baryon resonances. 2008.

[109] F. X. Lee, T. Mart, C. Bennhold, and L. E. Wright. Quasifree kaon photoproduction on nuclei. *Nucl. Phys.*, A695:237–272, 2001.

[110] F. E. Close and R. G. Roberts. Consistent analysis of the spin content of the nucleon. *Phys. Lett.*, B316:165–171, 1993.

[111] E. Oset and A. Ramos. ϕ decay in nuclei. *Nucl. Phys.*, A679:616–628, 2001.

[112] Ulf G. Meissner, Norbert Kaiser, H. Weigel, and J. Schechter. Realistic pseudoscalar - vector Lagrangian. 2. Static and dynamical baryon properties. *Phys. Rev.*, D39:1956, 1989.

[113] D. W. Thomas, A. Engler, H. E. Fisk, and R. W. Kraemer. Strange particle production from pi- p interactions at 1.69 gev/c. *Nucl. Phys.*, B56:15–45, 1973.

[114] J. J. Jones et al. Total cross-sections for $\pi^- p \to \Lambda K^0$ from threshold to 1.13 gev/c. *Phys. Rev. Lett.*, 26:860–863, 1971.

[115] R. C. Carrasco, E. Oset, and L. L. Salcedo. Inclusive (gamma, pi) reactions in nuclei. *Nucl. Phys.*, A541:585–622, 1992.

[116] R. G. T. Zegers et al. Beam polarization asymmetries for the $p(\gamma, K^+)\Lambda$ and $p(\gamma, K^+)\Sigma^0$ reactions at $E(\gamma) = $ 1.5-GeV - 2.4-GeV. *Phys. Rev. Lett.*, 91:092001, 2003.

[117] D. Drechsel. The Drell-Hearn-Gerasimov sum rule. *Prog. Part. Nucl. Phys.*, 34:181–200, 1995.

[118] J. Ahrens et al. First measurement of the Gerasimov-Drell-Hearn integral for Hydrogen from 200 to 800 MeV. *Phys. Rev. Lett.*, 87:022003, 2001.

[119] J. Ahrens et al. First measurement of the helicity dependence for the $\gamma p \to p\pi^+\pi^-$ reaction. *Eur. Phys. J.*, A34:11–21, 2007.

[120] J. C. Nacher and E. Oset. Study of polarization observables in double pion photoproduction on the proton. *Nucl. Phys.*, A697:372–387, 2002.

[121] D. P. Barber et al. Strangeness exchange in the photoproduction of $K^+\Lambda(1520)$ between 2.8-GeV and 4.8-GeV. *Zeit. Phys.*, C7:17, 1980.

[122] J. Barth et al. Low-energy photoproduction of ϕ mesons. *Eur. Phys. J.*, A17:269–274, 2003.

[123] V. Kubarovsky et al. Search for Θ^+ pentaquarks in the exclusive reaction $\gamma p \to K^+ K^- p$. *Phys. Rev. Lett.*, 97:102001, 2006.

[124] Takashi Nakano. Results and prospects from LEPS and LEPS2. *AIP Conf. Proc.*, 915:162–167, 2007.

[125] W. Roberts. A phenomenological Lagrangian approach to two kaon photoproduction and pentaquark searches. *Phys. Rev.*, C70:065201, 2004.

[126] Yongseok Oh, K. Nakayama, and T. S. H. Lee. Pentaquark $\Theta(1540)^+$ production in $\gamma N \to K \bar{K} N$. *Phys. Rept.*, 423:49–89, 2006.

[127] Alexander Sibirtsev, Johann Haidenbauer, S. Krewald, Ulf-G. Meissner, and Anthony William Thomas. K anti-K photoproduction from protons. *Eur. Phys. J.*, A31:221–232, 2007.

[128] E. Oset, Jose A. Oller, and Ulf-G. Meissner. Chiral dynamics and the reactions $pp \to dK^+ \bar{K}^0$ and $pp \to d\pi^+\eta$. *Eur. Phys. J.*, A12:435–446, 2001.

[129] C Hanhart, Yu. S Kalashnikova, Alexander Evgenyevich Kudryavtsev, and A. V Nefediev. Reconciling the X(3872) with the near-threshold enhancement in the $D^0\bar{D}^{*0}$ final state. *Phys. Rev.*, D76:034007, 2007.

[130] A. Dzyuba et al. Interpretation of $K^+\bar{K}^0$ pair production in pp collisions. *Eur. Phys. J.*, A38:1–8, 2008.

[131] T. Nakano. Private communication.

[132] S. I. Nam, A. Hosaka, and H. Ch. Kim. Production of the pentaquark Θ^+ in n p scattering. *Phys. Rev.*, D70:114027, 2004.

[133] Marek Karliner and Harry J. Lipkin. Why the Θ^+ is seen in some experiments and not in others: A possible explanation. *Phys. Lett.*, B597:309–313, 2004.

[134] Kenneth H. Hicks. Experimental search for pentaquarks. *Prog. Part. Nucl. Phys.*, 55:647–676, 2005.

[135] T. Nakano et al. Evidence of the Θ^+ in the $\gamma d \rightarrow K^+K^-pn$ reaction. *Phys. Rev.*, C79:025210, 2009.

[136] P. Bicudo and G. M. Marques. The $\Theta^+(1540)$ as a heptaquark with the overlap of a pion, a kaon and a nucleon. *Phys. Rev.*, D69:011503, 2004.

[137] N. G. Kelkar, M. Nowakowski, and K. P. Khemchandani. Time delayed K^+N reactions and exotic baryon resonances. *J. Phys.*, G29:1001–1009, 2003.

[138] J. S. Hyslop, R. A. Arndt, L. D. Roper, and R. L. Workman. Partial wave analysis of K^+ nucleon scattering. *Phys. Rev.*, D46:961–969, 1992.

[139] Norbert Kaiser. $\pi\pi$ S-wave phase shifts and non-perturbative chiral approach. *Eur. Phys. J.*, A3:307–309, 1998.

[140] V. E. Markushin. The radiative decay $\phi \rightarrow gamma\pi\pi$ in a coupled channel model and the structure of $f_0(980)$. *Eur. Phys. J.*, A8:389–399, 2000.

[141] M. F. M. Lutz and E. E. Kolomeitsev. On meson resonances and chiral symmetry. *Nucl. Phys.*, A730:392–416, 2004.

[142] Feng-Kun Guo and Peng-Nian Shen. Isospin and a possible interpretation of the newly observed X(1576). *Phys. Rev.*, D74:097503, 2006.

[143] Ulf-G. Meissner, E. Oset, and A. Pich. Chiral symmetry constraints on the K^+ interaction with the nuclear pion cloud. *Phys. Lett.*, B353:161–167, 1995.

[144] L. Alvarez-Ruso, J. A. Oller, and J. M. Alarcon. On the $\phi(1020)f_0(980)$ S-wave scattering and the Y(2175) resonance. *Phys. Rev.*, D80:054011, 2009.

[145] Susana Coito, George Rupp, and Eef van Beveren. Multichannel calculation of excited vector ϕ resonances and the $\phi(2170)$. hep-ph/0909.0051, 2009.

[146] B. Aubert et al. Observation of a broad structure in the $\pi^+\pi^- J/\psi$ mass spectrum around 4.26-GeV/c^2. *Phys. Rev. Lett.*, 95:142001, 2005.

[147] T. E. Coan et al. Charmonium decays of $Y(4260)$, $\psi(4160)$, and $\psi(4040)$. *Phys. Rev. Lett.*, 96:162003, 2006.

[148] Q. He et al. Confirmation of the Y(4260) resonance production in ISR. *Phys. Rev.*, D74:091104, 2006.

[149] C. Z. Yuan et al. Measurement of $e^+e^- \rightarrow \pi^+\pi^- J/\psi$ Cross Section via Initial State Radiation at Belle. *Phys. Rev. Lett.*, 99:182004, 2007.

[150] Felipe J. Llanes-Estrada. Charmonium's K2 peak. *Phys. Rev.*, D72:031503, 2005.

[151] L. Maiani, V. Riquer, F. Piccinini, and A. D. Polosa. Four Quark Interpretation of Y(4260). *Phys. Rev.*, D72:031502, 2005.

[152] Gui-Jun Ding. Are Y(4260) and Z_2^+(4250) are D_1D or D_0D^* Hadronic Molecules? *Phys. Rev.*, D79:014001, 2009.

[153] R. M. Albuquerque and M. Nielsen. QCD sum rules study of the $J^{PC} = 1^{--}$ charmonium Y mesons. *Nucl. Phys.*, A815:53–66, 2009.

[154] C. Z. Yuan, P. Wang, and X. H. Mo. The $Y(4260)$ as an $\omega\chi_{c1}$ molecular state. *Phys. Lett.*, B634:399–402, 2006.

[155] Xiang Liu, Xiao-Qiang Zeng, and Xue-Qian Li. Possible Molecular Structure of the Newly Observed Y(4260). *Phys. Rev.*, D72:054023, 2005.

[156] Shi-Lin Zhu. The possible interpretations of Y(4260). *Phys. Lett.*, B625:212, 2005.

[157] Cong-Feng Qiao. One Explanation for the Exotic State Y(4260). *Phys. Lett.*, B639:263–265, 2006.

[158] Eef van Beveren and George Rupp. Is the Y(4260) just a coupled-channel signal? 2006.

[159] Eef van Beveren and George Rupp. The X(4260) and possible confirmation of $\psi(3D)$, $\psi(5S)$, $\psi(4D)$, $\psi(6S)$ and $\psi(5D)$ in $J/\psi\pi^+pi^-$. 2009.

[160] Eef van Beveren and George Rupp. Interference effects in the X(4260) signal. *Phys. Rev.*, D79:111501, 2009.

[161] B. Aubert et al. Study of the $\pi^+\pi^-J/\psi$ Mass Spectrum via Initial-State Radiation at BABAR. 2008.

[162] B. Aubert et al. Exclusive Initial-State-Radiation Production of the $D\bar{D}$, $D\bar{D}^*$, and $D^*\bar{D}^*$, Systems. 2009.

[163] X. L. Wang et al. Observation of Two Resonant Structures in $e^+e^- \rightarrow \pi^+\pi^-\psi(2S)$ via Initial State Radiation at Belle. *Phys. Rev. Lett.*, 99:142002, 2007.

[164] Feng-Kun Guo, Christoph Hanhart, and Ulf-G. Meissner. Evidence that the $Y(4660)$ is a $f_0(980)\psi'$ bound state. *Phys. Lett.*, B665:26–29, 2008.

[165] D. Gamermann, E. Oset, D. Strottman, and M. J. Vicente Vacas. Dynamically Generated Open and Hidden Charm Meson Systems. *Phys. Rev.*, D76:074016, 2007.

[166] D. Gamermann and E. Oset. Axial Resonances in the Open and Hidden Charm Sectors. *Eur. Phys. J.*, A33:119–131, 2007.

[167] M. Bando, T. Kugo, S. Uehara, K. Yamawaki, and T. Yanagida. Is rho Meson a Dynamical Gauge Boson of Hidden Local Symmetry? *Phys. Rev. Lett.*, 54:1215, 1985.

[168] Masako Bando, Taichiro Kugo, and Koichi Yamawaki. Nonlinear Realization and Hidden Local Symmetries. *Phys. Rept.*, 164:217–314, 1988.

[169] Masayasu Harada and Koichi Yamawaki. Hidden local symmetry at loop: A new perspective of composite gauge boson and chiral phase transition. *Phys. Rept.*, 381:1–233, 2003.

[170] Ulf G. Meissner. Low-Energy Hadron Physics from Effective Chiral Lagrangians with Vector Mesons. *Phys. Rept.*, 161:213, 1988.

[171] Daniel Gamermann and Eulogio Oset. Isospin breaking effects in the $X(3872)$ resonance. *Phys. Rev.*, D80:014003, 2009.

[172] M. Ablikim et al. Resonances in $J/\psi \rightarrow \phi\pi^+\pi^-$ and $\phi K^+ K^-$. *Phys. Lett.*, B607:243–253, 2005.

[173] R. S. Bhalerao and L. C. Liu. Off-shell model for threshold pionic eta production on a nucleon and for ηN scattering. *Phys. Rev. Lett.*, 54:865–868, 1985.

[174] F. Klingl, T. Waas, and W. Weise. Nuclear bound states of omega mesons. *Nucl. Phys.*, A650:299–312, 1999.

[175] M. Ablikim et al. Observation of a broad 1– resonant structure around 1.5- GeV/c^2 in the K^+K^- mass spectrum in $J/\psi \to K^+K^-\pi^0$. *Phys. Rev. Lett.*, 97:142002, 2006.

[176] R. Molina, D. Nicmorus, and E. Oset. The $\rho\rho$ interaction in the hidden gauge formalism and the $f_0(1370)$ and $f_2(1270)$ resonances. *Phys. Rev.*, D78:114018, 2008.

[177] L. S. Geng and E. Oset. Vector meson-vector meson interaction in a hidden gauge unitary approach. *Phys. Rev.*, D79:074009, 2009.

[178] R. Molina, H. Nagahiro, A. Hosaka, and E. Oset. Scalar, axial-vector and tensor resonances from the ρD^*, ωD^* interaction in the hidden gauge formalism. *Phys. Rev.*, D80:014025, 2009.

[179] P. Gonzalez, E. Oset, and J. Vijande. An explanation of the $\Delta_{5/2^-}(1930)$ as a $\rho\Delta$ bound state. *Phys. Rev.*, C79:025209, 2009.

[180] Sourav Sarkar, Bao-Xi Sun, E. Oset, and M. J. Vicente Vacas. Dynamically generated resonances from the vector octet- baryon decuplet interaction. 2009.

[181] E. Oset and A. Ramos. Dynamically generated resonances from the vector octet- baryon octet interaction. hep-ph/0905.0973, 2009.